Regulation of the auxin response by an ancient small RNA pathway

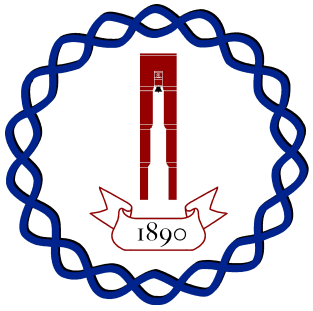

Yevgeniy Plavskin

Watson School of Biological Sciences

PhilosophiæDoctor (PhD)

August 2013

Acknowledgements

The work presented here was possible because of the support and, in some cases, direct participation of many people. I am very grateful for all of the discussions, technical help, ideas, mentoring, and timely distractions that I have received over the course of my thesis research.

I am fortunate to have a family that has encouraged my interest in biology for as long as I can remember. Without the support of my parents, grandparents, and sister, I would not have undertaken this work. Its completion would also not have been possible without my wife, Alex, whose tolerance of late nights in lab and experiment-induced emotional ups and downs is amazing, and whose advice throughout these years often gave me the perspective that I lacked. In addition, I am very grateful to many friends, both inside the lab and outside of it, for all of the teatimes, conversations, and general good times that have kept me in great spirits even when science wasn't going well.

At Cold Spring Harbor, I was lucky to have been a part of a fantastic community, and I have learned a great deal from my conversations with many of the scientists here. I am especially grateful to Dan Chitwood, for teaching me the basics of plant biology and introducing me to Physco; Elijah Salome-Diaz, for his work on growing moss in soil and his tireless enthusiasm; Carol Hu, for technical help; and Aman Husbands, for general support and especially for his critical reading of much of this thesis. Tim Mulligan's help was instrumental for many of the experiments described here. I am also incredibly grateful to the rest of my labmates for all that they have taught me over the years - it is difficult to imagine working with a better group of people.

This project would not have been possible if it were not for the help of my collaborators in Mitsuyasu Hasebe and Ralph Quatrano's labs. Pierre-François Perroud, Akitomo Nagashima, Tsuyoshi Aoyama, and Yosuke Tamada all helped with the experiments described here, and I am grateful to them and many other members of both labs for teaching me more than I ever thought I would know about moss.

I would like to thank my thesis committee - Greg Hannon, Dave Jackson, Ralph Quatrano, and Jan Witkowski - for all of their advice on this project, and Mike Scanlon for agreeing to be the external examiner during my thesis defense. I would also like to thank the administration of the Watson School, past and present, for making grad school run so smoothly and enjoyably.

Finally, I want to express my deep gratitude to Marja Timmermans. Much more than an advisor, Marja has been a true teacher to me over the course of my PhD. In her lab, I have enjoyed both a sense of scientific freedom and support for my work. If I have grown as a scientist over the past six years, it is primarily because of her mentorship.

Abstract

New organs and their associated developmental programs often evolve via the cooption of existing genetic pathways. Plants provide an excellent model for the study of such pathway neofunctionalization. Many genes that play a role in the development of flowering plant- or seed plant-specific organs are conserved in mosses, which diverged from the ancestors of flowering plants and other seed plants ~450 million years ago. We focused on one conserved set of genes, the miR390-dependent tasiRNA pathway. In flowering plants, tasiRNAs are involved in meristem mainternance, leaf polarity, and lateral root growth. The pathway is conserved in the moss *Physcomitrella patens*, although mosses lack roots, leaves, and layered meristems, suggesting a yet unknown ancestral function and repeated evolutionary cooption. With the goals of uncovering the miR390-dependent tasiRNA pathway's ancestral function and elucidating the reasons for its cooption, we studied its role in moss development.

To understand the tasiRNA pathway's function in moss, we generated *Ppsgs3* mutants, which are defective in tasiRNA biogenesis. These show defects in the filamentous stage of moss development, including an absence of caulonemal runners and a decrease in gametophore formation. These defects can be phenocopied by the overexpression of one set of tasiRNA targets, B-group *Auxin Response Factors* (*ARF*s). Abrogation of sRNA regulation of endogenous *PpARFb4* similarly recapitulates the developmental defects of *Ppsgs3*. Together, these results indicate that tasiRNAs regulate development by modulating ARF expression. Phenotypes similar to the ones observed in *Ppsgs3* are also observed in mutants defective in auxin signaling, suggesting that tasiRNA targets are repressive *ARF* genes, and that the tasiRNAs themselves function to modulate auxin signaling. Indeed, *Ppsgs3*

plants have decreased auxin sensitivity. Our work shows that the auxin response in *Physcomitrella* is modulated by a combination of tasiRNA-mediated regulation and auxin-dependent feedback loops.

We propose that the intricate structure of the auxin response network, with sRNA regulation of repressive ARFs across land plants, ensures a robust yet sensitive auxin response, which may have favored this network's repeated cooption. Intriguingly, in *Arabidopsis*, tasiRNAs play a role in lateral root development—a process that, like moss filament growth, is intricately tied to environmental conditions and auxin signaling. The ancestral function of the tasiRNA pathway may have thus been in sensitizing plants to environmental signals that affect plant development by feeding into auxin signaling.

Contents

List of Figures **ix**

1 Introduction: small RNA-regulated networks and the evolution of novel structures in plants **1**

Abstract 2

Introduction 2

Modes of cooption 5

Mechanisms of cooption 7

microRNAs as regulators of gene expression and development 9

Conservation and cooption of small RNAs during plant evolution 12

miR390-dependent tasiRNA biogenesis pathway 16

A conserved network for auxin response regulation 20

Conclusion and perspectives 23

2 tasiRNAs regulate protonemal development in *Physcomitrella patens* **25**

Introduction 26

Results 29

Creation of *Physcomitrella* tasiRNA biogenesis mutants 29

PpSGS3 plays a conserved role in tasiRNA biogenesis 32

Ppsgs3 mutants display protonemal development defects 34

Temporal expression pattern of tasiRNAs and tasiRNA targets 39

Discussion . . . 42
Conservation of tasiRNA biogenesis components . . . 42
tasiRNAs regulate the development of a complex tissue type . . . 43
tasiRNAs as temporal regulators of development . . . 44
Regulation of *ARF* genes by tasiRNAs in moss . . . 45
Ecological perspective on tasiRNA function . . . 46
Auxin signaling as a target for tasiRNA regulation . . . 46

3 tasiRNAs regulate protonemal development by silencing repressive *ARF* genes. 48

Introduction . . . 49
Results . . . 51
The *Ppsgs3* phenotype is consistent with a repression of auxin signaling . . . 51
Overexpression of *PpARFb2* and *PpARFb4* recapitulates the *Ppsgs3* phenotype . 52
tasiRNAs and miR1219 regulate protonemal development via *PpARFb4* . . . 57
sRNAs regulate protonemal development by restricting PpARFb4 to the tips of growing filaments . . . 61
Discussion . . . 65
A conserved role for B-group *ARF*s in repressing auxin signalling . . . 65
Functional redundancy among repressive ARFs in *P. patens* . . . 66
tasiRNAs and miR1219 limit the expression of *PpARFb4* to the protonemal periphery 69
Regulation of *ARF* genes by two sRNAs provides plant-to-plant robustness to protonemal development . . . 71
miR1219 and tasiRNAs provide spatial regulation of the auxin response . . . 72

4 tasiRNAs allow for a sensitive auxin response in *P. patens* 74

Introduction . . . 75
Results . . . 76

Ppsgs3 plants have an impaired auxin response 76
Induction of auxin-dependent gene expression is perturbed in *Ppsgs3* 80
Auxin signaling feeds back onto tasiRNAs and their targets 80
Ppsgs3 plants are impaired in the auxin-dependent induction of a gene regulating caulonemal differentiation 84
Discussion 86
Complex feedback regulation in the moss auxin response network 86
tasiRNAs as a dial to tune developmental response to auxin 90
5 Discussion and perspective **92**
Introduction 93
tasiRNAs modulate the auxin response in moss as part of a complex GRN 94
Spatial regulation by tasiRNAs allows for a robust and sensitive auxin response in cells at the protonemal edge 94
Stochastic local variation in the auxin response 97
tasiRNAs allow for a graded auxin response 98
Environmental regulation of moss development via modulation of the auxin response 100
The auxin response as a developmental effector of exogenous signaling 100
A role for tasiRNAs in mediating exogenous signals 102
Evolutionary perspective on the role of tasiRNAs 103
Regulation of diverse developmental processes by tasiRNAs 103
Regulatory properties of the auxin response GRN, and especially the role of tasiRNAs, may have contributed to its frequent cooption 105
Perspective 107

6 Materials and methods **109**

Identification of a *Physcomitrella* SGS3 homolog 110

Moss culture 110

Creation of transgenic plants 110

Cloning of transformation constructs 110

Moss transformation 111

PCR validation of targeted insertion 112

Transgene copy number quantification 112

Quantification of gene and sRNA expression 113

RNA Isolation 113

sRNA qRT-PCR 113

transcript qRT-PCR 114

RLM 5′ RACE 114

Phenotyping 115

Gametophore counts 115

Soil experiments 115

Branching analysis 116

Cell length measurements 116

Chemical treatments 116

Protein experiments 116

Histochemical staining 117

A Primers **118**

B Signals and prepatterns: new insights into organ polarity in plants. **122**

References **133**

List of Figures

1.1 Appearance of novel structures during the course of plant evolution 4

1.2 Evolution of sRNA regulation of *ARF* genes in land plants 14

1.3 Biogenesis of miR390-dependent tasiRNAs 17

2.1 An overview of *Physcomitrella* development 28

2.2 Creation of *Ppsgs3* mutant strains 31

2.3 *Ppsgs3* plants are defective in tasiRNA biogenesis 33

2.4 *Ppsgs3* affects caulonemal runner and bud formation 35

2.5 *Ppsgs3* protonema display high levels of branching and decreased cell length . 38

2.6 Temporal expression pattern of sRNAs and tasiRNA targets 40

3.1 The auxin response pathway 50

3.2 The *Ppsgs3* phenotype is consistent with a decreased auxin response 53

3.3 Overexpression of PpARFb2 and PpARFb4 recapitulates the *Ppsgs3* phenotype 56

3.4 Creation and validation of *PpARFb4-GUS* lines 58

3.5 sRNA regulation of *PpARFb4* is necessary for caulonemal runner development 60

3.6 sRNA regulation restricts PpARFb4 expression to the growing edge of the protonema 64

3.7 The role of tasiRNAs and B-group ARFs in moss development 67

4.1 *Ppsgs3* is resistant to low doses of auxin, but responds at high concentrations . 78

4.2 The molecular auxin response is decreased in *Ppsgs3* plants 81

4.3 tasiRNAs and their targets are auxin-regulated 83

4.4 Auxin-responsiveness of *PpRSL1* is compromised in *Ppsgs3* plants 85

4.5 tasiRNAs modulate the auxin response in moss 88

5.1 A model of spatial regulation of the auxin response in moss 96

5.2 Environmental conditions profoundly influence moss development and may feed into the auxin response GRN via tasiRNAs 101

5.3 Cooption of regulatory networks 108

List of Abbreviations

AGO	ARGONAUTE
AP2	APETALA2
ARE	Auxin Response Element
ARF	AUXIN RESPONSE FACTOR
At	*Arabidopsis thaliana*
bp	base pair
cDNA	complementary DNA
DCL	DICER-LIKE
FAA	Formaldehyde, alcohol, acetic acid
GRN	Gene Regulatory Network
GUS	β-Glucuronidase
HD-ZIPIII	HOMEODOMAIN LEUCINE ZIPPER CLASS III
IAA	Indole-3-acetic acid
lbl1	*leafbladeless1*
miRNA	microRNA
mRNA	Messenger RNA
NAA	1-naphthaleneacetic acid
nt	nucleotide
PAZ	PINHEAD, ARGONAUTE, ZWILLE
PCIB	p-Chlorophenoxyisobutyric acid
Pp	*Physcomitrella patens*
qPCR	quantitative PCR
RACE	Rapid amplification of cDNA ends
RDR	RNA-DEPENDENT RNA POLYMERASE
SGS	SUPPRESSOR OF GENE SILENCING
siRNA	small interfering RNA
sRNA	small RNA
tasiR-AP2	tasiRNAs targeting *AP2*-domain genes
tasiR-ARF	tasiRNAs targeting *ARF*s
tasiRNA	trans-acing siRNA
X-gluc	5-bromo-4-chloro-3-indoyl-β-D-Glucuronic acid
XS	rice gene X and SGS3
Zm	*Zea mays*

Chapter 1

Introduction: small RNA-regulated networks and the evolution of novel structures in plants

Published as Plavskin Y, Timmermans MCP. 2013. small RNA-regulated networks and the evolution of novel structures in plants. *Cold Spring Harb Symp Quant Biol*.

Abstract

The evolution of plants on land has produced a great diversity of organs, tissues, and cell types. Many of the genes identified as having a role in the development of such structures in flowering plants are conserved across all land plants, including in clades that diverged before the evolution of the structure in question. This suggests that novel organs commonly evolve via the cooption of existing developmental gene regulatory networks (GRNs). Although numerous examples of such cooptions have been identified, little is known about why those specific GRNs have been coopted. In this review, we discuss the properties of GRNs that may favor their cooption, as well as the mechanisms by which this can occur, in the context of plant developmental evolution. We especially focus on small RNA (sRNA)-regulated and auxin-signaling GRNs as intriguing models of regulatory network recruitment.

Introduction

The plethora of multicellular species that inhabit the earth today—with of all their tissue complexity—evolved from a handful of unicellular ancestors. As evolution proceeded, the appearance of novel organs and tissue types allowed organisms to occupy new niches. For example, the evolution of wings allowed insects to expand into the air column, and flowers allowed angiosperms to attract pollinators. Many of the developmental processes responsible for the formation of these organs, as well as their genetic basis, are now beginning to be understood. However, little is known about the origins of these processes. Elucidating the mechanisms by which novel developmental programs arise is essential for understanding how our unicellular ancestors evolved into extant multicellular organisms with their rich diversity of cell types, tissues, and organs.

Plants provide an especially attractive model for addressing this problem. Unlike animals, whose major clades diversified during the Cambrian explosion ∼550 million years ago (mya) (Peterson et al., 2009), land plants first began their diversification ∼450 mya (Kenrick and Crane, 1997), with some major clades such as the flowering plants not appearing until 130–90 mya (Crane et al., 1995). During the course of their evolution on land, plants evolved a

number of specialized organs and tissue types that have contributed to their diversity and success (summarized in Fig 1.1). The ancient plants that first emerged on land likely had a haploid gametophyte-dominant life cycle, with a diploid sporophyte dependent on the gametophyte for its nutrients. This life cycle is maintained today by bryophytes. Paleontological evidence of these early plants is scarce, but shared characteristics of many bryophytes suggest that their development proceeded by germination of a haploid spore, followed by emergence of filamentous or thalloid protonema and one or more gametophores (Kenrick and Crane, 1997). The highly branched filamentous protonema of most mosses (with the exception of *Sphagnum*) are likely to be a derived structure and are not found in hornworts or liverworts (Mishler and Churchill, 1984). After the divergence of bryophytes and tracheophytes ∼450mya, the latter evolved a nutrient-independent sporophyte generation (represented in fossils such as *Aglaophyton*) and a lignified vasculature (early examples of which can be found in *Cooksonia*) (Kenrick and Crane, 1997). These vascular, sporophyte-dominant plants are represented today by the lycophytes and euphyllophytes. In each of these phyla, the gametophyte became independently reduced to a tiny mass of cells from which the much bigger sporophytic plant develops (Kenrick and Crane, 1997). Among the euphyllophytes, ferns maintained the ancestral mode of dispersal by haploid spore, whereas their sister group, represented today by the gymnosperms and flowering plants, evolved diploid seeds as a primary mode of dispersal and further reduced their gametophyte, making it nutrient dependent on the sporophyte. After the divergence of gymnosperms and flowering plants, the latter evolved flowers, a layered tunica-corpus meristem (although this is also present in some groups of gymnosperms) and an ovary to enclose the developing seed (Gifford and Foster, 1989).

Many structures that appear widespread in plants actually hold independent evolutionary origins. This is true for anchoring structures, which can be found in every major clade of plants, such as the gametophytic rhizoids of bryophytes and the sporophytic roots of flowering plants (Pires and Dolan, 2012). A similar pattern holds true for the evolution of flattened photosynthetic structures. Such phyllids are present on the gametophores of both mosses and some species of liverworts, and these are believed to have independent evolutionary origins (Mishler and Churchill, 1984). Lycophytes independently evolved phyllids on the sporophytic

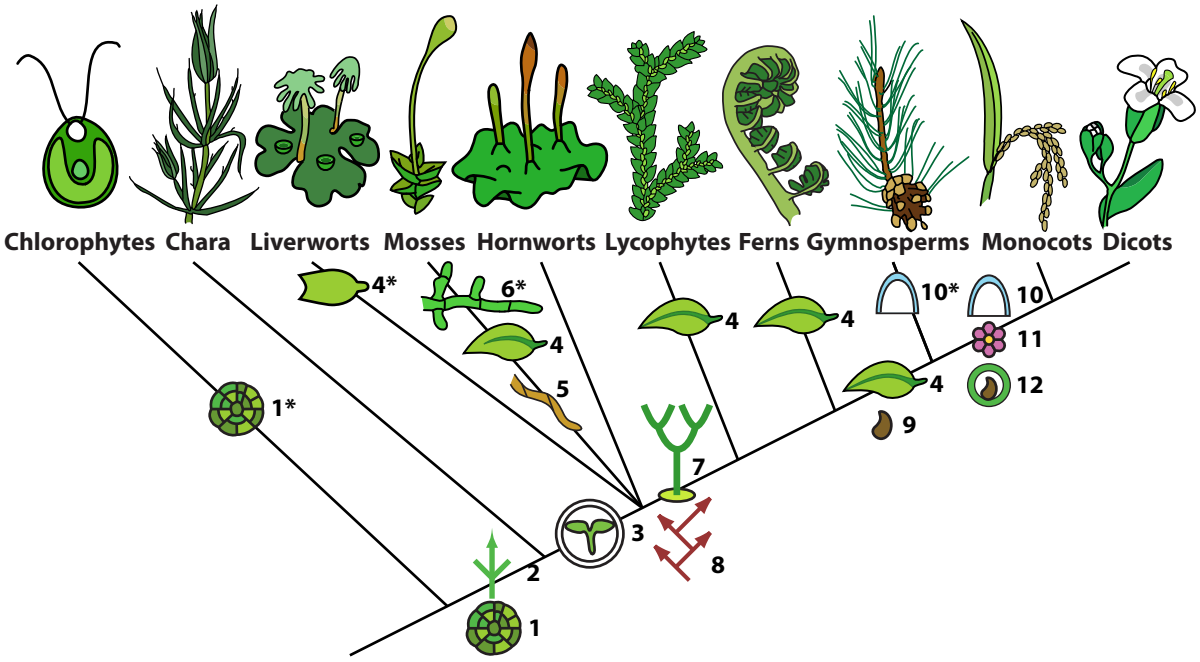

Figure 1.1: Appearance of novel structues during the course of plant evolution

Asterisks denote important structures present in only a subset of the plants in a clade. (1) Multicellularity appeared in some chlorophyte algae and at the base of streptophytes, which include land plants and Charales; (2) apical growth arose at the base of streptophytes; (3) protected development of the diploid embryo first appeared at the base of land plants; (4) flattened photosynthetic structures evolved independently in some groups of liverworts as well as in mosses, lycophytes, ferns, and at the base of seed plants; (5) multicellular rhizoids arose at the base of mosses; (6) branched protonemal filaments evolved in some mosses; (7) a dominant, branching sporophyte evolved at the base of vascular plants; (8) lignified vasculature arose at the base of vascular plants (although vascular tissue can be found in mosses as well); (9) seeds evolved at the base of seed plants; (10) layered "tunica-corpus" meristems arose in some gymnosperms and at the base of flowering plants; (11) flowers arose at the base of flowering plants; (12) seed development inside an enclosed ovary first evolved at the base of flowering plants.

Figure 1.1

generation, and even the true leaves that define euphyllophytes as a group evolved independently in ferns and in the ancestor of seed plants (Floyd and Bowman, 2006) (see Fig 1.1).

Genes that participate in development have primarily been studied in flowering plants. In recent years, however, genomic and genetic resources for a number of models outside of flowering plants have been developed, including the model liverwort *Marchantia polymorpha*, the model moss *Physcomitrella patens*, the model spikemoss *Selaginella*, and the model fern *Ceratopteris richardii*. The availability of genetically tractable models both within and outside of angiosperms provides an opportunity to study the evolution of the genes that underlie the development of novel structures across a wide range of evolutionary distances. Such studies have revealed that many key developmental regulators form complex hierarchical gene networks that are conserved throughout land plant evolution. In fact, a number of these appear to be significantly older than the developmental processes they are known to regulate. This suggests an ancestral role for some widely studied genes that is different from their role in flowering plants. Thus, cooption of existing genes or whole GRNs for a new function is an important way in which novel developmental processes may arise. In this review, we focus on the features of developmental circuits, especially those regulated by sRNAs, which make them amenable to repeated cooption during the course of plant evolution.

Modes of cooption

At the heart of developmental GRNs are so-called input/output circuits or genes. These integrate information from multiple inputs, such as developmental or environmental cues, and activate a set of downstream genes responsible for specific cellular processes associated with development (Erwin and Davidson, 2009). The hierarchical nature of GRNs means that redeployment of these input/output genes into a novel developmental context can also allow the GRNs complex downstream cellular processes to be transplanted. In this way, whole tissues or cell types can be recapitulated in a novel spatiotemporal pattern through the cooption of just one gene. A widely studied example in which a coopted GRN resulted in the redeployment of an existing tissue type is the evolution of teeth. The core gene network regulating tooth development has been deployed separately in at least two differ- ent contexts:

the endodermis-derived pharyngeal arches of fish and the ectodermis-derived oral jaws of jawed vertebrates (Fraser et al., 2009). This mode of cooption allowed an intact structure to essentially be transplanted by evolution into a novel developmental context.

However, regulatory networks are not always coopted in their entirety. The formation of novel structures during evolution is often driven by cooption of genes or circuits to regulate a novel set of downstream processes. In this case, rather than redeploying an existing network in a novel context, evolution is reusing a regulatory circuit for a different developmental purpose. A classic example is the evolution of wing spots in butterflies. These often complex pigmentation patterns are formed in response to the Hedgehog (Hh) signaling pathway (Keys et al., 1999). In fruit flies, *Hh* signaling has a crucial role in embryonic patterning. In the late stages of butterfly wing development, the developmental genes that this pathway regulates during embryonic patterning are replaced with pigmentation genes. Interestingly, the downstream targets of this circuit appear to be especially fluid, as the specific pigments in the wing spots vary among different species of butterflies (Carroll et al., 2004).

Examples of both modes of evolution are being identified in plants as well. For example, *ROOT HAIR DEFECTIVE SIX-LIKE* (*RSL*) transcription factors have been coopted multiple times during the course of plant evolution to specify tubular, tip-growing cell types including root hairs in *Arabidopsis* and gametophytic rhyzoids and caulonemal cells in *Physcomitrella* (Jang and Dolan, 2011; Jang et al., 2011; Menand et al., 2007a;b). A stunning variety of leaf developmental GRNs were coopted to regulate the development of floral organs (Kidner et al., 2002), whose similarity to leaves has long been recognized (von Goethe, 1790). In addition, multiple examples are found in plants of developmental circuits being coopted for a novel developmental function, similar to the cooption of the *Hh* signaling pathway in wing spot development. Two widely studied examples are *ERECTA*-family LEU-RICH RECEPTOR-LIKE KINASES and the *YODA* MAPKK kinase. Originally identified as key players in organ shape (Torii et al., 1996) and early embryonic development (Lukowitz et al., 2004), respectively, both genes have since been found to be key regulators of stomatal patterning (Bergmann et al., 2004; Shpak et al., 2005). Importantly, such repeated cooption of select circuits for the regulation of distinct processes results in many genes having very pleiotropic developmental functions.

Mechanisms of cooption

Mutation of protein-coding sequences constitutes one driver of phenotypic change. In the context of developmental GRNs, protein-coding mutations can alter the wiring of the network by changing the affinity of interactions with other proteins or nucleic acids or by creating new ones. Protein-coding changes in the *LEAFY* gene have, for instance, been shown to be important in plant evolution, with changes in the DNA-binding domain of this transcription factor leading to changes in its downstream targets (Maizel et al., 2005). However, across long divergence periods (e.g., among species), coding changes to genes do not appear to be the predominant cause of phenotypic adaptations (Stern and Orgogozo, 2008; 2009). Precisely because of the repeated cooption of the same developmental circuits for multiple functions, many input/output genes regulate more than one developmental process. Thus, any wiring changes caused by coding mutations in GRN components likely result in pleiotropic defects in the developing organism. For example, if changes to the network regulating wing spot patterning in butterflies occurred by coding-level mutations to the *Hh* gene, embryonic patterning would likely also be compromised. Examples of such changes are therefore more likely to be found in developmental regulators participating in select developmental processes, such as *LEAFY*.

Pleiotropic effects of protein-coding mutations may be partially alleviated by redundancy in the genome. Following a gene duplication event, the two paralogs are functionally redundant, and thus, mutations that affect the function of one are often better tolerated. As mutations accumulate, neofunctionalization of one or both paralogs often results. This pattern of duplication followed by neofunctionalization appears to be especially prevalent in plants, in which amplifications of individual genes are augmented by frequent whole-genome duplications and polyploidization events (Flagel and Wendel, 2009). Neofunctionalization of duplicated genes has, for instance, had a key role during the evolution of flower morphology within angiosperms (Kramer and Irish, 1999; Rosin and Kramer, 2009).

Unlike coding mutations, mutations in regulatory regions of genes avoid the problem of pleiotropy (Carroll et al., 2004; Stern and Orgogozo, 2008). Such mutations introduce novel

transcription factor-binding sites in the promoters or enhancers of genes or affect existing sites. These *cis*-regulatory changes alter the expression levels of genes or allow them to acquire novel spatiotemporal expression patterns without affecting their function in other contexts. Many of the known examples of cooption in plants are likely to reflect such regulatory changes, although the specific *cis* mutations have only been identified in select cases. The repeated evolution of compound leaves in dicots presents one example of how *cis*-regulatory changes that alter expression patterns of input/output genes can modify morphology. *KNOX* genes act as input/output genes, integrating multiple developmental signals to promote indeterminacy in the meristems of flowering plants (Rosin and Kramer, 2009; Townsley and Sinha, 2012). These genes are normally repressed in the determinate tissues of leaves by ASYMMETRIC LEAVES1 (AS1), AS2, and Polycomb group proteins that bind as a complex to sites in *KNOX* promoters (for review, see Lodha et al. (2008)). Expression of *KNOX* genes in developing leaves has been observed in many compound-leafed species (Bharathan et al., 2002). Studies from *Cardamine hirsuta* have identified differences in the 50 regulatory region of *KNOX* genes, including in the AS1-AS2 binding sites, which allow expression of these genes in the leaf primordia of this species (Guo et al., 2008; Hay and Tsiantis, 2006). Similarly, a study in Galapagean tomato *Solanum galapagense* identified a change in the promoter of a *KNOX*-like gene that is responsible for increased leaf complexity (Kimura et al., 2008). These examples point to repeated *cis*-regulatory cooption of the meristem indeterminacy GRN in multiple independent origins of leaf complexity.

A well-characterized example in which a *cis*-regulatory mutation selected for during plant evolution alters the expression level of a gene rather than its expression pattern comes from the domestication of maize. The increased apical dominance of maize, selected for during the domestication of its wild ancestor teosinte, results from a transposon insertion into the regulatory region of *teosinte branched1* (*tb1*) (Studer et al., 2011). This gene encodes a repressor of axillary meristem development, and its original function was in modulating teosinte plant architecture in response to environmental cues (Doebley et al., 1995). The insertion selected for during the evolution of maize uncouples expression from environmental inputs and leads to constitutive increases in the level of *tb1* that in turn keeps the growth of lateral branches

repressed (Studer et al., 2011).

The examples outlined above demonstrate the importance of *cis*-regulatory changes in altering the deployment of developmentally important regulatory genes, some of which likely function as input/output genes in their respective GRNs. The cooption of novel target genes by widely deployed regulatory circuits, such as that observed in the butterfly wing spot example, are likely to function by similar mechanisms. In fact, the evolution of wing spots in the *Drosophila* lineage has been traced to a novel *cis* element regulating the expression of the *Yellow* gene (Werner et al., 2010) that is predicted to encode an important component of the melanin synthesis pathway (Wittkopp et al., 2002). The novel element places *Yellow* under control of *Wingless* (*Wnt*) signaling, which—much like *Hh* signaling—regulates a wide range of processes in the developing embryo. Thus, cooption at various levels of developmental GRNs can occur via *cis*-regulatory changes.

Interestingly, in two of the animal examples of cooption identified above (butterfly wing spots and *Drosophila* wing spots), cooption occurs via redeployment of a morphogen. Such molecules are often at the heart of complex GRNs, whose readout depends on the level of the morphogen. In addition, the mobile nature of morphogens means that their redeployment in a small subset of cells in the developing organism can affect downstream targets far outside of the tissue in which they are synthesized. One potential advantage of mobile signals for evolution is that their deployment is not binary; downstream developmental effects can be carefully finetuned by altering levels of mobile signal synthesis, degradation, and the rate of mobility (Wartlick et al., 2009). Cooption of developmental GRNs via mobile signal redeployment likely has an especially important role in the evolution of plants, in which small RNAs and phytohormones act as mobile signals regulating many aspects of development.

microRNAs as regulators of gene expression and development

In addition to being regulated at the transcriptional level, many genes are regulated posttranscriptionally. microRNAs (miRNAs) have emerged as key posttranscriptional regulators of gene expression and important contributors to both animal and plant develop-

ment. miRNAs, which are ∼21 nucleotides in size, are processed from transcripts containing a foldback region before being loaded into an ARGONAUTE (AGO) protein to form an RNA-induced silencing complex (RISC) (for details on miRNA processing, see Axtell et al. (2011)). This AGO-miRNA complex binds to target transcripts and facilitates their site-specific cleavage or translational repression. Animal miRNAs bind to target RNAs based on complementarity within a short 6–8-nucleotide seed region and as a result, often have hundreds of predicted targets per genome. In contrast, plant miRNAs regulate transcripts to which they show complementarity across the length of the small RNA, and their target sets are usually limited to a few closely related genes per genome (Jones-Rhoades et al., 2006).

Much like the regulatory elements in promoters and enhancers described above, small RNAs can modulate levels and spatiotemporal patterns of gene expression in plants and animals. miRNAs are typically expressed in distinct and precisely defined spatiotemporal patterns (Javelle and Timmermans, 2012; Wienholds et al., 2005) that in turn act to limit the expression of their targets, often to complementary domains. The first miRNA discovered, lin-4, was found to negatively regulate LIN-14, clearing its transcript at the end of the first *Caenorhabditis elegans* larval stage and ensuring a timely developmental transition (Lee et al., 1993; Wightman et al., 1993). In flowering plants, miRNAs likewise have a role in regulating key developmental transitions. miR172 and miR156 regulate genes that promote juvenile and adult leaf traits, respectively (Chuck et al., 2007; Lauter et al., 2005; Wu et al., 2009; Wu and Poethig, 2006). miRNAs are also key players in the specification of distinct tissues and cell types in plants. For example, miR166 acts on the abaxial (bottom) side of developing leaves to limit expression of HD-ZIP III-class genes to the adaxial (top) leaf side. This is crucial to leaf development, because mutations yielding *HD-ZIPIII* genes insensitive to miR166 perturb proper adaxial-abaxial leaf patterning and, consequently, blade outgrowth (Emery et al., 2003; Juarez et al., 2004a) These, among numerous other examples, demonstrate the important role that miRNAs have in regulating the expression of key developmental genes (Chen, 2009).

In addition to their role in regulating the spatiotemporal expression patterns of target genes, miRNAs can also be important for increasing the robustness of GRNs, which is predicted to make networks more favorable for cooption (see next section). A miRNA can clear

out leaky transcription of its targets, increasing robustness of tissue specificity. Alternatively, a miRNA can stabilize the level of target gene expression by alleviating the inherent noisiness of transcription (Skopelitis et al., 2012; Voinnet, 2009). In this latter case, the miRNA and its target are coexpressed in the same spatiotemporal domain, and robustness of gene expression is increased because transcriptional activation tends to be noisier than translation (Ebert and Sharp, 2012; Hornstein and Shomron, 2006; Raser and O'Shea, 2005). Experimental evidence indeed suggests a role for some miRNAs in maintaining the robustness of gene expression in plants. *Arabidopsis* plants mutant for miR164a, b, and c display stochastic ectopic expression of *CUC1* and *CUC2*, suggesting a role for miR164 in clearing the leaky transcription of these targets. In addition, the expression domains of miR164 and its targets partially overlap, suggesting that miR164 may be functioning to mitigate noise in the transcription of *CUC1* and *CUC2* (Sieber et al., 2007).

Another property of sRNAs—their ability to move within the developing plant—has been shown to be an important contributor to the regulation of plant development. Movement of sRNAs outside of their biogenesis domain is important in regulating target gene expression in the developing leaf (Chitwood et al., 2009) and root (Carlsbecker et al., 2010; Miyashima et al., 2011). Computational modeling has shown that a gradient of sRNA concentration resulting from mobility can help to establish a sharp spatial boundary in target gene expression ((Levine et al., 2007), such that regulation via a mobile sRNA may have a key role in maintaining developmental robustness. (For a detailed review on sRNA mobility and its implications for plant development, see Skopelitis et al. (2012).)

Much as with the *cis*-regulatory elements controlling a genes transcription, multiple miRNAs may exert combinatorial control over a single target. Moreover, when sRNA-mediated repression is not catalytic, sRNAs have been shown to act cooperatively to create a switch-like threshold effect on gene expression (Mukherji et al., 2011) that can have profound impacts on GRN dynamics. This possibility may be especially relevant in animals, in which the presence of multiple imperfectly complementary miRNA sites on a single transcript is common (Shomron et al., 2009). However, examples of regulation of a single gene by multiple sRNAs also exist in plants. For example, the PPR-P family of genes is targeted in Arabidopsis by

miR161 and miR400 as well as trans-acting small interfering RNAs (tasiRNAs) derived from the *TAS1* and *TAS2* loci. At least five of the *PPR-P* genes are targeted by both miR161 and *TAS2*-derived tasiRNAs (Howell et al., 2007). The significance of such combinatorial—and possibly cooperative—regulation by multiple sRNAs is in need of further exploration, especially in plants.

Conservation and cooption of small RNAs during plant evolution

The role of miRNAs in regulating gene expression identifies them as potential key players in the process of evolutionary cooption. Additionally, a role for miRNAs in increasing GRN robustness underscores their importance in evolution. Robustness is important for heritability, and modeling shows that a gene such as a miRNA that increases the robustness of an adaptive allele will be coselected with that allele (Peterson et al., 2009). Besides its importance for heritability, robustness of developmental processes is itself adaptive, because development must remain consistent across variable environmental conditions. Thus, any factor that improves the robustness of a developmental GRN, such as miRNA, would also improve the chances of that GRN being evolutionarily coopted. Changes in miRNA-controlled GRNs can occur at multiple levels, including changes in the conservation of the miRNA arsenals across different species, losses/ gains of sRNA target sites during the course of evolution, and diversification in the function of small RNA targets. With the ever-increasing wealth of genome information, insights into each of these mechanisms are being elucidated.

The properties of miRNA precursor transcripts along with the nature of sRNA-target interactions make miRNAs amenable to computational investigation in species for which a genome sequence is available (Meyers et al., 2008). Putative targets can be found for known or predicted sRNAs by searching for genes with complementarity to the seed region and filtering the results by rules that help to identify high-quality targets (Addo-Quaye et al., 2008; Allen et al., 2005). The presence of sRNA deep sequencing information and transcript degradome data in many sequenced species has aided greatly in sRNA and target identification (for some examples, see Addo-Quaye et al. (2008); Arazi et al. (2005); Kasschau et al. (2007); Sunkar et al.

(2005)). This has revealed that, as with regulatory regions in promoters, miRNA complementary sites can appear and disappear from within a gene without changing its coding sequence. miRNA site evolution thus allows changes in the deployment of genes in specific spatiotemporal patterns without perturbing target function in other important developmental processes. A widely studied example has been identified in Texel sheep. Here, the 30 untranslated region (UTR) of a myostatin gene gained a novel site for two miRNAs, miR1 and miR206. These miRNAs are both expressed in skeletal muscle. In Texel sheep, they increase skeletal muscle production by decreasing myostatin levels in this tissue, leading to the meaty phenotype for which these sheep are known (Clop et al., 2006). Examples of miRNAs evolving novel targets also exist in plants. For example, miR156 has an evolutionarily conserved role in targeting SQUAMOSA BINDING PROTEIN-LIKE (SBP/SPL)-family genes across all land plants studied. However, in moss, this miRNA has been shown to also target the noncoding transcript *TAS6* (Arif et al., 2012). Existing targets can also lose miRNA regulation by mutations in the miRNA-binding site. For example, loss of a miR160 target site has occurred in some maize AUXIN RESPONSE FACTOR (ARF) genes (Fig 1.2b).

Interestingly, although the core RNAi machinery is conserved among eukaryotes, miRNAs appear to have evolved independently in animals and in plants (Bartel, 2004). Extensive sRNA sequencing in a number of plant species has revealed that miRNAs are frequently gained and lost during the course of plant evolution (for review, see Axtell and Bowman (2008); Cuperus et al. (2011)). For example, of 102 miRNA families in *Arabidopsis thaliana*, only 78 are conserved between *A. thaliana* and its close relative *A. lyrata*, 25 are conserved across the eudicots, and 22 have been identified in monocots (Cuperus et al., 2011; Fahlgren et al., 2010; Ma et al., 2010). Such limited evolutionary conservation implies that individual plant species generate numerous specific, recently evolved miRNAs. Novel miRNAs have been proposed to evolve by a partial inverted duplication of a member of a protein-coding gene family (Allen et al., 2004). When transcribed, this can result in long hairpin RNAs that in *Arabidopsis* are processed by one of four DICER-LIKE proteins, DCL4, into siRNAs. These repress expression of closely related homologs within the gene family. As the duplicated locus accumulates mutations, the transcripts begin to resemble a short hairpin-containing miRNA

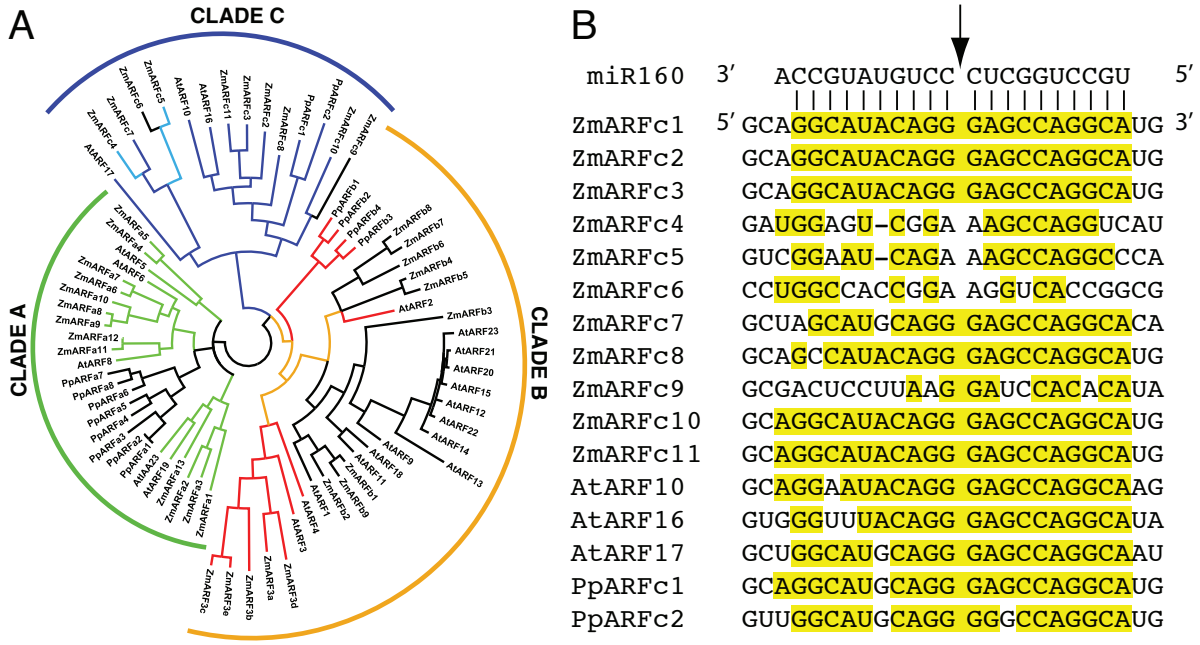

Figure 1.2: Evolution of sRNA regulation of *ARF* genes in land plants
(A) ARF proteins fall into three major clades, with a specific sRNA targeting members of each clade (colored branches); shown in black are branches representing *ARF* genes without an sRNA target site. Clade A contains activating ARF proteins including all of the miR167-targeted ARFs (green branches). Clade B includes the ARFs from *Arabidopsis*, maize, and *Physcomitrella*, which are targeted by miR390-dependent tasiRNAs (red branches); one interpretation of this tree is that tasiRNA targeting was the ancestral state for this clade (orange branches), with two independent losses within the flowering plants. Clade C includes all of the miR160-targeted ARFs (dark blue branches) and shows multiple losses of miRNA targeting occurring in maize, either by complete loss of the miR160 target site (black branches) or by mutation of the key central nucleotides in the miRNA cleavage site (light blue branches). Phylogeny was reconstructed using maximum likelihood; branches with an approximate-likelihood ratio test value of ,0.5 were collapsed. **(B)** Alignment of the miR160-target site from Clade C *ARF* genes. (Arrow) Site of RISC-mediated cleavage. Loss of the target site can be observed in *ZmARFc4*, *5*, *6*, and *9*. Accession numbers for moss and maize ARF proteins: GRMZM2G169820, GRMZM2G102845, GRMZM2G317900, GRMZM2G086949, GRMZM2G034840, GRMZM2G081158, GRMZM2G073750, GRMZM2G089640, GRMZM2G035405, GRMZM2G028980, GRMZM2G475882, GRMZM2G078274, GRMZM2G160005; ZmARFb1-9: GRMZM2G702026, GRMZM2G017187, GRMZM2G475263, GRMZM2G116557, GRMZM2G338259, GRMZM2G378580, GRMZM2G352159, GRMZM2G006042, GRMZM2G137413; ZmARFc1-11: GRMZM2G159399, GRMZM2G153233, GRMZM2G390641, GRMZM2G023813, GRMZM2G179121, GRMZM2G181254, GRMZM5G808366, GRMZM2G081406, GRMZM2G122614, GRMZM2G005284, AC207656.3_FGT002; ZmARF3a-e: GRMZM2G030710, GRMZM2G441325, GRMZM2G056120, GRMZM2G437460, GRMZM5G874163; PpARFa1-8: Pp1s86_1V6.1, Pp1s86_4V6.1, Pp1s119_32V6.1, Pp1s133_56V6.1, Pp1s6_240V6.1, Pp1s65_227V6.1, Pp1s48_147V6.1, Pp1s163_119V6.1; PpARFb1-4: Pp1s280_7V6.1, Pp1s341_4V6.1, Pp1s64_138V6.1, Pp1s14_392V6.1; PpARFc1-2: Pp1s339_47V6.1, Pp1s279_9V6.1.

Figure 1.2

precursor. Processing is shifted from DCL4 to DCL1, and the number of distinct sRNAs generated is greatly reduced. The continued accumulation of mutations ultimately leads to the production of a single prominent miRNA that targets members of the original gene family (for review, see Axtell and Bowman (2008); Chapman and Carrington (2007)). This mechanism of miRNA evolution explains why miRNAs often target multiple members of a specific gene family (Rhoades et al., 2002).

Despite the frequent gains and losses of miRNAs during the course of plant evolution, a conserved core of eight ancestral miRNAs (miR156, miR159/319, miR160, miR166, miR171, miR408, miR390/391, and miR395) remains in most embryophytes (Axtell and Bowman, 2008; Cuperus et al., 2011). The green alga *Chlamydomonas reinhardtii*, sister to the Streptophytes, shares no miRNAs with land plants (Zhao et al., 2007). This suggests the intriguing possibility that the miRNAs of land plants may have evolved alongside multicellularity or as a means of responding to a complex new environment during the transition to land. Indeed, many of the miRNAs conserved within land plants regulate development or environmental response. The latter include miR395 and miR408, which are conserved in every major group of land plants. miR395 regulates sulfur accumulation by targeting ATP sulfurylases and sulfur transporters (Liang et al., 2010). miR408 regulates the expression of the copper-containing proteins plantacyanin and laccases, down-regulating them to free up copper for essential cellular processes in response to low copper abundance (Abdel-Ghany and Pilon, 2008). Although studies examining the function of these two sRNAs were performed in flowering plants, it is not difficult to imagine that sulfur and copper availability may be important for many different groups of land plants.

The conservation of miRNAs important in developmental processes is more difficult to explain. Pan-embryophyte miRNAs include miR156, miR160, and miR166. The targets of these miRNAs, which are also largely conserved between mosses and flowering plants, have been shown to be important for seed plant-specific, and often even flowering plant-specific, developmental processes. SBP/SPL-family genes targeted by miR156 regulate traits associated with the transition from juvenile to adult growth, including leaf shape, root outgrowth, and flowering (Wu and Poethig, 2006). Interestingly, novel functions for these targets, such as

their role in bract suppression in maize (Chuck et al., 2007), can even be seen within flowering plants. Maize miR156 targets the gene *teosinte glume architecture*, a major target of selection during the domestication of maize from teosinte (Wang et al., 2005). The *ARF* genes targeted by miR160 influence processes such as leaf development and flowering (see, e.g., Mallory et al. (2005)), whereas the *HD-ZIPIII* genes regulated by miR166 are important in leaf polarity, meristem maintenance, and vascular patterning (Carlsbecker et al., 2010; Emery et al., 2003; Juarez et al., 2004a).

Although the function of miR395 and miR408 may be conserved across land plants, the function of the GRNs that miR156, miR160, and miR166 are parts of must have changed during the course of evolution. Mosses and vascular plants diverged long before the evolution of leaves, roots, and flowers, whose development these sRNAs and their targets participate in. In fact, because moss lacks a branched, vascularized sporophyte and because flowering plants have a much-simplified gametophyte, the existence of any homologous structures between mosses and flowering plants is questionable. This means that miR156, miR160, and miR166, as well as their targets, were redeployed during the evolution and elaboration of the sporophyte. Until the ancestral developmental function of the targets is elucidated, it will be difficult to precisely define why the GRNs containing these miRNA—target sets were coopted, multiple times, during the course of plant evolution. However, it is interesting to speculate that the ability of miRNAs to function as mobile signals and to provide robustness to GRNs has had a key role in the repeated cooption of sRNA-regulated GRNs.

miR390-dependent tasiRNA biogenesis pathway

Unlike the conserved miRNAs described above that target protein-coding genes in flowering plants, one miRNA present in the ancestor of all land plants, miR390, targets non-coding transcripts that give rise to a unique class of secondary sRNAs with roles in development (Fig 1.3b). . In *Arabidopsis*, miR390 uniquely associates with AGO7 (Mi et al., 2008; Montgomery et al., 2008), and this complex binds to two complementary sites on noncoding transcripts from the *TAS3* family (Allen et al., 2005). The transcripts are cleaved by AGO7 at the 3′ miR390-complementary site, stabilized by SUPPRESSOR OF GENE SILENCING3

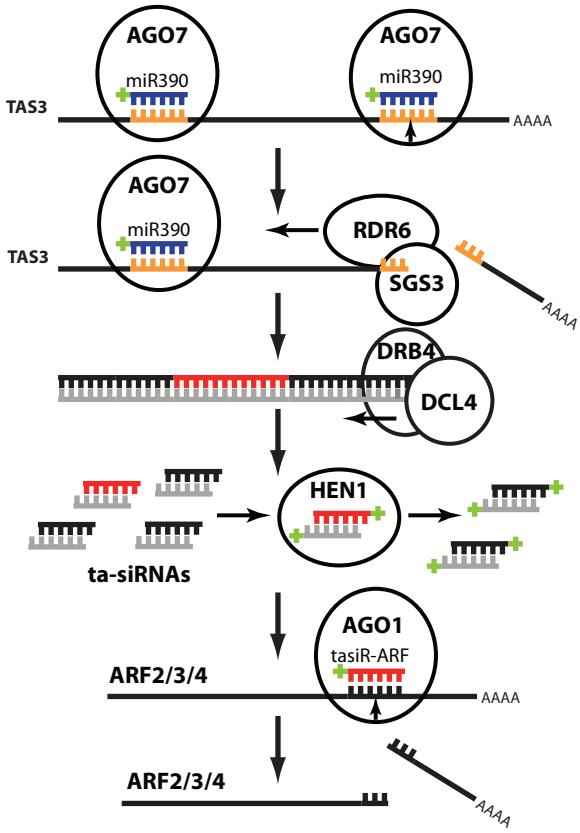

Figure 1.3: Biogenesis of miR390-dependent tasiRNAs
An AGO7-miR390 complex binds a noncoding *TAS3* transcript at two miR390-complementary sites and cleaves *TAS3* at the 3′ site. SGS3 stabilizes the *TAS3* cleavage product, and RDR6 converts it into a double-stranded transcript. Through the action of DCL4 and DRB4, this double-stranded RNA is then diced into 21-nucleotide tasiRNAs that are phased relative to the miR390 cleavage site. HEN1 methylates the 3′ end of these tasiRNAs, stabilizing them. A subset of the tasiRNAs in *Arabidopsis* goes on to target *ARF2*, *ARF3*, and *ARF4* transcripts.

(SGS3), and reverse transcribed by RNA-DEPENDENT RNA POLYMERASE6 (RDR6). The resulting double-stranded transcripts are then processed by DCL4 into phased 21-nucleotide tasi-RNAs. These are loaded into AGO1, and two of them, termed tasiR-ARFs, function to silence a set of *ARF* genes (*ARF2*, *3*, *4*) in *Arabidopsis* (Chapman and Carrington, 2007). Related tasiRNA biogenesis pathways have been identified, including those producing tasiRNAs from TAS loci targeted by miR173 and miR828 (Allen et al., 2005; Axtell et al., 2006; Rajagopalan et al., 2006; Yoshikawa, 2005), and those generating 21-nucleotide phasiRNAs from PPR and NB-LRR family genes (Howell et al., 2007; Shivaprasad et al., 2012; Zhai et al., 2011). However, in contrast to the miR390-dependent tasiRNA pathway, the latter seem to be limited to the dicot lineage of flow- ering plants.

The greater complexity of the miR390-dependent tasiRNA biogenesis pathway as compared with the relatively simple scheme of direct miRNA-mediated gene silencing allows more inputs for evolution to modulate the spatiotemporal pattern of the pathways activity. A striking example of this can be found when the expression patterns of miR390-dependent tasiRNA biogenesis components are compared between *Arabidopsis* and maize. In maize, miR390 localizes to the adaxial side of developing leaves (Nogueira et al., 2009), consistent with a role for this pathway in adaxial fate specification (Juarez et al., 2004b). In contrast, in *Arabidopsis*, in which miR390-dependent tasiRNAs are also important for specification of the adaxial side of the leaf, miR390 is expressed broadly throughout the developing shoot. However, *TAS3* and *AGO7* expression is adaxially restricted in *Arabidopsis* leaf primordia (Chitwood et al., 2009; Garcia et al., 2006), thus ensuring that tasiRNAs are only generated in that domain.

Components of the miR390-dependent tasiRNA biogenesis pathway have been identified in every major clade of plants studied except for lycophytes, whose model species *Selaginella* is conspicuously missing miR390 and many tasiRNA biogenesis components from its genome (Banks et al., 2011). Although the miR390-dependent tasiRNA biogenesis pathway is largely conserved in *Physcomitrella*, including its downstream *ARF* targets (Axtell et al., 2007; Talmor-Neiman et al., 2006), some important differences are worth noting. For example, although tasiR-ARF sequences are relatively conserved within seed plants (Allen et al., 2005; Axtell et al., 2006), *Physcomitrella* tasiR-ARFs lack significant sequence similarity to their

seed plant counterparts. This suggests the coevolution of target and sRNA sequences. Much like for the miRNAs described above, the downstream targets of tasiRNAs are evolutionarily fluid. In addition to their conserved *ARF* targets, *Physcomitrella* tasiRNAs also target at least two AP2-family genes (Axtell et al., 2007; Talmor-Neiman et al., 2006), suggesting either a gain of these targets within the moss lineage or their loss in the flowering plant lineage.

Further diversification of the tasiRNA pathway between bryophytes and seed plants is evident, as *Physcomitrella* generates tasiRNAs from *TAS* precursor transcripts targeted by miR156. These *TAS6* loci are arranged in tandem with three of the six *TAS3* loci, presenting the possibility of combinatorial regulation of tasiRNA biogenesis by miR156 and miR390 (Arif et al., 2012). Coregulation may also occur at the level of tasiRNA target silencing. In flowering plants, tasiRNA targets contain two tasiR-ARF complementary sites (Fahlgren et al., 2006; Nogueira et al., 2007; Williams et al., 2005). Although tasiRNA-targeted *ARF* genes in *Physcomitrella* contain only one tasiR-ARF complementary site, their transcripts are also processed by the bryophyte-specific miRNA miR1219 (Axtell et al., 2007). In moss, this combinatorial regulation may provide an extra layer of spatiotemporal control. Moreover, the conserved two-site regulation may allow for cooperativity in sRNA-mediated silencing of tasiR-ARF targets, lending extra robustness to this GRN. Whether such cooperativity between the two sRNA sites exists remains a key question.

The miR390-dependent tasiRNA biogenesis pathway is important for a number of developmental processes in flowering plants. For example, it has been shown to have a role in adaxial–abaxial leaf polarity in *Arabidopsis*, tomato, rice, and maize, with tasiRNAs specifying the adaxial side of the developing leaf by silencing the abaxial determinants *ARF3* and *ARF4* in that domain (Chitwood et al., 2009; Nagasaki et al., 2007; Nogueira et al., 2007; Yifhar et al., 2012). This function is especially crucial in monocots, and the pathway likely has a redundant role in leaf polarity in *Arabidopsis* (for review, see Husbands et al. (2009)). In monocots, tasiRNAs are also important for meristem maintenance, and null mutants in the tasiRNA biogenesis pathway are shoot meristemless (Nagasaki et al., 2007; Timmermans et al., 1998). In *Arabidopsis*, miR390-dependent tasiRNAs are important for lateral root outgrowth (Marin et al., 2010), and it has been proposed that their targets may serve as an integration point for

temporal developmental signals into leaf morphology (Hunter et al., 2003; 2006).

The miR390-dependent tasiRNA biogenesis pathway and its targets roles in development paint a complex picture. There is no easily identifiable cellular process that this pathway regulates in each of the above-mentioned developmental contexts. Furthermore, this pathway is conserved in bryophytes, which lack all of the structures (leaves, roots, layered meristems) whose development miR390-dependent tasiRNAs regulate in angiosperms. This suggest that the miR390-dependent tasiRNA pathway may have been coopted as a useful regulatory circuit, and that much like in the case of *Hh* signaling cooption during butterfly wing spot development, the processes downstream from this pathway are evolutionarily flexible. The fact that tasiRNAs integrate into responses to the phytohormone auxin may therefore be crucial to understanding their pleiotropic effects.

A conserved network for auxin response regulation

Much like the miR390-dependent tasiRNA biogenesis pathway itself, the network regulated by the tasiRNAs—the auxin response GRN—is an excellent model for studying the cooption of developmental networks during the course of plant evolution. Auxin is an ancient molecule. Putative auxin-efflux carriers and members of the auxin-signaling cascade have been identified in Streptophyte algae (De Smet et al., 2011), and auxin was shown to affect embryonic development in the brown alga *Fucus distichus* (Basu et al., 2002). Within flowering plants, the pathway has been coopted for a plethora of developmental processes (Finet and Jaillais, 2012; Guilfoyle and Hagen, 2007). Many of the themes important for GRN cooption discussed above have an important role in the auxin response network. These include mobile signals, sRNA regulation, hierarchical control, and feedback regulation. As such, an understanding of the evolution of auxin responses provides an excellent avenue into elucidating the role of each of these properties in the cooption of GRNs for novel developmental functions.

Auxin signaling proceeds via a baroque and highly regulated pathway. In the absence of auxin signaling, activating ARFs positioned at auxin response elements (AREs) in the promoters of auxin-responsive genes are kept in a repressed state by interacting with Aux/IAA

proteins (Ulmasov et al., 1999a). After entering the cell, auxin facilitates the interaction of its coreceptor TIR1 and related F-box proteins with Aux/IAA proteins, which results in the ubiquitination and degradation of the latter (Tan et al., 2007). As the levels of Aux/IAA proteins in the cell decrease, activating ARFs initiate transcription of auxin-responsive genes. These include members of the Aux/IAA family, establishing a negative feedback loop in the network (for review, see Finet and Jaillais (2012); Guilfoyle and Hagen (2007)). In addition to ARF proteins capable of activating transcription, all land plants contain genes that encode for ARF proteins that act as repressors. These most likely modulate the auxin response by competing with activating ARFs for AREs in the promoters of auxin-inducible genes. This level of regulation may be important to create a robust GRN and stabilize developmental response against short-term fluctuations in auxin levels (Vernoux et al., 2011). Tissue-specific expression of repressive ARFs likely also allows the auxin response to be differentially regulated across various spatiotemporal domains in the developing plant.

In addition to the extensive protein-mediated fine-tuning of the auxin-signaling GRN, many steps in the auxin-signaling cascade are regulated by sRNAs. The auxin receptors *TIR1*, *AFB2*, and *AFB3* are targets for the angiosperm-specific miRNA, miR393 (Parry et al., 2009), and expression of many *ARF* genes is also under sRNA control. A phylogeny of ARF proteins from *A. thaliana*, maize, and *P. patens* (Fig 1.2a) suggests that these may be subdivided into three clades (a recently published phylogenetic tree based on ARF proteins from a more extensive list of species supports this three-clade organization; see (Finet et al., 2012)). Clade A includes the activating ARF proteins from *Arabidopsis* (Guilfoyle and Hagen, 2007) as well as a number of proteins from *Physcomitrella* and maize. Members of this clade in *Arabidopsis* and maize are targeted by miR167 (Wu et al., 2006), which appears to be an angiosperm-specific sRNA (Cuperus et al., 2011). ARF proteins that have re- pressive functions appear to fall into two clades. Nearly all of the genes in clade C are regulated by miR160. Although this clade includes a number of maize genes in which regulation by miR160 has been lost, in all likelihood, ancient members of this clade were miR160 regulated (Fig 1.2a). Clade B contains ARF proteins from *Arabidopsis*, maize, and *Physcomitrella* known to be regulated by miR390-dependent tasiRNAs. Although the possibility that tasiRNA regulation of *ARF* genes evolved indepen-

dently three times during the course of evolution cannot formerly be excluded, the analysis suggests that members of this clade present in ancient land plants were regulated by tasiRNAs, with multiple losses of tasiRNA regulation occurring during the course of evolution. Such loss of tasiRNA regulation would be an example of the *cis*-regulatory sRNA site changes described above. Taken together, the phylogeny indicates that sRNA-mediated regulation of repressive *ARF* genes has likely remained in place during ∼450 million years of evolution.

Despite this high level of conservation within land plants, the developmental role of miR160- and tasiRNA-mediated *ARF* regulation outside of the angiosperms remains unknown. An investigation of the function of the auxin response GRN in the development of nonflowering land plants will be key to understanding the reasons for its repeated redeployment. In mosses, some of the developmental functions of auxin signaling have already been identified. Auxin has a role in controlling growth and cell elongation in *Physcomitrella* as well as in *Arabidopsis* (Chen et al., 2001; Fujita et al., 2008) and induces the formation of caulonemal filaments (Ashton et al., 1979; Johri and Desai, 1973). It is also important for the formation of rhizoid filaments on the leafy gametophore (Sakakibara et al., 2003), and an interplay of auxin and cytokinin signaling regulates the formation of gametophore-forming buds (Aoyama et al., 2012; Ashton et al., 1979).

In the absence of data on the specific functions of auxin response GRN components on moss development, it is tempting to speculate that the extensive repressive regulation and negative feedback in the auxin response GRN, both at the protein and RNA level, may contribute to the cooptability of this pathway. Repressive regulation is known to lend robustness to GRNs and their outputs (Alon, 2006). The multiple inputs into the auxin-signaling network (Middleton et al., 2012) that allow for fine-tuning of the auxin response based on developmental and potentially environmental cues may also make it more amenable to cooption. Finally, signal mobility may have promoted the auxin response GRNs repeated cooption during the course of plant evolution. The transport of auxin is essential during flowering plant development, in which it is necessary for key processes, such as organ initiation, vasculature formation, and apical dominance (Leyser, 2011), to occur. However, the extent to which auxin transport is conserved remains unclear. Polar auxin movement has been shown to occur in

the moss sporophyte, and although no apical-basal auxin transport was observed in the leafy gametophore of many moss species (Fujita et al., 2008), transport within other gametophytic tissues has not been ruled out. In addition to auxin, sRNAs that regulate auxin response also act as a mobile signal (Chitwood et al., 2009; Skopelitis et al., 2012). Interestingly, recruitment of a mobile signal to pattern an evolutionarily novel feature has occurred multiple times in animal development, such as the repeated cooption of *Hh* and *Wnt* described above. The extent to which auxin transport and sRNA movement are conserved across land plants remains to be determined, and the answer to these questions may be key in understanding the reasons for the adaptability of the auxin response GRN.

A broader regulatory question addresses the outputs of auxin signaling across land plants. The connection among the developmental processes for which auxin is responsible in flowering plants and mosses is not immediately apparent; thus, understanding the genes downstream from the auxin response GRN in these two groups is crucial. Are the genes regulated by auxin evolutionarily static, or is auxin signaling a convenient module used to regulate a wide range of cellular processes? Equally important is to understand the developmental and environmental signals that feed into and modulate auxin signaling. Are regulators of auxin signaling—such as ARFs and sRNAs—turned on and off in response to the same upstream signals in bryophytes and flowering plants, or has the plethora of inputs into the auxin response GRN been used to plug in regulators specific to each plant's lifestyle? Clearly, the complexity of the auxin response module makes it an ideal model for understanding cooption and redeployment of GRNs during the course of evolution.

Conclusion and perspectives

The redeployment of existing GRNs and regulatory circuits is an important mode of evolution of novel tissues and organs. This cooption often occurs by changes in regulatory promoter sites, signaling molecule deployment, or sRNA control. The wealth of genomic data available for evolutionarily distant species provides valuable insight into the conservation of individual circuits or networks. However, many key questions about regulatory network cooption and redeployment remain. The conservation of signals that feed into a GRN and

the diversity of downstream processes regulated by a GRN in development across different species remain a mystery. Insights gained from studies of development in flowering plants suggest that inherent robustness and the use of mobile signals are properties that might favor repeated cooption of GRNs during the course of evolution, and sRNA regulation has emerged as an intriguing way to lend these evolutionarily favorable properties to GRNs. The relative importance of these properties and others, such as feedback regulation, in determining which networks are successfully coopted for specific novel functions is in need of further exploration. Finally, coopted GRNs carry considerable baggage, including the factors that feed into the GRN, its outputs, and the internal properties of the network. It is important to understand how evolution selectively changes specific aspects of a newly recruited GRN without perturbing desirable network properties or compromising its functions in other developmental processes. To answer these questions, functional studies must be performed in phylogenetic groups in which conserved GRNs are likely to have divergent roles. Studying complex conserved pathways such as miR390- and miR160-dependent regulation of auxin responses provides an opportunity to simultaneously explore the importance of multiple network properties for cooption. The emergence of new model organisms across the land plants promises that many of these questions can be addressed.

Chapter 2

tasiRNAs regulate protonemal development in *Physcomitrella patens*

Introduction

Comparative developmental studies have revealed repeated cooption of select complex gene regulatory networks throughout evolution (Carroll et al., 2004). The properties that favor the recurring cooption of certain developmental pathways, and the ways in which these are integrated into existing regulatory networks, remain largely unknown. Addressing these questions will require data on the function and properties of such networks across a variety of evolutionary divergent species. The miR390-dependent tasiRNA pathway has been extensively studied in flowering plants, and offers a promising model for studying gene regulatory network cooption. Despite its origin at the base of land plants (Axtell and Bartel, 2005), in flowering plants the miR390-dependent tasiRNA pathway functions in the development of organs—such as leaves and roots—that are seed plant-specific, and have no homologous structures in bryophytes. Thus, elucidating the function of this pathway in mosses may in turn lead to a better understanding of how novel organs evolve, and which network properties are favored by evolution for cooption. Indeed, the properties of this pathway—which include multiple levels of regulatory control, inputs in the form of mobile signals, and a potential role in regulating the response to the ancient hormone auxin—all suggest that it may lend favorable qualities to the developmental processes it controls (see Chapter 1). We therefore decided to explore the developmental function of the miR390-dependent tasiRNA biogenesis pathway in the moss *Physcomitrella patens*, with the goal of gaining insight into its role in this bryophyte and shedding light on its ancient functions and evolution.

Physcomitrella patens is rapidly emerging as the model system of choice for bryophyte genetic and development analyses (Quatrano et al., 2007). It has a short life cycle ($\sim$2 months), can be cultured under laboratory conditions with relative ease, and is amenable to efficient gene targeting, facilitating reverse genetics approaches (Schaefer, 2001). Extensive genomic resources are available for *Physcomitrella*, including a genome sequence (Rensing et al., 2008), small RNA profiling data (Axtell et al., 2007), and extensive expression data. Finally, the function of a number of developmentally important genes has already been uncovered (for example Eklund et al. (2010); Menand et al. (2007b); Okano et al. (2009)), allowing us to link the miR390-dependent tasiRNA pathway with a variety of other regulatory networks.

Bryophytes, like all plants, undergo an alteration of haploid and diploid generations. However, unlike the life cycles of extant vascular plants, their life cycle is haploid-dominant. Moss development (Fig 2.1a) begins with the germination of a haploid spore, which produces filaments called protonema. These protonema elongate via the growth and division of a single tip cell, although older cells also divide to produce side branches. At first, the majority of protonemal cells are chloroplast-rich chloronema, characterized by a crosswall that is perpendicular to the plane of cell division. However, some chloronema later give rise to caulonema, comprised of longer filamentous cells with fewer chloroplasts and a crosswall oblique to the cell division plane (Reski, 1998). These caulonemal filaments can form long runners capable of colonizing a wide area of the substratum around the plant. The timing of caulonemal runner formation depends on the growth conditions, but on BCD media supplemented with diammonium tartrate (BCDAT media) (see Materials and Methods), this usually occurs 2–3 weeks after spore germination, or 1.5–2 weeks after transplantation of a single plantlet from protonemal subculture (Fig 2.1d). Soon after the plant begins producing caulonemal runners, protonema initiate modified side branches that give rise to gametophore buds. These cease tip growth, and instead grow by division of a single tetrahedral apical stem cell (Harrison et al., 2009). The gametophore produces flattened light-capturing phyllids and filamentous anchoring rhizoids. Under short-day and low-temperature conditions, gametophores produce archegonia (containing a single egg cell each) and antherrhidia (containing the swimming sperm typical of non-seed plants). When fertilization occurs, the resulting diploid sporophyte plant is embedded at the tip of the haploid gametophore. The moss sporophyte is dependent on the gametophytic tissue for nutrition and signaling (Reski, 1998). By contrast, in seed plants, the tiny gametophytes are embedded in and nutritionally dependent on the sporophyte. The sporophytes of mosses are determinate, unlike those of their vascular plant counterparts. The *Physcomitrella* sporophyte contains an apical stem cell with two planes of division (Okano et al., 2009). After undergoing a period of growth and differentiation, cells within the sporophyte undergo meiosis, and form haploid spores.

Utilizing the genomic tools developed in *Physcomitrella*, as well as the ability to perform targeted gene replacement, we set out to create moss mutants defective in tasiRNA biogenesis

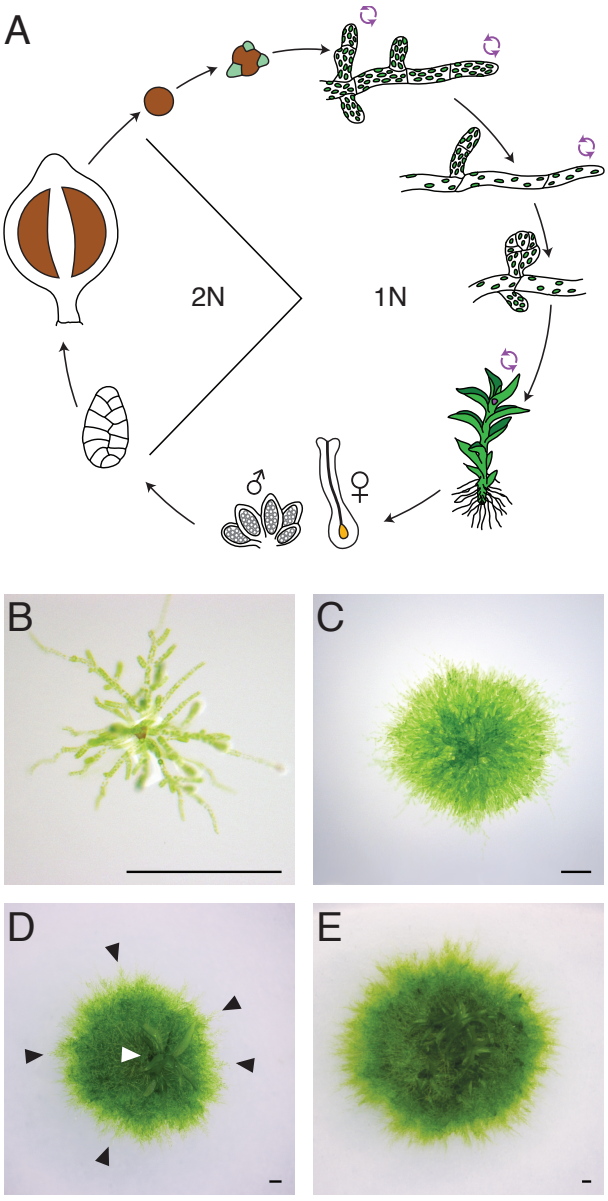

Figure 2.1: An overview of *Physcomitrella* development
(A) Moss development begins with the germination of a haploid spore, which produces protonema comprised mostly of short, chloroplast-rich chloronemal cells. These undergo apical growth through division of an apical cell and branching to produce a dense filamentous network. Some protonemal cells then switch to caulonema, which form long, chloroplast-poor runners that give rise to chloronemal branches. Protonema also give rise to buds, which grow by division of a single tetrahedral stem cell and produce a gametophore. Archegonia and antherrhidia are produced at the gametophore tip. Fertilization results in a diploid embryo embedded within the haploid gametophore. This sporophyte undergoes determinate apical growth. Cells within the sporophyte undergo meiosis and form new spores. **(B)** A six-day-old germinated spore. **(C-E)** Moss plants eight, fifteen, and twenty-two days post-transplantation, respectively. Largely chloronemal growth is visible in (C), with gametophores (white arrowhead) and caulonemal runners (black arrowheads) first appearing in (D). Scalebar = 0.5mm

and to assay the effect of this perturbation on development. We found that the moss homolog of *Suppressor of Gene Silencing 3* plays a conserved role in tasiRNA biogenesis. Perturbation of the tasiRNA biogenesis pathway in *P. patens* results in the upregulation of tasiRNA-targeted *Auxin Response Factor* (*ARF*) genes. It also leads to the loss of caulonemal runners, increased protonemal density as a result of decreased cell size and high-order chloronemal branching, and a decrease in the number of gametophores. The involvement of tasiRNAs in these processes suggests that they may play a role in the temporal regulation of development and in regulating the auxin response.

Results

Creation of *Physcomitrella* tasiRNA biogenesis mutants

In flowering plants, tasiRNA biogenesis proceeds by the miR390-dependent, AGO7-mediated cleavage of a non-coding transcript, TAS3. This triggers the production of a double-stranded RNA by RDR6, which is stabilized by SGS3, and processed by DCL4 into 21-nt tasiRNAs, which are formed in phase with the miR390-dependent cleavage site. These are loaded into another AGO and two of them, the tasiR-ARFs, target ARF transcripts for degradation (Fig 1.3). Many components of the tasiRNA biogenesis machinery are conserved in *P. patens*, including one RDR6, one DCL4, three miR390 precursors, and six TAS3 loci, although there is no clear moss homolog of AGO7 (Arif et al., 2012; Axtell et al., 2006; 2007; Talmor-Neiman et al., 2006). We identified a single *Physcomitrella* homolog of SGS3, Pp1s169_116V6, termed herein PpSGS3 (Fig 2.2a). In the defining XS domain, PpSGS3 shares 67% sequence similarity with AtSGS3 and 69.6% with LBL1. *SGS3* is an essential component of tasiRNA biogenesis in flowering plants (Nogueira et al., 2007; Peragine et al., 2004). Some of the targets of tasiRNAs are conserved in mosses, where tasiRNAs target four ARF genes (Axtell et al., 2007). In addition, tasiRNAs targeting three additional, non-conserved targets—*Apetala2*-domain genes (*AP2a–c*)—are produced in *P. patens* (Talmor-Neiman et al., 2006).

To study the developmental role of the miR390-dependent tasiRNA biogenesis pathway in *Physcomitrella*, we used homologous recombination-based targeted mutagenesis to create plants deficient in tasiRNA biogenesis. We created stable transformants in which the es-

Figure 2.2: Creation of *Ppsgs3* mutant strains
(A) Alignment of XS domains of SGS3 homologs from *A. thaliana*, maize, and *P. patens*. Conserved amino acid identity is highlighted in yellow. **(B)** Diagram of WT (top) and knockout (bottom) *PpSGS3* locus. HR, homology regions for targeted recombination; arrows, positions of primers used in (D). **(C)** diagram of two tandemly inserted knockout cassettes in *Ppsgs3.20*. Homologous regions are shown in black, *AphIV* resistance cassette in white, probe in green. Arrowheads represent restriction sites for *Bgl*II (black) and *Hind*III (white). **(D)** PCR tests confirming targeted transgene insertion in three *Ppsgs3* mutant strains. Green highlighting marks primer pairs from (B) with a product expected only in the case of a targeted recombination event. **(E)** Southern blots performed on *Ppsgs3.20* moss are consistent with a tandem insertion of the transformation cassette at the target site.

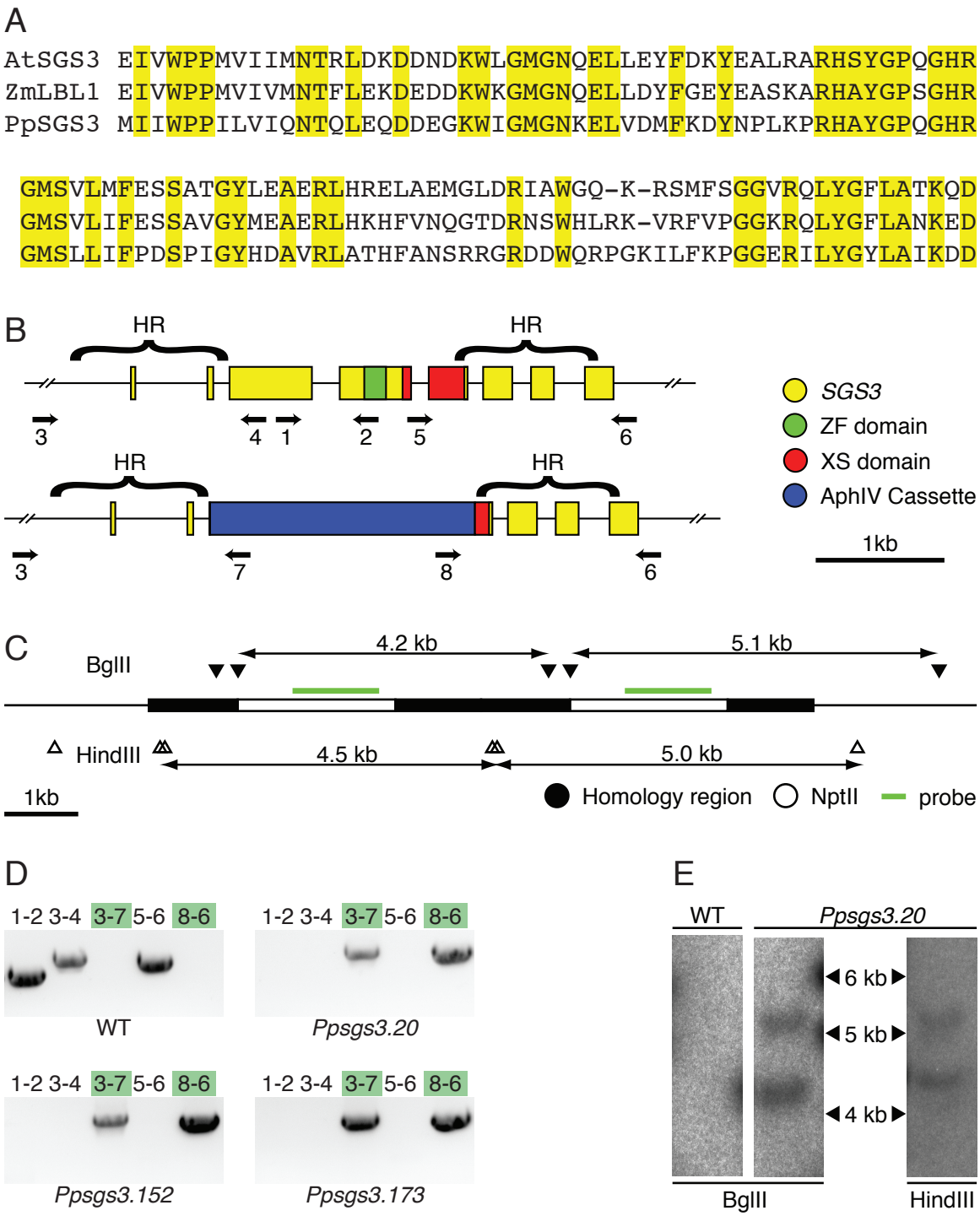
A
AtSGS3 EIVWPPMVIIMNTRLDKDDNDKWLGMGNQELLEYFDKYEALRARHSYGPQGHR
ZmLBL1 EIVWPPMVIVMNTFLEKDEDDKWKGMGNQELLDYFGEYEASKARHAYGPSGHR
PpSGS3 MIIWPPILVIQNTQLEQDDEGKWIGMGNKELVDMFKDYNPLKPRHAYGPQGHR
GMSVLMFESSATGYLEAERLHRELAEMGLDRIAWGQ-K-RSMFSGGVRQLYGFLATKQD
GMSVLIFESSAVGYMEAERLHKHFVNQGTDRNSWHLRK-VRFVPGGKRQLYGFLANKED
GMSLLIFPDSPIGYHDAVRLATHFANSRRGRDDWQRPGKILFKPGGERILYGYLAIKDD
B
HR
HR
3
4
1
2
5
6
HR
HR
3
7
8
6
SGS3
ZF domain
XS domain
AphIV Cassette
1kb
C
BglII
4.2 kb
5.1 kb
HindIII
4.5 kb
5.0 kb
1kb
Homology region
NptII
probe
D
1-2 3-4 3-7 5-6 8-6
WT
Ppsgs3.20
Ppsgs3.152
Ppsgs3.173
E
WT
Ppsgs3.20
6 kb
5 kb
4 kb
BglII
HindIII

Figure 2.2

sential zinc finger-XS domain (Nogueira et al., 2007) of *PpSGS3* is replaced by a cassette with a transgene conferring hygromycin resistance (Fig 2.2b). PCR genotyping using *PpSGS3*-specific primers, as well as primers within the resistance cassette, was used to identify mutants with targeted transgenes (Fig 2.2d), which made up 47% of stable transformants. Southern blot or genomic qPCR was used to screen and eliminate lines carrying additional non-targeted transgene insertions (see Materials and Methods). *Ppsgs3.20* contains tandem insertions of the resistance cassette at the target locus but nowhere else in the genome (Fig 2.2d), while *Ppsgs3.152* and *Ppsgs3.173* contain a single targeted insertion site (data not shown). All three strains displayed similar phenotypes, indicating that the extra insertions of the resistance cassette at the target site of *Ppsgs3.20* did not affect development beyond the effect of the *Ppsgs3* mutation itself. The detailed analyses presented here were performed on *Ppsgs3.20*, unless stated otherwise.

*PpSGS*3 plays a conserved role in tasiRNA biogenesis

In *Arabidopsis*, loss of SGS3 function abolishes the production of tasiRNAs (Peragine et al., 2004). To query the presence of tasiRNA biogenesis in *Ppsgs3* mutants, we performed sRNA qPCR and examined the abundance of miR390 and select tasiRNAs. As miR390 is upstream of SGS3 in tasiRNA biogenesis, no significant difference in miR390 levels was expected between WT and *Ppsgs3* plants, and this is indeed what we observed (Fig 2.3a). However, the levels of tasiRNAs targeting *ARF* transcripts (tasiR-ARFs) and *AP2* transcripts (tasiR-AP2s) are significantly lower in *Ppsgs3* than in WT (Fig 2.3a). The apparent low levels of tasiRNAs persisting in *Ppsgs3* likely reflect the limitations of this technique rather than the presence of residual tasiRNAs. The loss of tasiRNAs in *Ppsgs3* mutants demonstrates the key role of PpSGS3 in tasiRNA biogenesis in *Physcomitrella*.

We next sought to determine the effect of tasiRNA loss on the sRNA-dependent cleavage of target transcripts. In plants, sRNA-dependent repression works primarily via AGO-mediated slicing of the target transcript between the nucleotides complementary to the tenth and eleventh nucleotides of the sRNA (reviewed in Jones-Rhoades et al. (2006)). Given the absence of tasiRNA accumulation in *Ppsgs3* mutants, we examined whether tasiRNA-mediated

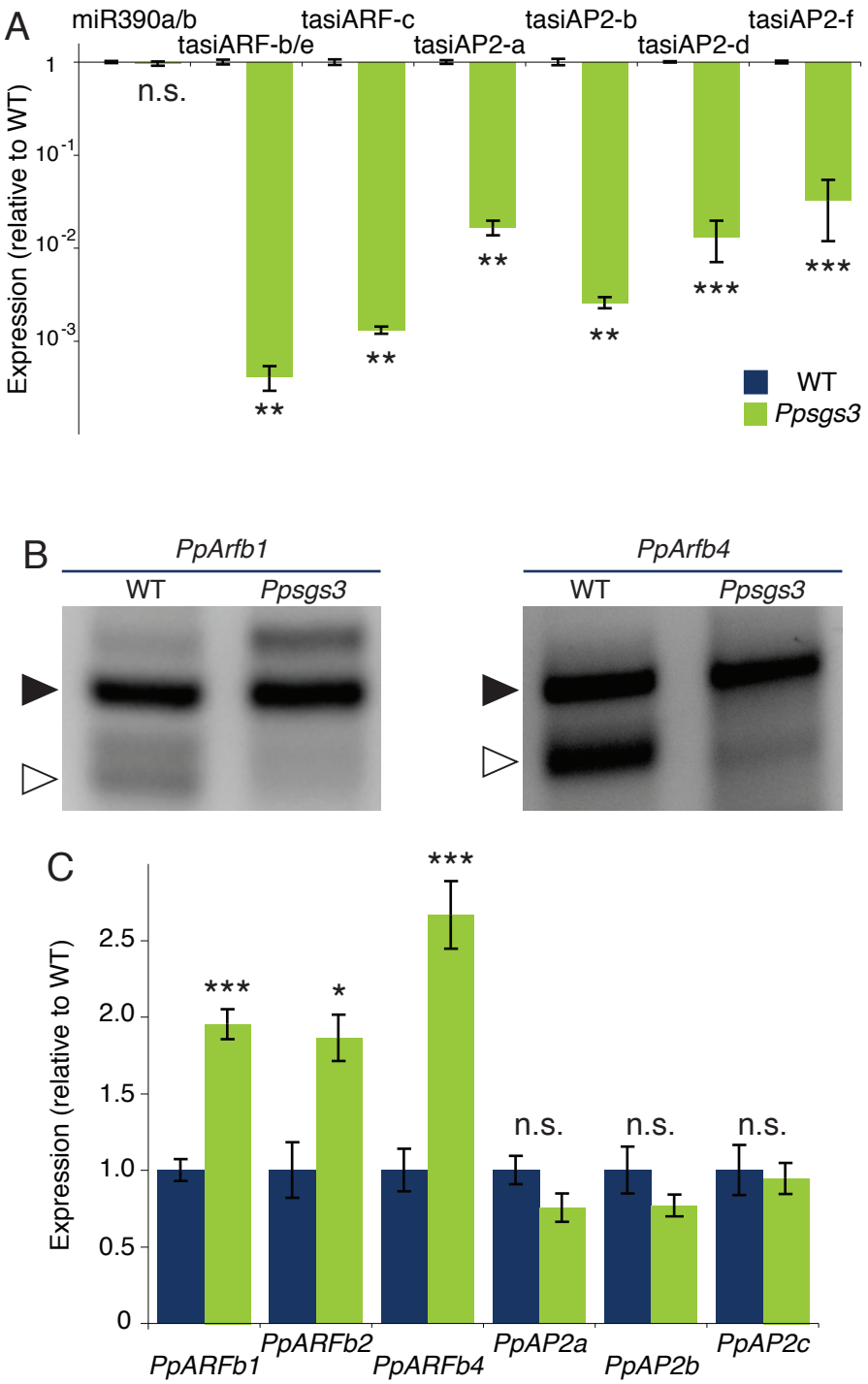

Figure 2.3: Ppsgs3 plants are defective in tasiRNA biogenesis
(A) In contrast to miR390, *TAS3*-derived tasiRNA levels are significantly lower in *Ppsgs3* plants. (B) RLM 5′ RACE demonstrates a loss of tasiRNA-dependent cleavage of *PpARFb1* and *PpARFb4* (white arrow) in *Ppsgs3*, with no change in the level of miR1219-dependent cleavage (black arrow). (C) tasiRNA targets *PpARFb1*, *PpARFb2*, and *PpARFb4* show significantly increased expression in *Ppsgs3*; *PpAP2a-c* show no significant change. *p< .05, **p < .01, ***p < .001

cleavage of target transcripts was abolished. Cleavage sites can be identified using a modified 5′ RACE protocol, RNA ligase-mediated amplification of cDNA ends (RLM 5′ RACE) (Liu and Gorovsky, 1993). We assayed the transcripts of two tasiRNA targets, *PpARFb1* and *PpARFb4*, which have previously been shown to undergo tasiRNA-mediated cleavage. In addition to a tasiRNA-complementary site, these transcripts also contain a site complementary to miR1219, a miRNA not found in vascular plants (Axtell et al., 2007). RLM 5′ RACE on WT moss transcripts shows two dominant cleavage products, consistent with tasiRNA- and miR1219-mediated processing (Axtell et al., 2007; Talmor-Neiman et al., 2006) (Fig 2.3b). A similar analysis of *Ppsgs3* mutant plants demonstrates that, as expected, cleavage products corresponding to the tasiRNA-mediated cleavage site are lost or decreased in level, while products corresponding to miR1219-mediated cleavage remain unaffected (Fig 2.3b).

To determine whether the loss of tasiRNA-mediated cleavage affected target transcript levels, we performed qPCR on 15-day-old plants and measured the expression levels of tasiRNA targets. Of the four tasiRNA-targeted *ARF* genes, *PpARFb3* is expressed minimally in protonema and young gametophores. In *Ppsgs3* plants, all three protonemally expressed tasiRNA-targeted *ARF* genes are upregulated 1.5–3-fold relative to WT levels. Surprisingly, none of the *AP2* genes show significant differences in their expression levels (Fig 2.3c). This may reflect a lack of spatial overlap between tasiRNAs and *AP2ac*.

Taken together, these results demonstrate that *Ppsgs3* plants are defective in tasiRNA biogenesis, and that this defect results in a failure to post-transcriptionally regulate a subset of tasiRNA targets, resulting in increased accumulation of these targets. This indicates that the role of *PpSGS3* in tasiRNA biogenesis is conserved across land plants.

Ppsgs3 mutants display protonemal development defects

To determine the effects of tasiRNA biogenesis loss and target misregulation on *P. patens* development, we characterized the phenotype of *Ppsgs3* mutants throughout their life cycle (Fig 2.4). *Ppsgs3* produce both sporophytes and viable spores, and display no obvious defects in gametophore morphology (Fig 2.4a–f). We observed a significant decrease in the rate of gametophore initiation in *Ppsgs3*. In WT plants, gametophore buds with phyllids first

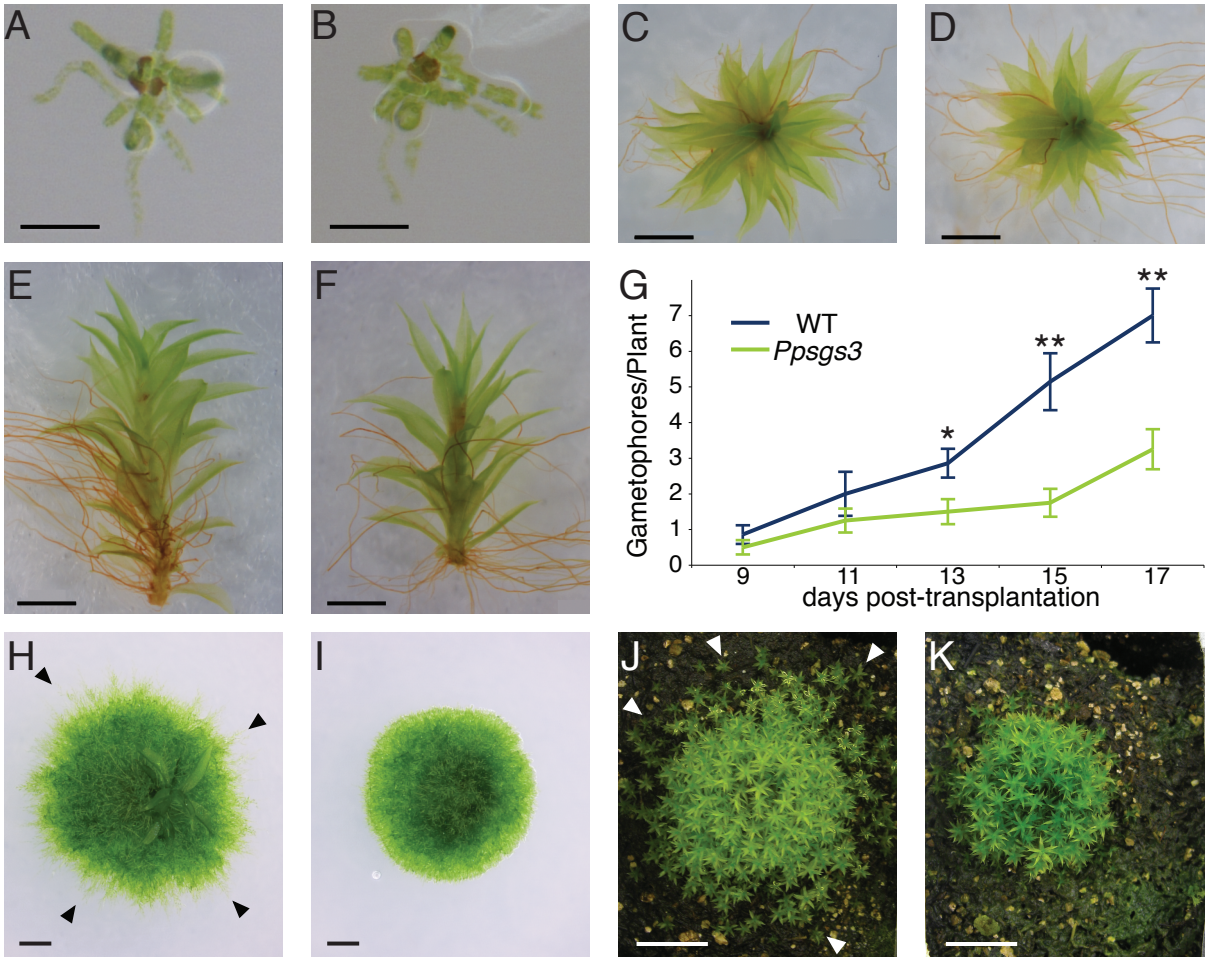

Figure 2.4: *Ppsgs3* affects caulonemal runner and bud formation
(A-B) Four- to six-day-old spores of WT (A) and *Ppsgs3* (B), showing that *Ppsgs3* spores are viable. Scalebar: 0.1mm **(C-F)** WT (C, E) and *Ppsgs3* (D, F) gametophores grown for ~1 month on BC(D) media are morphologically indistinguishable. Scalebar: 1mm. **(G)** Gametophore initiation is decreased in *Ppsgs3*. *p < .05, **p < .01 **(H-I)** 15-day-old WT (H) plants grown on BCDAT media form caulonemal runners (black arrowheads), whereas *Ppsgs3* (I) plants of the same age fail to form caulonemal runners. Scalebar: 1mm **(J-K)** Early phenotypes of *Ppsgs3* result in defects in adult plants. Following ~2 months growth on soil, WT plants (J) often form 'satellite' gametophores away from the main plant (white arrowheads). *Ppsgs3* plants (K) form far fewer satellite gametophores, have a more compact plant size, and appear greener. Scalebar: 1cm

Figure 2.4

start to appear around day 9 post-transplanation, and are located primarily at the center of the plant. Their numbers increase with time, and around the end of the third week post-transplantation, gametophore buds begin forming at the periphery of the plant, potentially on young caulonemal runners. We observe a decrease in the number of gametophore buds with phyllids in *Ppsgs3* plants as early as 13 days post-transplantation (Fig 2.4g).

Protonemal development is also perturbed in *Ppsgs3* mutant plants, which form denser chloronemal networks than their WT counterparts. Additionally, the *Ppsgs3* protonemal mat maintains a smooth, circular shape. By contrast, by day 15 post-transplantation the caulonemal runners of WT plants extend beyond the edges of the protonemal mat, creating a rough appearance (Fig 2.4h–i). The *Ppsgsg3* protonemal phenotype reflects the failure of these mutants to form caulonemal runners. It is important to note that careful dissection of *Ppsgs3* protonema revealed some cells with cross-walls oblique to their plane of division, a feature characteristic of caulonemal cells, suggesting that runners may represent a unique caulonemal subtype specifically lost in *Ppsgs3*.

Caulonemal runners typically form in moss plants $\sim$2 weeks post-transplantation (Fig 2.1d). We tested whether the lack of caulonemal runners in *Ppsgs3* results from a developmental delay by scoring for their presence in WT and *Ppsgs3* moss grown on media for extended periods of time ($>$2 months). We do not observe caulonemal runner formation in *Ppsgs3* even after this extended growth period. Thus, the absence of caulonemal runner formation in tasiRNA biogenesis mutants is not the result of a developmental delay.

To understand the function of tasiRNA-mediated developmental regulation in their natural environment, we tested the effects of the *Ppsgs3* mutation in moss grown on soil, which is a more ecologically relevant substratum than BCDAT media. It is not possible to directly observe protonemal development on soil; however, single 'satellite' gametophores growing apart from the main gametophore tuft can be used as a proxy to indicate the position of caulonemal runners. Two months after transplantation to soil, WT *P. patens* have a central tuft of gametophores, $\sim$2cm wide, usually surrounded by a multitude of satellite gametophores. By contrast, *Ppsgs3* plants have a smaller central tuft and few, if any, satellite gametophores (Fig 2.4j–k). This indicates that the loss of caulonemal runner formation observed in *Ppsgs3* plants

on BCDAT media also occurs in soil-grown plants, and that it impacts their ability to colonize distant substratum.

In addition to a loss of caulonemal runners and a decrease in gametophore formation, we noted an increase in the density of the protonemal networks of *Ppsgs3* plants. Two possible causes can be envisioned for this phenotype. A decrease in cell size or an increase in branching could both result in a denser appearance. To assess these possibilities, we assessed branching and cell size in *Ppsgs3* and WT protonema. To characterize branching in WT protonema, we assessed how many chloronemal cells produced a branch. 'Main filaments' of protonema, which extend from the center of the plant out towards its periphery, display a stereotyped pattern of branching, producing one or occasionally two branches at nearly every cell along the filament (Fig 2.5a, c). In addition, a subset of cells along these primary branches form secondary branches, but tertiary branches are rarely observed (Fig 2.5c). This result shows that not all chloronemal cells are equally potent in their ability to form a branch, and that protonemal branching is effectively determinate, with a progressive loss of competence as branching order increases. Although high variability in branching frequency makes a quantitative comparison of branching levels between WT and *Ppsgs3* difficult, *Ppsgs3* filaments showing exceptionally high numbers of secondary and tertiary branches were common. One such filament is shown (photograph—Fig 2.5b, diagram—Fig 2.5d). This filament shows more secondary branches than the WT filament, and the *Ppsgs3* secondary branches are longer (contain more cells) than their WT counterparts. The number and length of tertiary branches is also increased. On *Ppsgs3* branches close to the center of the protonemal mat, quarternary branches can regulary be observed, which are very rarely detected in WT plants. The extensive branching pattern of the primary branch of the 29th *Ppsgs3* filament cell shown in Fig 2.5d suggests that with respect to branching, this branch is behaving as a main filament, rather than as a branch cell. These data suggest that loss of tasiRNA biogenesis results in a partial loss of determinacy in protonemal cells.

In addition, we measured the cell length in the 3rd, 4th, and 5th cells of 7–10 chloronemal filaments in *Ppsgs3* and WT. We observed a significant $\sim$6% decrease in chloronemal cell length in *Ppsgs3* plants (Fig 2.5e). Together, these results indicate that the increase in protone-

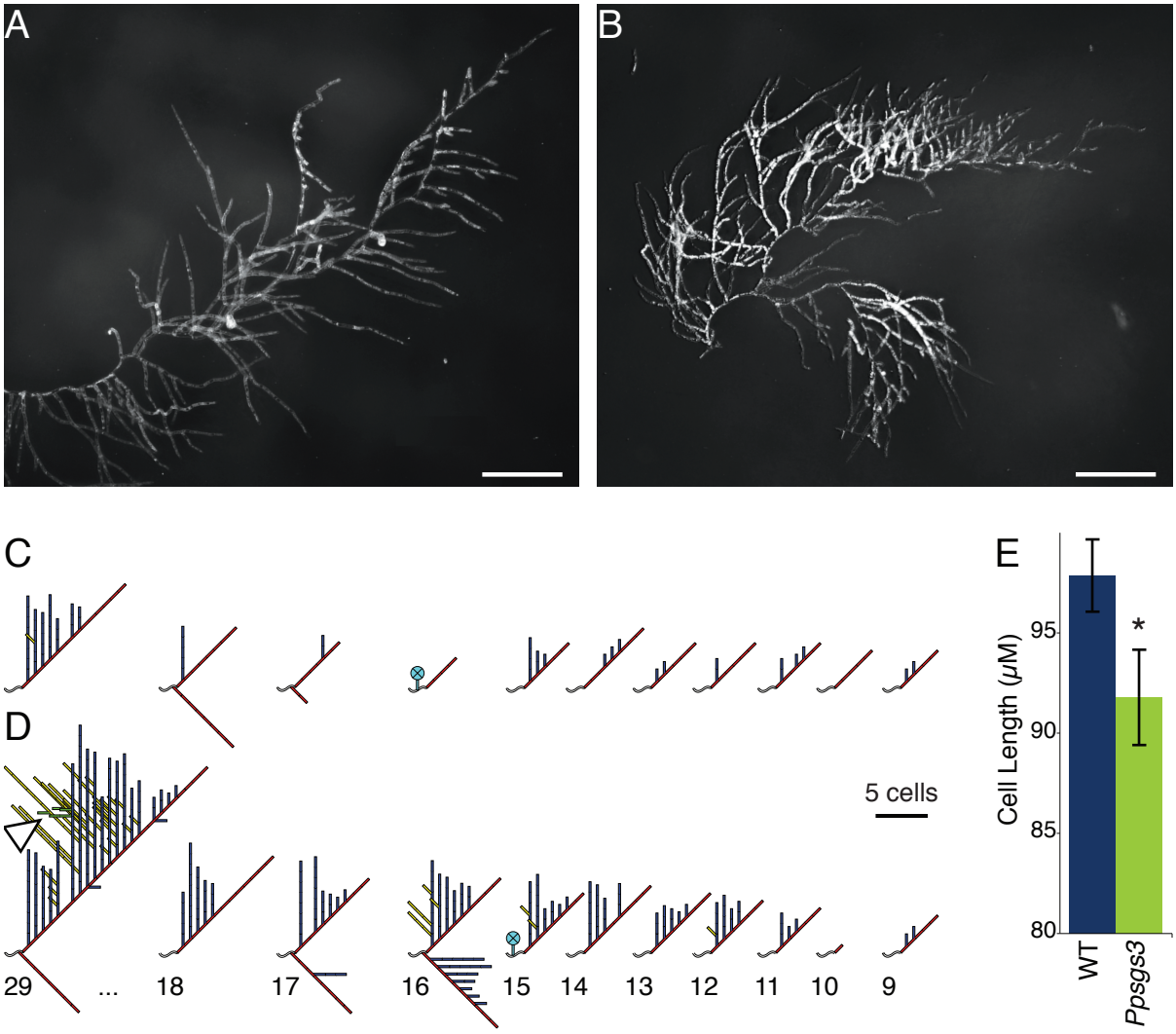

Figure 2.5: *Ppsgs3* protonema display high levels of branching and decreased cell length

(A-B) Primary filaments from ~3-week-old WT (A) and *Ppsgs3* (B) plants, with the growing tip of the primary filament in the top right of each photo. *Ppsgs3* shows an increased number of branches along the primary filament. Scalebar = 0.5mm. **(C-D)** Branching patterns of the cells along the filaments shown in (A) and (B), respectively, between cells 9-18 from the tip cell, as well as at cell #29 from the tip, close to the center of the protonemal mat. Wavy white lines represent cells of the main filament; red lines - primary branches; blue lines - secondary branches; yellow lines - tertiary branches; green lines - quarternary branches (white arrow-head); and cyan circles represent gametophore buds. Branch lengths are proportional to the number of cells in the branch. WT filaments (C) typically have fewer secondary, tertiary, and quarternary branches than *Ppsgs3* filaments (D). **(E)** Chloronemal cells in *Ppsgs3* filaments are shorter than in WT, $p < 0.05$. $n > 20$ cells.

Figure 2.5

mal density observed in *Ppsgs3* results from increased branching and decreased protonemal cell size in tasiRNA biogenesis mutants.

Our results indicate that *Ppsgs3* mutants are defective in protonemal development. These defects include decreased chloronemal cell size and increased branching, likely as a consequence of a loss of chloronemal determinacy, as well as an absence of caulonemal runners. We also observe a decrease in the formation of gametophore buds in *Ppsgs3*. A decrease in caulonemal runner number can indirectly result in lower gametophore bud formation, since buds often form on caulonemal runners. However, the decrease in bud numbers in *Ppsgs3* can be observed at a developmental stage when bud formation does not yet occur on caulonemal runners, as it does later in development. Thus the reduction in gametophore initiation in *Ppsgs3* plants is likely to be uncoupled from their caulonemal defect.

Temporal expression pattern of tasiRNAs and tasiRNA targets

In *Arabidopsis*, tasiRNA biogenesis mutants, including *sgs3*, display defects in developmental timing. This manifests itself in the precocious appearance of mature traits, such as abaxial trichomes and elongated leaf shape (Hunter et al., 2006). Protonemal development in *Physcomitrella* is also temporally regulated, with runners and gametophore buds beginning to appear $\sim$1.5–2 weeks after the transplantation of individual plantlets onto media (Fig 2.1d). Since our data point to tasiRNAs as regulators of these processes, we asked whether tasiRNAs might similarly control developmental timing in *Physcomitrella*. However, in contrast to *Arabidopsis*, where tasiRNAs maintain juvenile traits, the *Ppsgs3* phenotypic data suggest that tasiRNAs may promote maturation in moss.

Phenotyping experiments, such as the ones described above, are typically performed by subculturing moss protonema on cellophane-overlaid plates 3–5 times by homogenizing the tissue, and transplanting individual plantlets onto solid media 5 days after the final subculture. To explore the possibility of *Physcomitrella* developmental timing regulation by tasiRNAs, we monitored the levels of tasiRNAs, miR1219, and their targets throughout moss development following the transplantation of individual plantlets (Fig 2.6), focusing specifically on those targets that were upregulated in *Ppsgs3*. sRNA and target levels were analyzed in

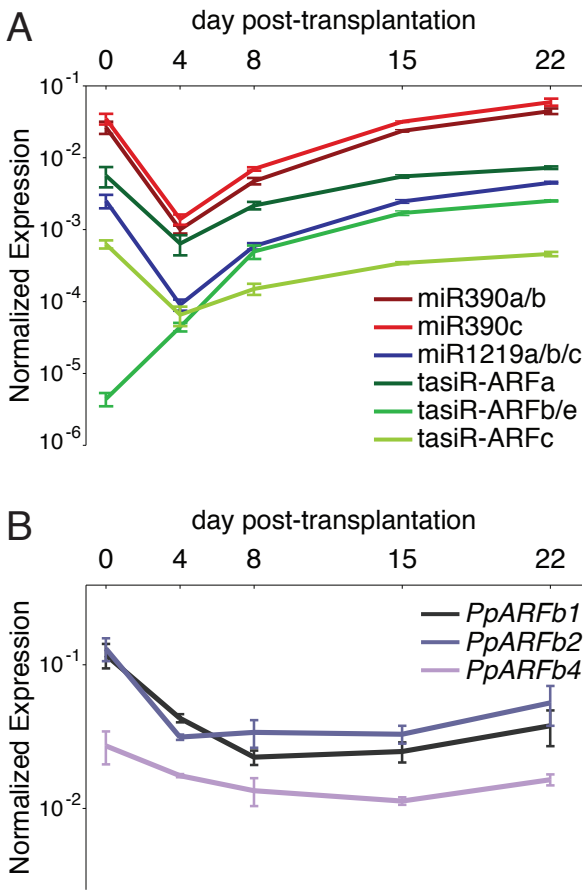

Figure 2.6: Temporal expression pattern of sRNAs and tasiRNA targets
(A) Expression levels of miR390, miR1219, and tasiRNAs rise dramatically between day 4 and day 22 post-transplantation. **(B)** Expression levels of tasiRNA-targeted *PpARF* genes over the same timecourse. Temporal changes in tasiRNA-targeted *PpARF* genes are more subtle than what is observed for tasiRNAs and miR1219.
All expression values were normalized to U6 in (A) and GAPDH in (B). n = 3. "day 0" denotes 5-day-old cellophane-subcultured protonema.

Figure 2.6

subcultured protonema grown for 5 days on cellophane-overlaid media ('day 0'), as well as in plantlets transplanted individually onto solid BCDAT media and grown for 4, 8, 15, and 22 days.

qRT-PCR analyses of miR390, miR1219, and tasiR-ARFs from four *TAS3* loci, including the most abundant one, *TAS3a*, showed an increase in expression between day 4 and day 22 post-transplantation (Fig 2.6a). This increase is quite dramatic, varying between ∼10-fold for tasiR-ARFa and tasiR-ARFc and 40–60-fold for the other sRNAs. These data also provided us with key information for future experiments. Protonemal tissue grown on cellophane plates is commonly used to quantify gene expression in moss (for example, Cho et al. (2012); Prigge et al. (2010), among many others). Levels of most sRNAs and protein-coding transcripts tested are much higher in cellophane-grown tissue than in any of the whole-plant tissue we collected. This convinced us of the importance of assaying gene expression in the developmental contexts in which we observe our phenotypes, namely in individual solid media-grown plantlets. Cellophane-grown samples were thus excluded from our further analyses and from additional experiments.

Temporal changes in tasiRNA target levels are ambiguous, and generally fail to reflect the strong increase in tasiR-ARF and miR1219 expression over developmental time (Fig 2.6b). *PpARFb1* has a significant ∼2-fold decrease in expression between day 4 and day 8 of development, and *PpARFb4* decreases significantly between day 4 and day 15. However, despite an increase in tasiR-ARF and miR1219 levels, both *PpARFb1* and *PpARFb4* approach their day 4 expression levels by the third week post-transplantation. One possible explanation for these observations is that the increase in sRNA levels occurs in a spatial domain that does not overlap with the expression domain of the tasiRNA targets. Overall, these results do not strongly support or refute the hypothesis that tasiRNAs may play a role in the regulation of developmental timing.

Discussion

Conservation of tasiRNA biogenesis components

Previous studies in *Physcomitrella* have identified homologs of many tasiRNA biogenesis components, including miR390, *TAS* loci, *DCL4* (Axtell et al., 2007), and *RDR6* (Talmor-Neiman et al., 2006). Here, we report the identification of another conserved component, *SGS3*, and show it is required for the biogenesis of tasiRNAs in moss. Interestingly, a previous study failed to identify the *Physcomitrella* homolog of *AGO7* (Axtell et al., 2007), a critical tasiRNA biogenesis component in *Arabidopsis* (Hunter et al., 2006), maize (Douglas et al., 2010), and rice (Nagasaki et al., 2007). AGO7 plays a highly specialized role in tasiRNA biogenesis in *Arabidopsis*, associating almost exclusively with miR390 to cleave the *TAS3* transcript and trigger downstream tasiRNA production (Mi et al., 2008; Montgomery et al., 2008). In *Arabidopsis*, miR390 is likely sorted into AGO7 and another AGO, AGO2, due to its 5′ Adenine. Although the 5′ Adenine is conserved in the two most abundant miR390 species of *Physcomitrella*, AGO2 and AGO3—both members of the same clade as AGO7—are also missing from moss (Axtell et al., 2007). These findings demonstrate that *Physcomitrella* AGO genes fall into only two of the three plant *AGO* clades. Future research will be critical for determining which moss AGO functions in place of AGO7 to initiate tasiRNA biogenesis, and whether that AGO similarly forms exclusive complexes with miR390 to effect its function. Another important evolutionary question is whether members of the specialized *AGO7* clade were present in the common ancestor of all plants and then lost in mosses, or whether this gene evolved after the appearance of the vascular plants. Examining *AGO* sequences from other bryophytes, such as liverworts or hornworts, may help address this question.

In *Physcomitrella*, every gene encoding a protein component of the tasiRNA biogenesis pathway is present in one copy (Axtell et al. (2007); Talmor-Neiman et al. (2006); and this study), despite a recent genome duplication in the moss (Rensing et al., 2008). A similar phenomenon is observed in maize, which has also had a recent genome duplication (Schnable et al., 2009). One possible interpretation of these findings is that there is selective pressure to maintain tasiRNA biogenesis components as single-copy genes. Importantly, in maize, sRNA

pathway genes that are not involved in tasiRNA biogenesis are present in multiple copies. For example, most *AGO* genes, with the noteable exception of *AGO7*, are present in the genome in pairs of paralogs (Marcela Dotto, personal communication). This suggests that the pressure to maintain sRNA biogenesis components as single-copy genes is specific to the tasiRNA biogenesis pathway.

Despite its origins at the base of land plants and high degree of conservation across embryophytes, the miR390-dependent tasiRNA biogenesis pathway is entirely missing in *Selaginella moellendorfii* (see Banks et al. (2011) and Chap 1). It is not known whether the loss of this pathway is evolutionarily recent, or occurred at the base of the lycophyte lineage, although future genome sequencing in *Lycopodium*—a lycophyte genus evolutionarily distant from *Selaginella*—may address this. sRNA control over *ARF* expression is not entirely lost in *Selaginella*, however, as its genome still encodes miR160, an ancient miRNA that regulates Clade C *ARF*s.

tasiRNAs regulate the development of a complex tissue type

Moss protonema are usually described as a simple tissue, consisting of a mix of caulonema, chloronema, and gametophore-derived rhizoids (Bopp, 1980). The 'stem cell-like' tip cells have been further singled out as representing a unique cell type, with little research on the developmental heterogeneity of other protonemal cells. Our results uncover additional complexity in protonemal development. *Ppsgs3* mutant plants demonstrate multiple protonemal defects, the most striking of which is an absence of caulonemal runners. However, these plants produce protonemal cells with caulonema-like oblique crosswalls. These observations may be reconciled if caulonema do not become runners in *Ppsgs3* because they are more determinate. However, the increase in branching in *Ppsgs3* instead suggests a decrease in protonemal determinacy. I thus favor an alternate explanation, whereby the caulonemal runners absent in *Ppsgs3* represent just one of a number of distinct caulonemal cell types. Together with the observed increase in chloronemal branching, this finding may contribute to a more sophisticated view of protonemal development in *Physcomitrella* than is often presented. We propose that the protonema is a complex tissue that consists of cells at various levels of indeterminacy

and branching competency, as well as with distinct differentiation states at different positions along the chloronema–caulonema spectrum. Interestingly, tasiRNAs appear to regulate multiple dimensions of this differentiation space, specifically chloronemal indeterminacy and the specification of caulonemal runners.

Previous studies have shown accelerated bud formation in tasiRNA biogenesis-defective *Pprdr6* mutant plants, suggesting that tasiRNAs may play a conserved role in maintaining juvenile developmental characteristics across land plants (Cho et al., 2008; Talmor-Neiman et al., 2006). Inversely, we found that gametophore bud initiation is decreased in *Ppsgs3* plants. This discrepancy could indicate non-overlapping functions of PpRDR6 and PpSGS3. Interestingly, *Ppdcl3* mutant plants also have increased gametophore production. PpDCL3 is not involved in tasiRNA biogenesis, but is necessary for the production of 22–24 sRNAs, a process that PpRDR6 likely contributes to (Cho et al., 2008). These data suggest that the accelerated gametophore formation observed in *Pprdr6* may be the result of 22–24 nt sRNA loss, rather than the loss of tasiRNAs. An exploration of gametophore formation in moss lines with sRNA-resistant tasiRNA targets is necessary to resolve the role of tasiRNAs in gametophore formation.

tasiRNAs as temporal regulators of development

tasiRNAs are important for the regulation of developmental timing in *A. thaliana*, where they are thought to set a threshold that must be passed in order to begin a mature developmental program. tasiRNA biogenesis mutants thus demonstrate precocious expression of the mature program (Hunter et al., 2003). By contrast, tasiRNA biogenesis mutants in maize do not display precocious developmental phenotypes. Previous studies had reported precocious gametophore bud initiation in a *Physcomitrella* tasiRNA biogenesis mutant (Talmor-Neiman et al., 2006). However, our data contradicts this, indicating instead that tasiRNAs in moss are required for the expression of adult developmental programs, such as the initiation of gametophore buds and caulonemal runners. Nonetheless, because the developmental processes affected in *Ppsgs3* mutants are temporally regulated in moss, we explored the possibility that tasiRNAs are playing a role in regulating the timing of moss development. tasiRNAs, miR390, and miR1219 are all strongly upregulated as development proceeds, hinting at a role

for these sRNAs in developmental progression, although we cannot exclude the possibility that this temporal expression pattern is a general property of sRNAs in *Physcomitrella*. In order for temporal changes in sRNA levels to drive developmental transitions, they must be reflected in temporal changes in target levels; however, the expression levels of *PpARFb1*, *2*, and *4* change only moderately, if at all, over the course of plant development. Our results are thus inconclusive with respect to tasiRNA-mediated regulation of developmental transitions in *Physcomitrella*, and further research will be required to disambiguate their role as temporal regulators of moss development.

Regulation of *ARF* genes by tasiRNAs in moss

Our results demonstrate a conserved role for *SGS3* in tasiRNA biogenesis across land plants. Perturbation of tasiRNA biogenesis in *Ppsgs3* leads to an increase in the levels of *PpARFb1*, *PpARFb2*, and *PpARFb4* transcripts. This shows that tasiRNAs are key regulators of these repressive *ARF* genes in early moss development. Transcripts of all three genes are 1.5–2.5-fold higher in *Ppsgs3* plants than in WT, a level of upregulation that is consistent with what is seen in *Arabidopsis* and maize (Nogueira et al., 2007; Peragine et al., 2004). This modest change in transcript levels may underestimate the upregulation of PpARFb1,2, and 4 proteins, since tasiRNAs may act partially through translational repression of their targets. For example, in *Arabidopsis*, an abrogation of tasiRNA regulation causes drastic changes in AtARF3 protein expression levels (Chitwood et al., 2009), despite only a $\sim$2-fold increase in transcript levels. Translational reporters of tasiRNA targets are necessary in *Physcomitrella* to fully assess the impact of sRNA regulation on PpARF levels. Nevertheless, even subtle changes in expression level could have dramatic effects on phenotype, especially if they result in the misexpression of the target in a cell type that it is not normally found in.

In contrast to the changes we observed in *ARF* gene expression, the levels of tasiRNA-targeted *AP2* genes are not significantly altered in *Ppsgs3* mutants. This is surprising since a previous study found that one of these genes, *PpAP2c*, was expressed at a higher level in cellophane-grown *Pprdr6* tissue than in WT tissue (Talmor-Neiman et al., 2006). The absence of an increase in *PpAP2c* levels in our study likely reflects differences between the tissue types

in which expression levels were assayed: for example, tasiRNAs and their target *AP2* genes may be coexpressed in cellophane-grown protonema but not in individual 15-day-old plants.

Ecological perspective on tasiRNA function

Environmental signals—including light levels and substratum nutrient content—regulate caulonemal runner growth and bud formation in moss (Reski, 1998). Our results demonstrating a role of *Ppsgs3* in these processes raise the intriguing possibility that tasiRNAs may contribute to the modulation of moss development in response to its environment. For plants, which are sessile, the ability to respond to environmental cues by adjusting development is essential. Our data hint that such adjustments may occur via an ancient genetic network, which evolved at the same time that plants first colonized land and began to struggle with many of the environmental challenges of this new habitat. However, further work will be needed to address the role of tasiRNAs in regulating developmental response to the environment in *Physcomitrella*.

The phenotype of *Ppsgs3* plants grown on soil suggest that these mutants' protonemal defects, especially the plants' failure to produce caulonemal runners, would likely impact their fitness in the wild. Caulonema allow WT plants to spread through the substratum, and as our soil experiments show, caulonema-derived gametophores form at sites distant from the central plant. Since in the wild, gametophores go on to bear the gametangia and spore-producing sporophytes, such spreading is essential for sperm and spore dispersal. Perhaps more importantly, it may allow plants that germinated on nutrient-poor patches of soil to spread to more favorable nearby locations. The absence of caulonemal runners in *Ppsgs3* plants prevents them from colonizing distant areas of the substratum. As a result, these plants' gametophores are concentrated on small patches of soil, competing for a limited set of resources and unable to expand. tasiRNA biogenesis is thus likely to be crucial for plant fitness in the wild, especially in nutrient-poor or other high-stress conditions.

Auxin signaling as a target for tasiRNA regulation

tasiRNAs exert their effect on development by regulating the expression of target genes;

in moss, these include four *ARF* genes and three *AP2*-domain transcription factors. It remains to be determined which of tasiRNA targets are responsible for the phenotypes observed in *Ppsgs3* mutants.

In flowering plants, AP2-domain transcription factors have been identified as key regulators in a number of developmental processes, particularly the regulation of flowering time and floral organ development (Rosin and Kramer, 2009). A number of *AP2*-domain genes were found to regulate bud formation in *Physcomitrella* (Aoyama et al., 2012); however, none of these are tasiRNA targets. Our data indicate that tasiRNAs limit the expression of *ARF* genes. The role of *ARF* genes in *Physcomitrella* development has also not been explored; however, in *Arabidopsis*, *ARF* genes are involved in the regulation of the auxin response network (Middleton et al., 2012).

We noted that auxin regulates many of the same processes that are perturbed in *Ppsgs3* mutants. The role of auxin in *Physcomitrella* development has been extensively studied (Ashton et al. (1979); Jang and Dolan (2011); Johri and Desai (1973); Prigge et al. (2010); Sakakibara et al. (2003) among many others). For example, it has long been known that auxin application induces caulonemal formation (Ashton et al., 1979; Johri and Desai, 1973). Additionally, gametophore bud initiation is regulated by a fine balance between auxin and cytokinin signaling, and when this balance is perturbed, gametophore formation is affected (Aoyama et al., 2012). The high level of overlap between the developmental processes under tasiRNA control and those regulated by auxin points to a potential mechanism by which tasiRNAs can affect development. The defects observed in *Ppsgs3* plants may be due to aberrant auxin signaling, perhaps as a result of *ARF* misregulation.

Chapter 3

tasiRNAs regulate protonemal development by silencing repressive *ARF* genes.

Introduction

The developmental processes perturbed in *Ppsgs3* mutants are known to be regulated by auxin signaling. Auxin (primarily indole-3-acetic acid, IAA) plays a key role in plant development by regulating the expression of auxin-responsive genes. Work in *Arabidopsis* has uncovered the molecular mechanism of this regulation (reviewed in Finet and Jaillais (2012)). The promoters of these genes are bound by 'activating' ARF transcription factors, but in the absence of auxin, Aux/IAA proteins heterodimerize with these activating ARFs to block transcription. In the presence of auxin, Aux/IAAs are degraded via TIR1/AFB-family receptors, leading to the induction of auxin-responsive gene expression (see Chap 1 and Fig 3.1).

In mosses, auxin plays an important role in protonemal development, especially in branching suppression and the induction of caulonema (Johri and Desai, 1973). A collection of *Physcomitrella* mutants resistant to synthetic auxin (1-napthalene-acetic acid, NAA) treatment demonstrated phenotypes that included an absence of caulonema and, in some cases, a decrease in gametophore bud formation (Ashton et al., 1979). Seven of the strongest mutants were found to harbor lesions in the three *Physcomitrella Aux/IAA* genes. These mutations prevent the auxin-dependent degradation of Aux/IAA proteins, rendering the plant unable to respond to auxin signaling (Prigge et al., 2010). In addition, moss plants carrying mutations in *DIAGEOTROPICA*, which has a conserved role in auxin signaling, are also defective in caulonema formation (Prigge et al., 2010). This auxin-dependent formation of caulonema occurs via the induction of auxin-regulated *PpRSL1* and *PpRSL2* (Jang and Dolan, 2011), whose homolog *RHD6* regulates auxin-induced root hair formation in *Arabidopsis* (Menand et al., 2007b) (see Chap 1).

The similarity between the phenotypes of *Ppsgs3* plants and auxin signaling mutants is particularly intriguing considering the upregulation of tasiRNA-targeted *ARF* genes in *Ppsgs3*. *ARF* genes have been grouped into activators (group A) or repressors (groups B and C) (Finet et al., 2012; Ulmasov et al., 1997; 1999a). The binding of 'repressive' ARF proteins to the promoters of auxin-responsive genes can repress the transcription of the latter (Ulmasov et al., 1997; 1999a;b) (Fig3.1c). In *Arabidopsis*, tasiRNAs target *AtARF2-4*, which are repressive (Ti-

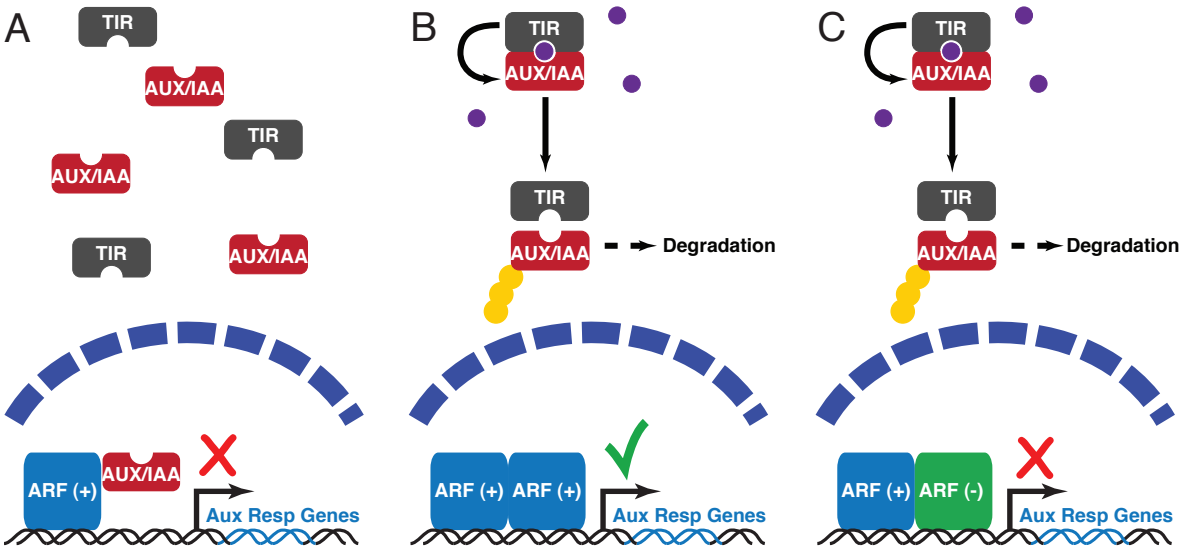

Figure 3.1: The auxin response pathway
(A) Aux/IAA repressors associate with activating ARF transcription factors (blue boxes), preventing the transcriptional activation of auxin-responsive genes. **(B)** In the presence of the phytohormone auxin (purple circle), TIR-family F-box ubiquitin ligases bind auxin and Aux/IAAs, ubiquitinating the latter and targeting them for degradation. This allows activation of auxin-responsive genes. **(C)** Repressive ARF proteins (green boxes) repress the activation of auxin-responsive genes in an auxin-independent manner.

Figure 3.1

wari et al., 2003). Phylogenetic studies show that the *Physcomitrella* tasiRNA targets are also members of group B of repressive *ARF*s. (see Chap 1; Finet et al. (2012)).

Both expression data and the nature of the *Ppsgs3* phenotype pointed to the possibility that misregulation of *ARF* genes was responsible for the developmental defects we observed in these plants. We sought to test whether this was the case by directly probing the developmental effects of *PpARFb* misregulation. In flowering plants, *ARF* genes have diverse developmental roles (for example, Hardtke (1998); Mallory et al. (2005); Pekker et al. (2005)), with different family members regulating the auxin response in distinct spatiotemporal contexts (Rademacher et al., 2011). Nothing is known about the mechanistic roles of the ARFs in regulating auxin response in moss, or about individual *ARF* genes' contribution to moss development. Detailed examination of the roles of ARFs in *P. patens* development may provide a basis for an evolutionary comparison of their developmental function between mosses and angiosperms. Investigations of *ARF* function in moss may also yield further insights into the mechanisms of auxin response across land plants.

In this chapter, we show that moderate levels of overexpression of *PpARFb2* and *PpARFb4* results in phenotypes similar to those observed in *Ppsgs3*. These phenotypes are also observed when sRNA control of endogenous *PpARFb4* is abolished. Our data indicate that tasiRNAs act partially redundantly with miR1219 to limit *PpARFb4* expression to the growing edge of the protonemal mat to regulate caulonemal runner formation.

Results

The *Ppsgs3* phenotype is consistent with a repression of auxin signaling

The phenotypic similarities between *Ppsgs3* and known auxin-insensitive mutants led us to investigate a connection between tasiRNA biogenesis and auxin signaling. Protonemal development is very sensitive to environmental factors (Reski, 1998). Therefore, it was important to establish the effects of auxin treatment and auxin signaling inhibition on moss development in the same laboratory growth conditions under which *Ppsgs3* mutants were examined.

When grown on BCDAT media, WT plants produced variable numbers of caulonemal runners, with most plants displaying some caulonemal runner formation by 15–22 days post-transplantation (Fig 3.2a). As previously reported, growth of moss on 1 μM NAA resulted in a dramatic increase in caulonema formation (Fig 3.2b). To test the effects of repressing auxin signaling, we grew moss on media supplemented with the 'antiauxin' *p*-chlorophenoxyisobutyric acid (PCIB). PCIB treatment causes the conversion of caulonema to chloronema and a decrease in bud formation (Bopp, 1980). We observed particularly severe phenotypes in moss grown on BCDAT supplemented with 30 μM PCIB. These include the formation of very small, dense plants consisting entirely of short chloronemal cells (data not shown). Plants grown on media supplemented with 10 μM PCIB display a less pronounced plant size defect, and phenotypes that are very similar to those of *Ppsgs3* grown on media without PCIB (Fig 3.2c–d). These include a slight decrease in the diameter of the protonemal mat, a lack of caulonemal runners, increased protonemal density, and an apparent decrease in bud formation. In fact, PCIB-treated WT plants are virtually indistinguishable from non-treated *Ppsgs3* plants, with the exception of a dome-like protrusion of the protonemal mat over the surface of the growth media in the former.

These results demonstrate that the *Ppsgs3* phenotype can be recapitulated by perturbing auxin signaling in moss. Considering the elevated expression levels of *PpARFb1–4*, which are closely related to repressive *ARF* genes in flowering plants, these data lend support to the hypothesis that tasiRNAs influence protonemal development by regulating the levels of repressive *ARF* gene expression.

Overexpression of *PpARFb2* and *PpARFb4* recapitulates the *Ppsgs3* phenotype

To investigate the hypothesis that *PpARFb1–4* act as effectors of the *Ppsgs3* phenotype, we characterized lines, created by Akitomo Nagashima in the Hasebe lab, that allow the inducible overexpression of tasiRNA-targeted ARFs. These lines use the XVE system to induce expression of HA-tagged, miR1219- and tasiRNA-resistant *PpARFb2* or *PpARFb4* in a dose-responsive, estradiol-dependent manner (Ishikawa et al., 2011; Zuo et al., 2000).

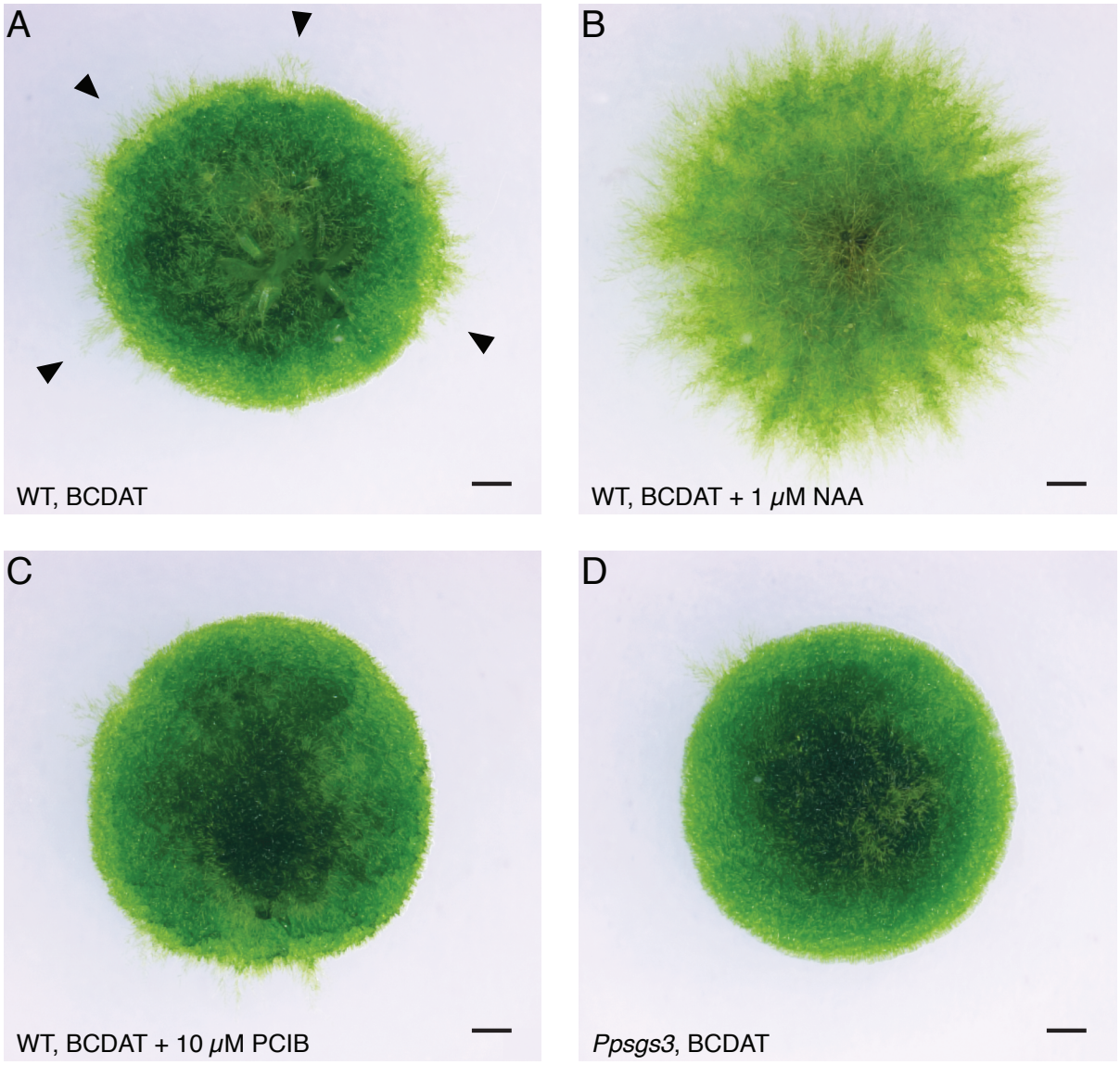

Figure 3.2: The *Ppsgs3* phenotype is consistent with a decreased auxin response

(A) WT plants on BCDAT media form caulonemal runners (black arrowheads). **(B)** Caulonemal runner formation is dramatically increased on media supplemented with 1 μM NAA. **(C)** Supplementing media with 10 μM PCIB, an auxin response inhibitor, decreases gametophore and caulonemal formation in WT plants, resulting in a phenotype very similar to that of *Ppsgs3* plants grown on media without PCIB. **(D)** *Ppsgs3* plant on BCDAT media. Plants shown are ~3 weeks post-transplantation. Scalebar = 1mm

Figure 3.2

XVE::PpARFb2 and *XVE::PpARFb4* cassettes, as well as a control *XVE::NLS-GUS-GFP* cassette, were integrated into the neutral *PIG1* locus. For each construct, multiple lines representing independent transformations were planted out on BCDAT medium and grown for 15 days, when caulonema formation becomes apparent. Growth on 1 μM estradiol results in a very mild decrease in caulonemal runner formation that is *ARF*-independent (Fig 3.3a–c). Nevertheless, this effect is not significant enough to hamper analysis of *ARF* overexpression strains.

Although all *XVE::PpARFb2* and *XVE::PpARFb4* lines represent single-site targeted integrations into a neutral genomic locus, different lines overexpressing the same *ARF* gene display a wide range of phenotype intensities. 'Weak' lines for both *XVE::PpARFb2* (e.g. line #11, Fig 3.3d–f) and *XVE::PpARFb4* (e.g. line #3, Fig 3.3g-i) show a loss of caulonemal runners, increased protonemal density, and a decrease in gametophore formation when grown on media containing 0.01–1 μM estradiol (Fig 3.3d–i). In most lines tested (for example, Fig 3.3g–i), higher concentrations of estradiol (1 μM) result in more severe phenotypes, including a progressive decrease in the number of caulonemal runners formed and in plant diameter, as well as an increase in the density of the protonema.

'Strong' lines of both *XVE:: PpARFb2* (e.g. line #6, not shown) and *XVE::PpARFb4* (e.g. line #10, Fig 3.3j–l) display very severe phenotypes, even when grown on low concentrations of estradiol (0.01 μM). These phenotypes include a very dense protonemal mat, small cells, and a strong decrease in plant diameter; similar phenotypes are observed when WT moss is grown on high concentrations of PCIB (30 μM). Importantly, in all lines except one, no phenotype is detected without estradiol treatment, indicating that the phenotypes observed are the result of *ARF* overexpression.

Differences in phenotype severity between lines overexpressing the same protein may be due to unknown background mutations in some of the overexpression lines. A more likely explanation, however, is that these differences stem from disparities in the levels of overexpressed protein. To test this possibility, we measured ARF-HA protein levels in every *XVE::PpARFb* line (Fig 3.3m–o). Our results show that 'strong' lines do indeed correlate with the highest levels of ARF-HA estradiol-dependent upregulation.

Figure 3.3: Overexpression of PpARFb2 and PpARFb4 recapitulates the *Ppsgs3* phenotype

Estradiol-inducible overexpressors of **(A-C)** GUS-GFP or sRNA-resistant, HA-tagged **(D-F)** PpARFb2 and **(G-L)** PpARFb4 were grown on various concentrations of estradiol. **(M)** HA-tagged protein overexpression level was quantified by western blot (bottom panel). A very mild decrease in caulonemal runner formation can be observed in the *XVE:: GUS-GFP* control strain on 1 μM estradiol (C). Overexpression of PpARFB2 and PpARFb4 to low levels recapitulates the decrease in caulonemal runners and gametophore buds seen in *Ppsgs3* (E-F, H-I), and results in a mild decrease in overall plant size. Stronger overexpression (K-L, M) results in very small, dense plants, similar to the effect observed in WT moss grown on high concentrations of PCIB. Scalebar = 1mm.

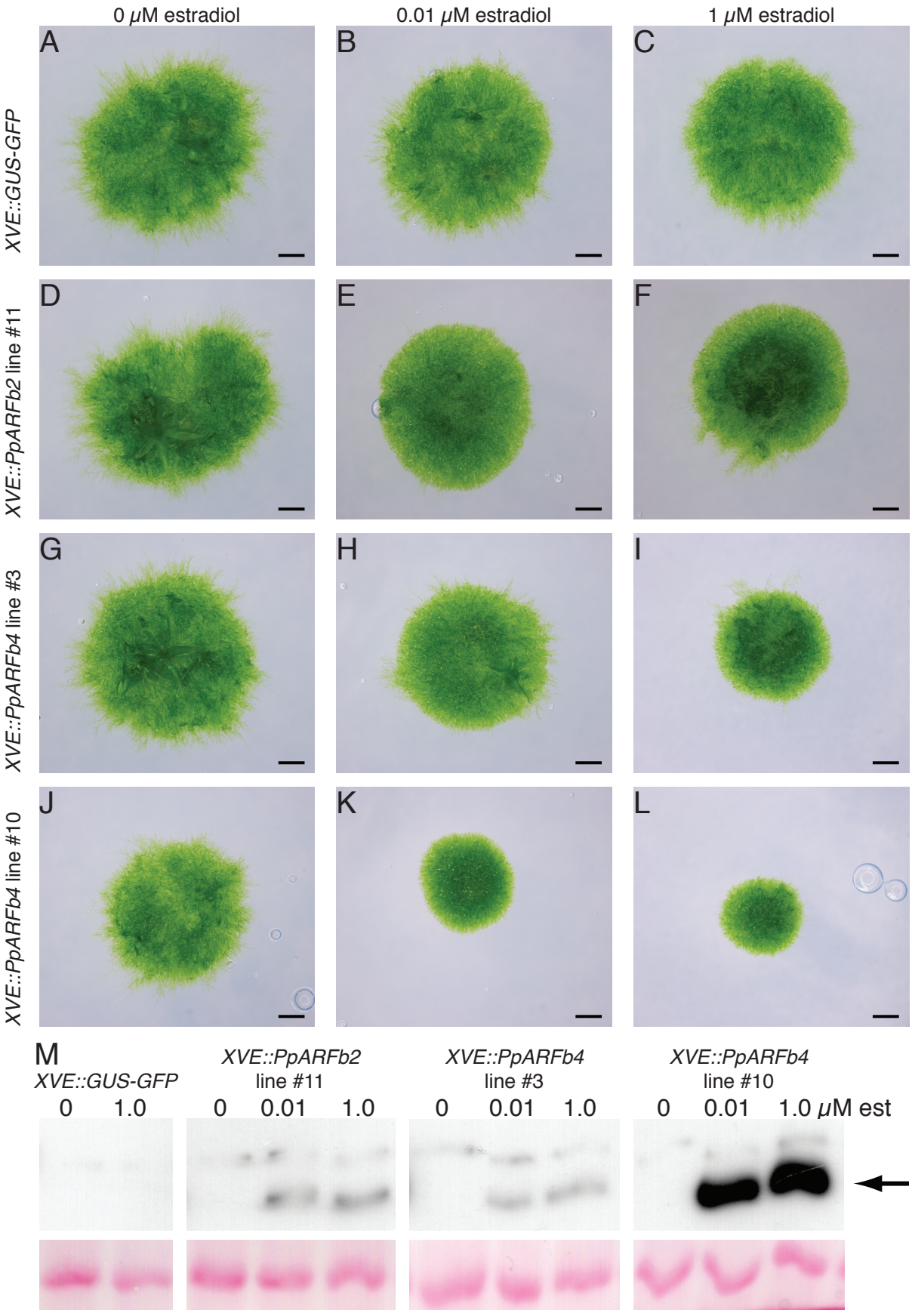
0 μM estradiol
0.01 μM estradiol
1 μM estradiol
A
B
C
XVE::GUS-GFP
D
E
F
XVE::PpARFb2 line #11
G
H
I
XVE::PpARFb4 line #3
J
K
L
XVE::PpARFb4 line #10
M
XVE::GUS-GFP
0 1.0
XVE::PpARFb2
line #11
0 0.01 1.0
XVE::PpARFb4
line #3
0 0.01 1.0
XVE::PpARFb4
line #10
0 0.01 1.0 μM est

Figure 3.3

The phenotypes of plants overexpressing PpARFb2 and PpARFb4 confirm that these proteins likely play similar roles in repressing auxin signaling, as phylogenetic analysis had suggested. These data further support the hypothesis that the tasiRNA-targeted *PpARFb* genes are the effectors of the phenotypes observed in *Ppsgs3*.

tasiRNAs and miR1219 regulate protonemal development via *PpARFb4*

The phenotypes of *XVE::PpARFb2* and *XVE::PpARFb4* plants point to the misexpression of these repressive *ARF* genes as the driver of the phenotypes observed in *Ppsgs3*. However, those experiments do not take into account the endogenous spatiotemporal expression patterns of these genes. Additionally, they do not permit the roles of miR1219 and tasiRNAs in regulating their targets to be studied individually. To directly test the role of sRNA-mediated regulation of tasiRNA targets in moss development, we decided to create sRNA-insensitive *PpARFb* mutants that maintain the target's native genomic context.

Of the tasiRNA targets, *PpARFb4* is the most highly overexpressed in *Ppsgs3* mutants (Fig 2.3c), showing that this gene is especially sensitive to changes in tasiRNA regulation. This makes *PpARFb4* an especially attractive model to study the regulation of *PpARFb* genes by tasiRNAs as well as miR1219. We used targeted gene replacement to create stable transformants in which the WT endogenous *PpARFb4* gene was tagged with the *GUS* reporter gene to allow monitoring of the spatial expression pattern of *PpARFb4* (Fig 3.4a). To study the role of sRNA-mediated regulation of *PpARFb4* in moss development, we also created plants in which, in addition to a *GUS* tag, silent mutations are introduced into the endogenous *PpARFb4* sequence that prevent targeting of the transcript by miR1219, tasiRNAs, or both sRNAs (Fig 3.4b).

The transformation cassette used to create the strains described above contains a ∼1-kb homology region between the sRNA sites and the *GUS* reporter and resistance cassette (Fig 3.4a). This raised the concern that recombination would occur in this intervening region, producing transgenic plants that retain WT sRNA sites despite being transformed with sRNA-resistant constructs. To allow for an efficient way to assay sRNA site mutations in the transgenic plants, new restriction sites were introduced into the mutated sRNA sites (Fig 3.4b–c).

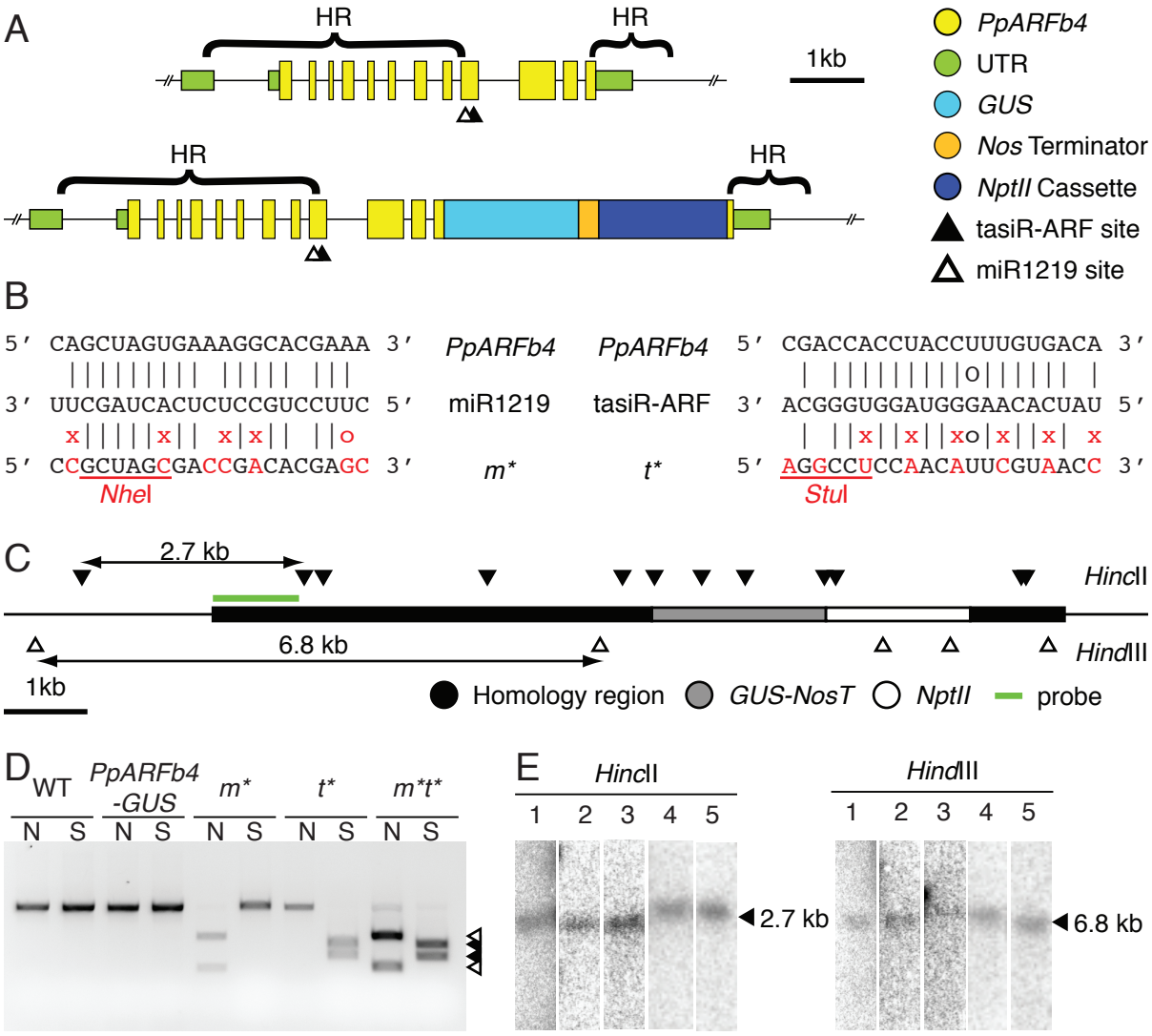

Figure 3.4: Creation and validation of *PpARFb4-GUS* lines
(A) Strains were created by recombining a cassette containing a *GUS* transgene, the *Nos* Terminator, and a resistance cassette directly upstream of the stop codon of *PpARFb4*. Arrows represent primers used in (D). **(B)** *miR1219** (‘*m**’), *tasiR-ARF** (‘*t**’), or *miR1219**+*tasiR-ARF** (‘*m*t**’) strains were created by integrating cassettes in which the 5′ homology region contains a mutant version of the sRNA site; this mutant site could be distinguished from the WT by the introduction of a restriction enzyme site. **(C)** Diagram of Southern blot analysis of transgenic plants showing *Hinc*II and *Hind*III restriction sites. **(D)** Strains in which the miR1219- and/or the tasiRNA-complementary site was mutated were validated by restriction digest. White arrows: products in *m** mutants; black arrows: products in *t** mutants. **(E)** Southern blots were performed with a probe in the 5′ homology region (5′ UTR of *PpARFb4*). Single bands in transgenic lines indicate single-locus, targeted integrations of the transgene cassette. All other lines in this study were verified similarly.

Figure 3.4

~50% of transgenic plants contained these restriction sites, consistent with replacement of the WT sRNA sites. All *PpARFb4-GUS* transgenic lines were validated as single insertions by qPCR of 5′ and 3′ homology regions or by Southern blot, probing for the 5′ homology region (Fig 3.4d–e).

To gauge the impact of sRNA-mediated regulation of *PpARFb4* on moss development, we characterized WT, miR1219-resistant (m^*), tasiRNA-resistant (t^*), and miR1219+tasiR-ARF-resistant (m^*t^*) *PpARFb4-GUS* plants grown on BCDAT media. 2–3 lines of each genotype were analyzed, with no significant differences detected between different lines of the same genotype. As expected, *PpARFb4-GUS* plants resemble WT plants (Fig 3.5a), although we detect a very subtle decrease in caulonemal runner formation, perhaps due to a stabilizing effect of the GUS tag on the PpARF4 protein. However, highly variable phenotypes are observed across plants within each of the m^* and t^* lines, ranging from WT-like to completely lacking caulonemal runners; examples displaying intermediate phenotypes for these lines are shown in Fig 3.5b–c. m^*t^* plants consistently lack caulonemal runners (Fig 3.5d), closely mimicking the protonemal phenotype observed in Ppsgs3. Unlike *Ppsgs3* plants, however, m^*t^* plants do not appear to have a significantly decreased protonemal mat diameter. These results indicate that tasiRNAs and miR1219 likely act partially redundantly to regulate caulonemal runner formation via *PpARFb4*, consistent with data showing that the *PpARFb4* transcript is cleaved at both tasiRNA- and miR1219-complementary sites (see Fig 2.3b and Axtell et al. (2007)). Additionally, the failure of t^* plants to fully recapitulate the *Ppsgs3* phenotype suggests that misexpression of other tasiRNA targets contributes to the protonemal defects observed in *Ppsgs3*. The phenotypic similarity between strains overexpressing PpARFb2 and PpARFb4 implies that the *Ppsgs3* phenotype likely results from the combined overexpression of B-group *ARF* genes.

Ppsgs3 plants and *Pprdr6* plants have opposite phenotypes with respect to gametophore numbers (Fig 2.4, Arif et al. (2012); Talmor-Neiman et al. (2006)). This result confounds the role of tasiRNA biogenesis, and more specifically the misregulation of *PpARFb1–4*, in gametophore development. To address this, we compared gametophore formation in *PpARFb4-GUS* and m^*t^* strains. We observe a highly significant and very strong decrease in gametophore num-

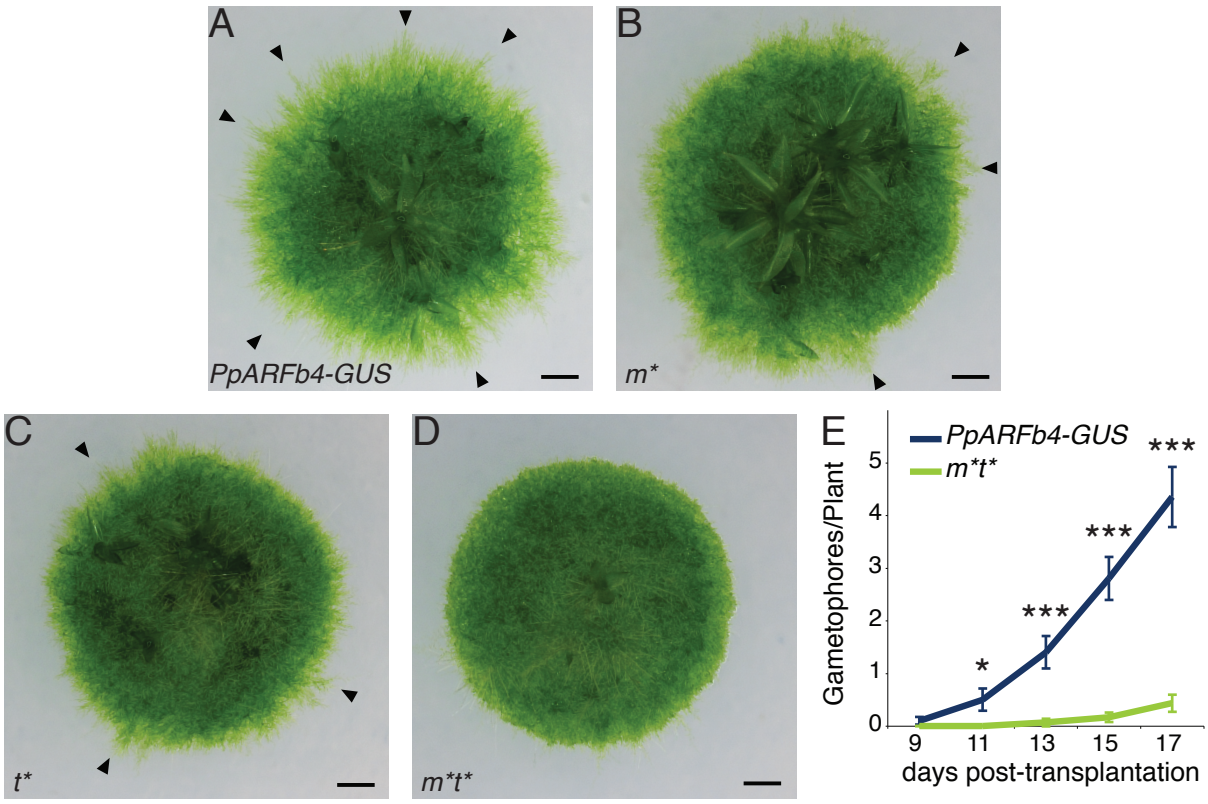

Figure 3.5: sRNA regulation of *PpARFb4* is necessary for caulonemal runner development

(A) 22-day-old *PpARFb4-GUS* plants grown on BCDAT media demonstrate WT levels of caulonemal runner formation (arrowheads). **(B, C)** Plants in which the miR1219- (B) or tasiR-ARF- (C) complementary sites of *PpARFb4* are mutanted demonstrate a wide range of phenotypes, from no runners at all to WT levels of runner formation; intermediate phenotypes are shown here. **(D)** Plants in which both the miR1219- and tasiR-ARF-complementary sites of *PpARFb4* are mutated, however, consistently lacked caulonemal runners, instead displaying a round protonemal mat with a smooth edge. **(E)** Mutating the miR1219- and tasiR-ARF-complementary sites of *PpARFb4* also results in a severe delay in gametophore formation. *p < .05, **p < .01, ***p < .001. Scalebar = 1 mm.

Figure 3.5

ber in m^*t^* mutants, with what appears to be nearly a week-long-day delay in the onset of gametophore formation (Fig 3.5e). This phenotype is even stronger than that observed in *Ppsgs3* mutants, and suggests that the gametophore initiation defects observed in those plants may indeed result from *PpARFb4* misregulation. The cause of the increase in gametophore number in *Pprdr6* plants remains unclear; however, in addition to the loss of tasiRNA biogenesis, the *Pprdr6* mutation also results in a partial loss of the 22–24nt sRNA population (Cho et al., 2008), and we suspect that this loss may underlie the increase in gametophore formation observed in *Pprdr6* plants. I favor an explanation for the increased gametophore numbers in *Pprdr6*, proposed by Cho et al. (2008), whereby siRNAs targeting repetitive elements may contribute to the repression of gametophore formation, although the mechanism by which this occurs remains to be elucidated.

Together, these data suggest that protonemal development and gametophore initiation in *Physcomitrella* are regulated through the coordinate action of miR1219 and tasiRNAs, which exert their effect by fine-tuning the levels of multiple repressive *ARF* genes with overlapping functions.

sRNAs regulate protonemal development by restricting PpARFb4 to the tips of growing filaments

sRNAs often act by limiting the expression of their target genes to specific domains (Javelle and Timmermans, 2012; Wienholds et al., 2005). This is true for tasiRNAs, which—in *Arabidopsis* and rice—act to limit expression of their targets to the abaxial side (Chitwood et al., 2009; Itoh et al., 2008). We reasoned that an understanding of the spatiotemporal domains of miR1219 and tasiRNA activity in *Physcomitrella* would help elucidate how these sRNAs regulate caulonemal runner and gametophore bud formation.

Attempts to monitor PpARFb2 and PpARFb4 accumulation using fluorescent tags were unsuccessful, possibly due to low levels of these proteins in developing protonema (data not shown). To circumvent this problem we took advantage of the *GUS*-tagged WT and sRNA-resistant *PpARFb4* transgenic lines described above. As GUS activity is enzymatic, it is a significantly more sensitive assay for detecting tagged protein expression in plant tissue. Extended

staining times (up to 2 weeks) are necessary to detect PpARFb4 expression, showing that the protein is indeed present in cells at very low levels. To determine whether the staining pattern observed under these extended conditions is specific to PpARFb4-GUS expression, WT plants were stained alongside the transgenics. No staining is observed in any WT control plants. In addition, staining in transgenic plants is nuclear localized (see insets in Fig 3.6), consistent with PpARFb4 acting as a transcription factor. This indicates that the observed staining represents specific signal caused by accumulation of PpARF4b-GUS protein.

GUS staining patterns in *PpARFb4-GUS*, m^*, t^*, and m^*t^* plants were examined one, two, and three weeks after transplantation to solid media. Although reporter activity levels in all genotypes seems to increase as development proceeds, we do not observe any striking differences in spatial expression patterns between the three timepoints. A more detailed analysis was performed on plants 15 days post-transplantation, since this is the time point closest to the initiation of caulonemal runners and gametophore buds.

We observe expression of sRNA-sensitive PpARFb4-GUS at the edges of young phyllids in a low number of gametophores. Within the protonema, PpARFb4 expression is sporadic, occurring in less than a third of protonemal filaments (Fig 3.6a). Filaments showing GUS activity are not distributed evenly along the circumference of the plant; rather, PpARFb4-expressing filaments appear to occur most frequently in a couple of contiguous sectors along the edge of the protonemal mat. Furthermore, in filaments where PpARFb4-GUS is expressed, it is only present in the 1–3 cells nearest the filament tip.

Mutation of the miR1219-complementary site of *PpARFb4* results in a slightly higher number of PpARFb4-expressing filaments than the *PpARFb4-GUS* plants (Fig 3.6b). More significant differences from the WT expression pattern are observed in t^* lines (Fig 3.6c), which show expression in most filaments. In addition, the PpARFb4-GUS expression level in individual cells appears higher in t^* plants than in *PpARFb4-GUS* and m^* plants. Given the strong phenotypes observed in m^*t^* plants (Fig 3.5d), we expected that the expression of *PpARFb4* would be highest in these plants, and indeed GUS staining reveals expression of PpARFb4 in nearly every filament. Staining of individual cells appears stronger, and PpARFb4-expressing cells often extended further down the filament, than in any of the WT or single sRNA-resistant

Figure 3.6: sRNA regulation restricts PpARFb4 expression to the growing edge of the protonema

(A) PpARFb4-GUS is expressed in the first 1-3 cells from the tips of the protonema, although most filaments lack expression entirely. As expected for a translational reporter of the expression of an ARF, which are transcription factors, staining is primarily nuclear. **(B)** Plants in which the miR1219-complementary site of *PpARFb4* has been mutated show expression in more filaments. **(C)** plants with tasiR-ARF-resistant *PpARFb4* show stronger expression in even more filaments and, in some cases, in more cells along the filament. Staining is also stronger. **(D)** Expression of miR1219- and tasiR-ARF-resistant *PpARFb4* is expanded even further from filament tips than in the other genotypes; inset shows expression in the 6th cell from the tip (the 5th cell has no expression). Staining is stronger than in other genotypes, although the apparent increase in staining strength compared to other genotypes is partially the result of a higher density of filaments at the protonemal edge in these mutants. Arrowheads indicate expression of PpARFb4-GUS in young gametophore buds. **(E)** Activity of the *PpRSL1* promoter is strongest towards the center of the protonemal network, and is weak in cells closest to the tip. Inset shows overstained plant demonstrating weak promoter activity at the edge of the protonemal mat. This expression domain is complementary to that of PpARFb4.

Scalebar = 0.1 mm. Asterisks in inset mark cells along one filament expressing PpARFb4-GUS; red asterisks denote tip cells.

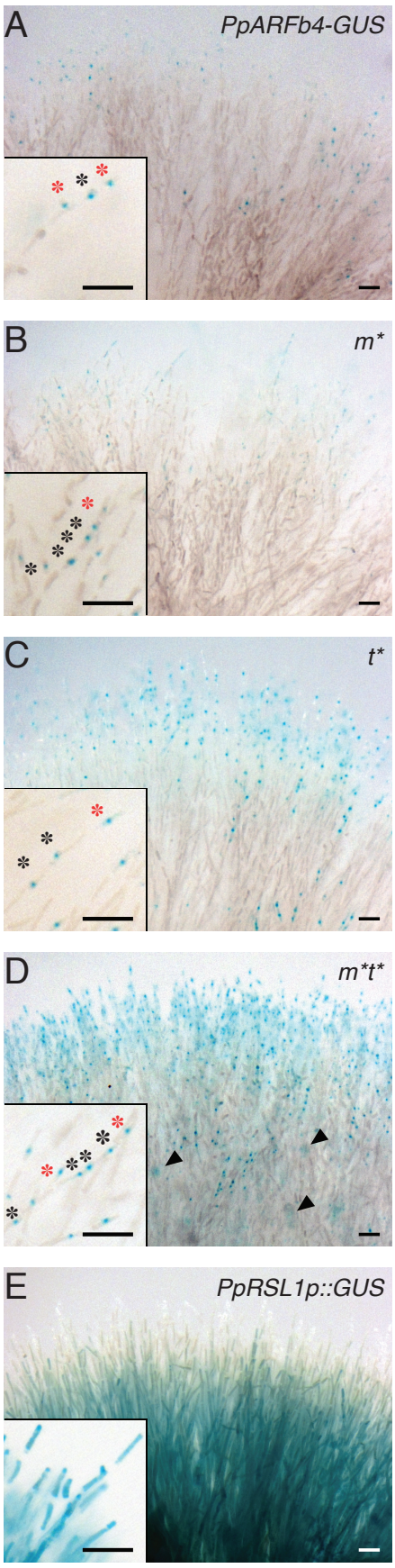

Figure 3.6

lines. Finally, we also detect weak staining at the bases of gametophore buds (Fig 3.6d), as well as in the tips of some young phyllids (data not shown).

Considering the role of PpRSL1 in regulating caulonemal specification in moss (Jang and Dolan, 2011; Jang et al., 2011), we sought to compare its expression pattern to that of PpARFb4 . We used a transcriptional reporter, *PpRSL1p::GUS*, to assay *PpRSL1* promoter activity in 15-day-old plants (Fig 3.6e) (Jang and Dolan, 2011). We found strong *PpRSL1* expression throughout the protonemal mat, with the exception of the growing edges, where expression was significantly weaker. The spatial domain of *PpRSL1* promoter activity thus appears complimentary to the domain of PpARFb4 expression.

This insight into the spatial regulation of tasiRNA targets highlights the partially redundant roles of miR1219 and tasiR-ARFs in target regulation, as well as the importance of the leading edge of the protonemal mat in filament differentiation.

Discussion

A conserved role for B-group *ARF*s in repressing auxin signalling

In flowering plants, Auxin Response Factors fall into two groups—activating and repressive—that have opposing roles in regulating the auxin response (Fig 3.1). Auxin signaling is highly variable over time, and modeling suggests that repressive ARFs may stabilize the transcriptional auxin response against these fluctuations. The activating/repressive ARF dichotomy has also been proposed to be important in spatially modulating the auxin response, since distinct patterns of activating and repressive ARF expression can create zones of high or low auxin sensitivity (Vernoux et al., 2011). Despite extensive research on auxin signaling and ARF function in flowering plants, especially in *Arabidopsis*, the function of these transcription factors remains unexplored in other land plant clades. Phylogenetic data suggests that the repressive-activating dichotomy observed in flowering plant *ARF* genes may represent an ancient mode of auxin response regulation that dates back to the earliest land plants (Fig 1.2a, Finet et al. (2012)). Our results are the first to lend support to this hypothesis. We tested the phenotypic effects of overexpressing two of the four *Physcomitrella* B-group *ARF*s, which are

most closely related to repressive *ARF* genes from *Arabidopsis*. In both cases, overexpression of these genes results in phenotypes consistent with a decrease in auxin signaling. This, along with the phenotypes of *Ppiaa* mutants (Prigge et al., 2010), reveals that the framework of auxin response modulation outlined in Fig 3.7 —activation of auxin-responsive genes by activating ARFs, and repression by AUX/IAAs and repressive ARFs—was likely an ancient feature of land plant development.

The inducible *ARF* lines allow us to decouple *PpARFb2* and *PpARFb4* expression from the complex auxin response network. The extensive regulatory feedback in this network and redundancy between *ARF* genes can confound traditional mutant-based analyses. Using the inducible system, we can induce various levels of repressive *ARF* expression independently of the state of the auxin response network in the cell, which makes these strains valuable tools for exploring the effect of modulating auxin response levels on plant development. The similarity of phenotypes between lines overexpressing *PpARFb2* and *PpARFb4* at low levels and those of *Ppsgs3* plants lends support to the hypothesis that tasiRNAs regulate plant development by modulating the levels of auxin response via the B-group *ARF* genes.

Functional redundancy among repressive ARFs in *P. patens*

Multiple paralogous genes exist at each step in the auxin response pathway. The *Arabidopsis* auxin response network, for example, consists of 6 *TIR1/AFB* auxin receptors, 29 *Aux/IAA* genes, 5 activating *ARF* genes, and 18 putative repressive *ARF* genes (Fig 1.2a; Parry et al. (2009); Vernoux et al. (2011)). This network is somewhat simpler in *Physcomitrella*, but still demonstrates a high degree of gene duplication. The moss genome encodes 4 *TIR1/AFB* auxin receptors (and an additional two related genes not found in flowering plants), 3 *Aux/IAA* genes, 8 putative activating *ARF* genes, and 6 putative repressive *ARF* genes (Axtell et al. (2007); Prigge et al. (2010) and Fig 1.2a). The high number of paralogous genes responsible for every step in the auxin response pathway may reflect a high degree of subspecialization in auxin response, with subtly different functions for every gene. For example, proteins could have unique interaction partners or bind to different gene targets. Evidence of such subspecialization exists among the *Arabidopsis* AUX/IAA and TIR1/AFB proteins. The degradation

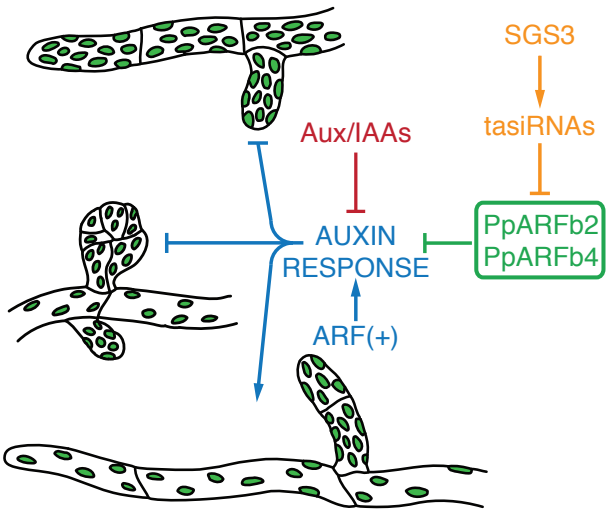

Figure 3.7: The role of tasiRNAs and B-group ARFs in moss development
SGS3 is necessary for the production of tasiRNAs, which regulate the expression of PpARFb1-4. PpARFb2 and PpARFb4 repress the plant's auxin response, derepressing chloronemal side branch formation and suppressing the formation of caulonemal runners and the initiation or maturation of gametophore buds.

Figure 3.7

dynamics of AUX/IAAs in response to auxin differ depending on the particular TIR1/AFB coreceptor and AUX/IAA protein forming the interaction (Havens et al., 2012). Some very preliminary evidence for such subspecialization was also found in moss repressive ARF proteins: a yeast two-hybrid assay demonstrated that the general repressor TOPLESS interacts with only a subset of the putative repressive ARF proteins (Causier et al., 2012).

An alternative model is that, rather than providing a way to differentially regulate distinct targets in response to the same auxin input, the high number of paralogs at each step in the auxin response pathway are more or less biochemically equivalent, and serve to provide modular spatiotemporal regulation of the auxin response. In animals, such modular regulation is often achieved via cis-regulatory element evolution (Carroll et al., 2004), but gene duplications appear to be a common solution to this problem in plants (Flagel and Wendel, 2009). Evidence for this model has also been found in *Arabidopsis*. Yeast two-hybrid assays group ARFs almost perfectly into groups that correspond with their identity as activators or repressors based solely on their ability to interact with each other and Aux/IAA proteins. This suggests a high degree of biochemical similarity within ARF paralog groups. The same study found that Aux/IAAs and ARFs are expressed in highly diverse patterns throughout the developing floral meristem and organ primordia (Vernoux et al., 2011). A number of additional studies have also identified distinct spatiotemporal domains of *ARF* expression, especially in the root and developing embryo (for example, Rademacher et al. (2012; 2011)). Together, these studies provide evidence for the idea that the high number of *ARF* and *Aux/IAA* genes in *Arabidopsis* is necessary for modular spatial regulation of the auxin response.

Our work begins to approach the question of divergence between auxin response regulator activity in moss from a functional perspective. Overexpression of *PpARFb2* and *PpARFb4* yields very similar phenotypes: dense protonema, a decrease in caulonemal runner production, and—at high overexpression levels—a decrease in gametophore formation and plant size. Indeed, PpARFb2 and PpARFb4 overexpression level seems to play a greater role in determining a plant's phenotype than which of the two proteins is overexpressed. This suggests that, at least in the case of PpARFb2 and PpARFb4, repressive ARF paralogs target the same downstream genes. In addition, the similarity of these phenotypes to those of various *Ppiaa* mutants

(Prigge et al., 2010) and to moss grown on high levels of PCIB suggest that PpARFb2 and PpARFb4 are able to repress most, or all, auxin-regulated developmental processes. It should be noted, however, that subtle differences between the function of these two transcription factors, especially differences in the strength of auxin response regulation such as the ones observed in *Arabidopsis* TIR1/AFB receptors (Havens et al., 2012), would likely have been missed in our assay.

Although overexpression experiments showed that induction of either PpARFb2 or PpARFb4 to sufficiently high levels could recapitulate the *Ppsgs3* phenotype, they do not take into account the endogenous expression levels of these genes. t^* lines allowed us to explore the effects of abolishing the tasiRNA-mediated regulation of just one repressive *ARF*. While some t^* plants lack caulonemal runners, the phenotype of most mutants was less severe than that observed in *Ppsgs3*. This observation suggests that, as expected, overexpression of *PpARFb4* only partially contributes to the *Ppsgs3* protonemal defects. Studies of tasiRNA-resistant mutants of *PpARFb1–2* may determine the contribution of these genes to the *Ppsgs3* phenotype, and analysis of *Pparfb* knockouts will help elucidate the degree of functional redundancy between them. However, our preliminary results paint a complex picture. For example, the ability of the m^*t^* mutation in *PpARFb4* to fully recapitulate the caulonemal defect of *Ppsgs3* but not its effect on plant size suggests some degree of subspecialization among the tasiRNA targets. Because moss uniquitously overexpressing PpARFb4 has a plant size defect, such subspecialization is more likely the result of differences in the expression patterns of tasiRNA targets rather than in their downstream target genes.

tasiRNAs and miR1219 limit the expression of *PpARFb4* to the protonemal periphery

In both plants and animals, sRNAs can regulate development by restricting the spatiotemporal expression domain of their targets (Skopelitis et al., 2012). This is the mode of action of tasiRNAs in flowering plants, which regulate leaf polarity by restricting the expression of their targets to the abaxial side of developing leaves (Chitwood et al., 2009; Itoh et al., 2008). In line with previous studies, our work demonstrates that the loss of sRNA-mediated regulation leads to an increased accumulation of the repressive *ARF*s in moss (Axtell et al., 2007;

Talmor-Neiman et al., 2006), Fig 2.3a). However, the question of whether moss tasiRNAs act to restrict *PpARFb* expression to a specific spatiotemporal domain, as they do in flowering plants, previously remained unanswered. We were able to address this question with *PpARFb4-GUS* strains that define the endogenous expression pattern of this tasiRNA target in *Physcomitrella*, allowing us to infer the spatiotemporal domain of tasiR-ARF and miR1219 activity based on the expression pattern of sRNA-resistant versions of the PpARFb4-GUS transgene.

The phenotypic effect of the m^*t^* mutation was stronger than that of either the m^* or the t^* mutation on its own, suggesting that miR1219 and tasiRNAs have overlapping roles in repressing *PpARFb4*. This conclusion is supported by the expanded expression domain and higher expression levels of m^*t^* relative to m^* or t^* alone. These data indicate that miR1219 and tasiRNAs act near the edge of protonema to limit *ARF* expression to the protonemal edge. The *PpARFb4* promoter does not seem to be active at the center of the plant, so additional reporters will be necessary to elucidate the levels of miR1219 and tasiRNA activity in this domain.

t^* plants accumulate PpARFb4 in the $\sim$3 tip cells of nearly all protonemal filaments, and show higher levels of accumulation in each cell than tasiRNA-sensitive *PpARFb4-GUS* plants. Despite this, the suppression of caulonemal runner formation in this strain is highly variable. Caulonemal runner formation is only fully abolished in *PpARFb4-GUS.*m^*t^* mutants, in which *PpARFb4* expression is expanded to additional cells towards the protonemal center. One possible interpretation of this observation is that expression of PpARFb4 in cells distant to the tip are able to suppress caulonemal runner formation, or that runner formation is non-cell-autonomous. Indeed, at first glance, the high activity of the promoter of *PpRSL1*, a key inducer of caulonemal formation in *P. patens*, in cells away from the protonemal edge seems to support this conclusion. This is surprising, since the conversion of chloronema to caulonema occurs in the growing tip of filaments, and some evidence exists that this conversion occurs in a cell-autonomous manner (Bopp, 1980). The weak activity of the *PpRSL1* promoter at the protonemal edge may provide the key piece of information for understanding this apparent inconsistency. We propose that this weak *PpRSL1* expression is near the threshold for what is sufficient to drive caulonemal runner formation. As *PpRSL1* promoter activity

is auxin-regulated (Jang and Dolan, 2011), the increase in repressive ARF expression in cells at the protonemal edge in the absence of tasiRNA regulation, and perhaps a further increase in levels of these repressors in the absence of downregulation by miR1219, may drive expression of PpRSL1 in chloronemal tip cells far below the threshold needed to induce caulonemal differentiation.

It is unlikely that the expansion of protonemal PpARFb4-GUS expression observed in m^*t^* is responsible for the decrease in gametophore buds that we observed in these plants. At ~2 weeks post-transplantation, gametophores in WT plants were observed primarily at the center of the protonemal network, whereas PpARFb4-GUS in m^*t^* plants is expressed at the protonemal edges. However, in addition to its expanded expression in the protonema, PpARFb4-GUS is also expressed in young gametophore buds in m^*t^* plants. This raises the possibility that rather than being deficient in bud initiation, m^*t^* plants (and potentially *Ppsgs3* plants) initiate buds, and that ectopic PpARFb4 expression arrests their further development. The gametophore counts performed in this study included only those gametophores forming phyllids, and counts of younger gametophore buds present an interesting direction for future studies.

Regulation of *ARF* genes by two sRNAs provides plant-to-plant robustness to protonemal development

Plants overexpressing PpARFb4 showed a progressive decrease in the developmental output of auxin response, such as plant size and caulonemal runner formation, with increasing PpARFb4 levels. We thus expected that a small increase in the expression levels of repressive *ARF* genes, such as the one observed in t^* or m^*, would moderately decrease the rate of caulonemal runner formation. Instead, we observed a highly variable phenotype, with different m^* and t^* individuals displaying a range of phenotypes, from WT-like to a complete absence of caulonemal runners. On the other hand, *PpARFb4-GUS*.m^*t^* plants consistently lacked caulonemal runners and were significantly delayed in gametophore initiation.

One explanation for this observation is that the levels of the tasiRNA-targeted *ARF* genes vary from plant to plant. Such stochastic variations can be caused by variable pro-

moter activity, variable regulatory sRNA levels, or both. We propose that in WT plants, the variation in repressive *ARF* levels remains well below the threshold above which caulonemal runner formation is inhibited; when sRNA regulation is completely absent, target levels increase well above the threshold and caulonemal runners are consistently repressed. However, when *PpARFb4* is under the regulation of only one sRNA, it is expressed at levels close to the threshold of caulonemal repression. Small plant-to-plant fluctuations in *PpARFb4* expression would result in stochastic crossing of this threshold, leading to the highly variable phenotypes seen in m^* and t^* plants. miR1219 appears to be a moss-specific sRNA, but flowering plant tasiRNA targets contain two closely spaced tasiRNA binding sites. Our results suggest that this double targeting may be necessary to robustly regulate downstream developmental processes. Interestingly, preliminary results in *Arabidopsis* suggest that variation in leaf width is higher in tasiRNA biogenesis mutants than in WT plants when they are grown at high temperatures (C. Quietsch, personal communication). These data present the intriguing possibility that tasiRNAs were conserved over ∼450 million years of evolution because of their ability to lend robustness to the regulation of the auxin response.

miR1219 and tasiRNAs provide spatial regulation of the auxin response

Our data indicate that B-group *ARF* genes are regulated by tasiRNAs and miR1219, and that these *ARF*s in turn repress auxin signaling in developing moss protonema (summarized in Fig 3.7). The sRNAs appear to act together to regulate targets that are likely expressed in partially overlapping domains and create a fine-tuned pattern of auxin response regulation in the developing protonema.

sRNA-dependent regulation of auxin signaling appears to be widespread. Another ancient sRNA, miR160, regulates C-group *ARF* genes across all land plants, and flowering plants have evolved a third sRNA, miR167, to regulate activating *ARF* gene expression as well. We hypothesize that this sRNA-mediated regulation may be important to lend robustness to developmental processes regulated by auxin; however, the auxin regulatory network is complex and contains many instances of feedback, making it difficult to predict the effect of specific

inputs on the behavior of the network. Detailed experimental tests may yield surprising explanations for the importance of sRNAs in modulating the auxin response in plants.

Chapter 4

tasiRNAs allow for a sensitive auxin response in *P. patens*

Introduction

The auxin response GRN demonstrates a great deal of complexity in flowering plants. The network includes two mechanisms that transcriptionally silence the auxin response: one via Aux/IAAs, and the other via repressive ARFs; additionally, multiple members of the network are regulated by sRNAs, including both activating and repressive *ARF* genes (see Chap 1). The complexity of the network is further increased by multiple instances of regulatory feedback. These include negative feedback, whereby expression of repressive *Aux/IAA*s and a subset of repressive *ARF*s is activated in response to auxin signaling (Paponov et al., 2008), as well as at least one case of positive feedback, in which the activating *ARF5* is upregulated in response to auxin (Lau et al., 2011).

This high level of complexity has been proposed to lend a number of favorable properties to the auxin response network. Computational modeling has demonstrated that a simple network consisting of one activating ARF and one Aux/IAA, both transcriptionally induced by auxin, is sufficient to produce a switch-like auxin response (Lau et al., 2011). This may be important to allow cells making auxin-regulated cell fate decisions to 'commit' to a cell fate once a certain level of auxin signaling is reached. However, such a network may be sensitive to fluctuations in auxin levels. Experiments have demonstrated that in the *Arabidopsis* meristem, such fluctuations are common, but do not result in the activation of auxin-regulated genes. This robustness of the auxin response is likely the result of the activity of repressive ARFs. By decreasing cells' sensitivity to auxin, they prevent spurious fluctuations in auxin signaling from triggering the auxin response and its associated cell fate changes. In addition, differential expression of auxin response network components throughout the meristem creates distinct auxin-responsive and auxin-insensitive domains (Vernoux et al., 2011).

Previous studies have demonstrated that the role of Aux/IAAs in repressing the auxin response is conserved in *Physcomitrella*, as is their upregulation in response to auxin signaling (Prigge et al., 2010). Our work identifies another key component of the auxin response GRN in moss, the repressive ARFs. We found that least one of these repressors, PpARFb4, is expressed at the edge of the developing protonemal mat. The overexpression of these ARFs re-

presses auxin-regulated developmental processes, including chloronemal branch determinacy and caulonemal runner and gametophore bud formation. Moreover, our data suggests that by regulating the expression of repressive ARFs, tasiRNAs may act as modulators of the auxin response in *Physcomitrella*. We set out to explore the effect of this modulation on the ability of *P. patens* to respond to auxin treatment, and to further explore the regulatory properties of the *Physcomitrella* auxin response GRN.

Our results demonstrate that tasiRNA biogenesis mutants are impaired in their ability to respond to low concentrations of exogenous auxin. This defect is detectable both in terms of the absence of a developmental response to auxin, as well as a decrease in the upregulation of auxin-responsive genes. We also detect complex feedback of auxin signaling onto tasiRNAs and their targets. We propose that the activity of tasiRNAs allows moss to produce a sensitive, graded developmental response to increasing auxin concentrations.

Results

Ppsgs3 plants have an impaired auxin response

Ppsgs3 mutants demonstrate phenotypes consistent with a decrease in auxin signaling, as well as an upregulation of repressive *ARF* genes. These results suggest that tasiRNA biogenesis mutants may be impaired in their ability to respond to auxin. We sought to directly assay the auxin response in *Ppsgs3* plants by examining the effects of exogenous auxin on their development. WT moss grown on BCDAT media with 1 μM NAA produces large amounts of caulonema, including many caulonemal runners (Fig 3.2b, 4.1e), and gametophores on which phyllids are replaced by filaments (Bopp, 1980). Previous studies have shown that strong auxin-resistant *Ppiaa* mutants do not respond to 1 μM NAA by forming caulonema (Ashton et al., 1979; Prigge et al., 2010). However, 1 μM NAA has the same effect on both WT and *Ppsgs3* (Fig 4.1j), showing that *Ppsgs3* mutants, in contrast to *Ppiaa*, are still capable of forming caulonemal runners when induced with exogenous auxin.

This result indicates that unlike the previously described *Ppiaa* mutants, which contain genetic lesions that prevent the degradation of Aux/IAAs in the presence of auxin, *Ppsgs3*

Figure 4.1: *Ppsgs3* is resistant to low doses of auxin, but responds at high concentrations

(A-E) WT and **(F-J)** *Ppsgs3* plants grown on BCDAT media with 0, 0.03, 0.1, 0.3, or 1.0 μM NAA. Caulonemal runners (some highlighted by arrowheads) are strongly induced in WT by growth on NAA concentrations as low as 0.03 μM (B). As auxin concentration is increased, more and more caulonemal runners are formed (C-E). On 0.3 μM NAA and higher, chloronema in the primary protonemal mat begin to be converted into caulonema as well (D and E), as evidenced by lighter filament color; protonemal mat density also decreases siginificantly. *Ppsgs3* plants grown without auxin do not form caulonemal runners, with rare exceptions (F). Unlike WT plants, they also fail to form caulonemal runners when grown on 0.03 or 0.1 μM NAA (H-I). However, higher auxin concentrations partially rescue this defect, and *Ppsgs3* plants begin to resemble their WT counterparts with respect to caulonemal formation and protonemal mat density on 0.3 and 1 μM NAA (I-J). Plants were grown for 22 days post-transplantation. Scalebar = 5 mm

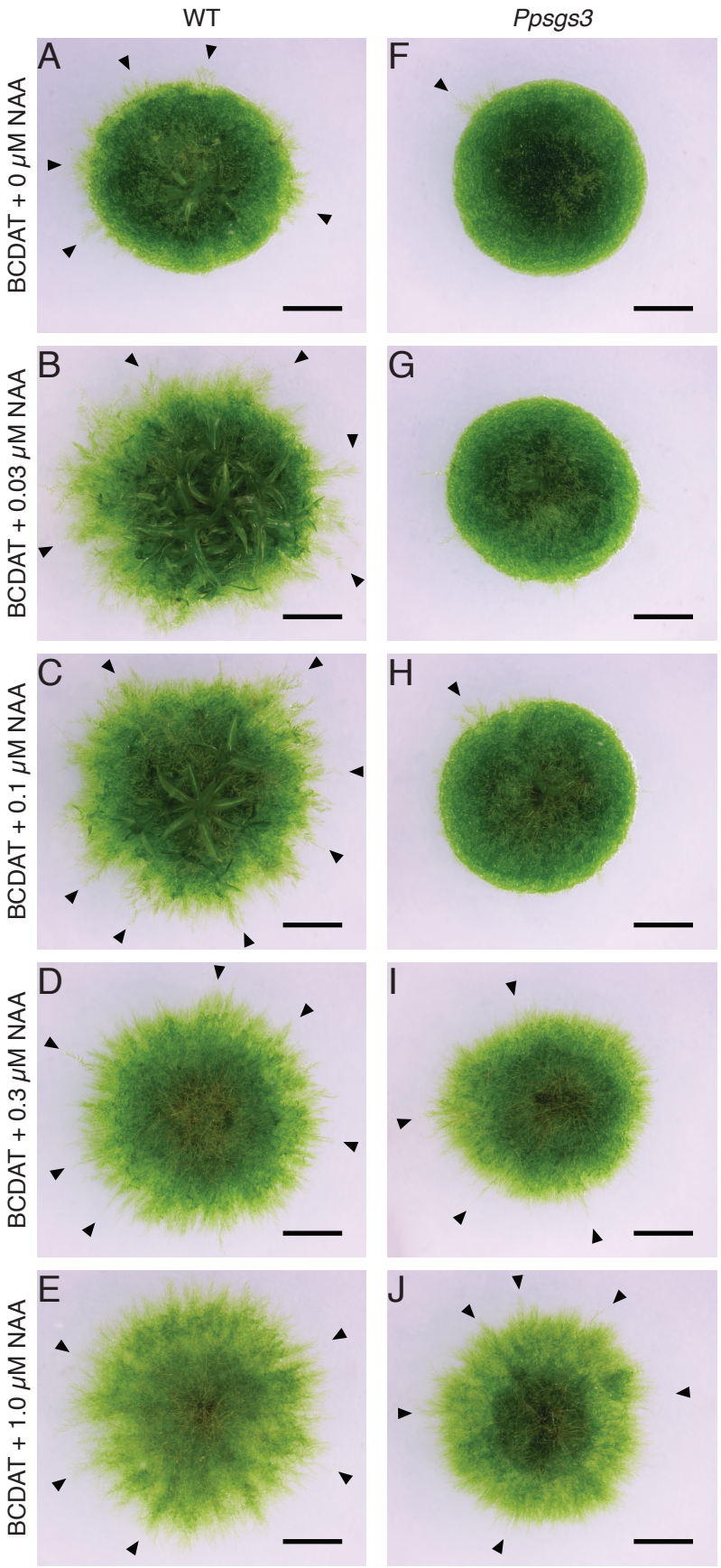
WT
Ppsgs3
A
F
BCDAT + 0 μM NAA
B
G
BCDAT + 0.03 μM NAA
C
H
BCDAT + 0.1 μM NAA
D
I
BCDAT + 0.3 μM NAA
E
J
BCDAT + 1.0 μM NAA

Figure 4.1

mutants are not auxin-resistant. Instead, these mutants may have a decreased sensitivity to auxin as a result of repressive ARF upregulation. If so, the effect of tasiRNA loss should be more apparent at lower concentrations of auxin. To test this hypothesis, we grew WT and *Ppsgs3* plants on an NAA concentration series, i.e. media supplemented with 0, 0.03, 0.1, 0.3, and 1.0 μM NAA (Fig 4.1). WT plants respond to these auxin concentrations with phenotypes of increasing severity. After 22 days of growth on BCDAT media without any NAA, WT *P. patens* has a number of caulonemal runners in multiple places around the circumference of the protonemal mat (Fig 4.1a). Plants grown on media supplemented with 0.03 μM NAA produce many more caulonemal runners (Fig 4.1b). On 0.1 μM NAA, caulonemal runners emerge along most of the circumference of the protonemal mat (Fig 4.1c). On 0.3 μM NAA, more caulonemal runners are formed, and the protonema become sparser and lighter in color, likely reflecting the formation of caulonema, rather than chloronema, within the main protonemal mat itself (Fig 4.1d). On this auxin concentration, filaments also replace phyllids on the gametophores. Finally, on 1 μM NAA, much of the WT protonemal mat consists of caulonema (Fig 4.1e). Thus, as exogenous auxin concentration increases, WT plants show a smooth transition from a primarily chloronemal mat with a few caulonemal runners to a caulonemal mat with extensive caulonemal runner formation.

Ppsgs3 plants did not undergo the same graded response to increasing auxin concentrations. As noted before, *Ppsgs3* plants rarely produce caulonemal runners when grown on BCDAT media (Fig 4.1f). This does not change as they are treated with auxin, and *Ppsgs3* plants grown on 0.03 and 0.1 μM NAA are phenotypically indistinguishable from untreated plants (Fig 4.1g–h). However, on 0.3 μM NAA, *Ppsgs3* plants begin to resemble WT plants grown on the same auxin concentration, with sparse, light-colored protonemal mats, caulonemal runners, and filaments replacing phyllids. As in WT, caulonemal formation further increased on 1 μM NAA.

These phenotypic data demonstrate that *Ppsgs3* plants are indeed impaired in their ability to respond to exogenous auxin, although treatment with high levels of NAA ($>$0.1 μM) can override this defect. Thus, in contrast to the graded auxin response observed in WT, *Ppsgs3* plants appear to be insensitive to low concentrations of auxin, but respond strongly to high

concentrations.

Induction of auxin-dependent gene expression is perturbed in *Ppsgs3*

We sought to probe the molecular basis of the auxin response defect observed in *Ppsgs3* plants. Our data suggests that the phenotypes observed in *Ppsgs3* are the result of the repression of auxin-responsive genes by repressive ARFs. One group of well-known auxin-regulated genes is the *Aux/IAA*s, which are downstream of auxin signaling in flowering plants (Abel and Theologis, 1996). These genes are also upregulated in response to auxin signaling in *Physcomitrella* (Lavy et al., 2012; Prigge et al., 2010). To assay the effect of the *Ppsgs3* mutation on auxin-responsive genes, we measured the levels of the three moss *Aux/IAA* genes, *PpIAA1a*, *PpIAA1b*, and *PpIAA2a* (Prigge et al., 2010), on 0, 0.03, and 0.1 μM NAA in 15-day-old WT and *Ppsgs3* plants (Fig 4.2a-c). No statistically significant differences in *PpIAA2* levels are observed between *Ppsgs3* and WT in any of these conditions. This is consistent with what is found in *Ppdgt* mutants, which are defective in auxin signaling and display decreased expression of a number of other auxin response genes but not *PpIAA2* (Lavy et al., 2012). By contrast, we observe a significant decrease in the induction of *PpIAA1a–b* in response to auxin in *Ppsgs3* plants. In WT plants grown on 0.03 μM NAA, *PpIAA1a* and *PpIAA1b* transcript levels are upregulated 2.6- and 2.7-fold, respectively, relative to their levels on media without auxin. In *Ppsgs3* moss grown in the same conditions, *PpIAA1a* expression is only upregulated 1.6-fold, and *PpIAA1b* transcript levels are not significantly changed. Although a stronger increase in the expression of both genes is observed in *Ppsgs3* on 0.1 μM NAA, levels of *PpIAA1b* remain significantly lower in *Ppsgs3* plants than in WT.

The decrease in both the molecular and developmental response to exogenous auxin in *Ppsgs3* mutants is consistent with an increased repression of auxin target genes due to the upregulation of repressive ARFs. These data provide further support for our hypothesis that the function of tasiRNAs in *Physocmitrella* is to modulate the auxin response.

Auxin signaling feeds back onto tasiRNAs and their targets

Feedback regulation, especially negative feedback loops, represent a common tran-

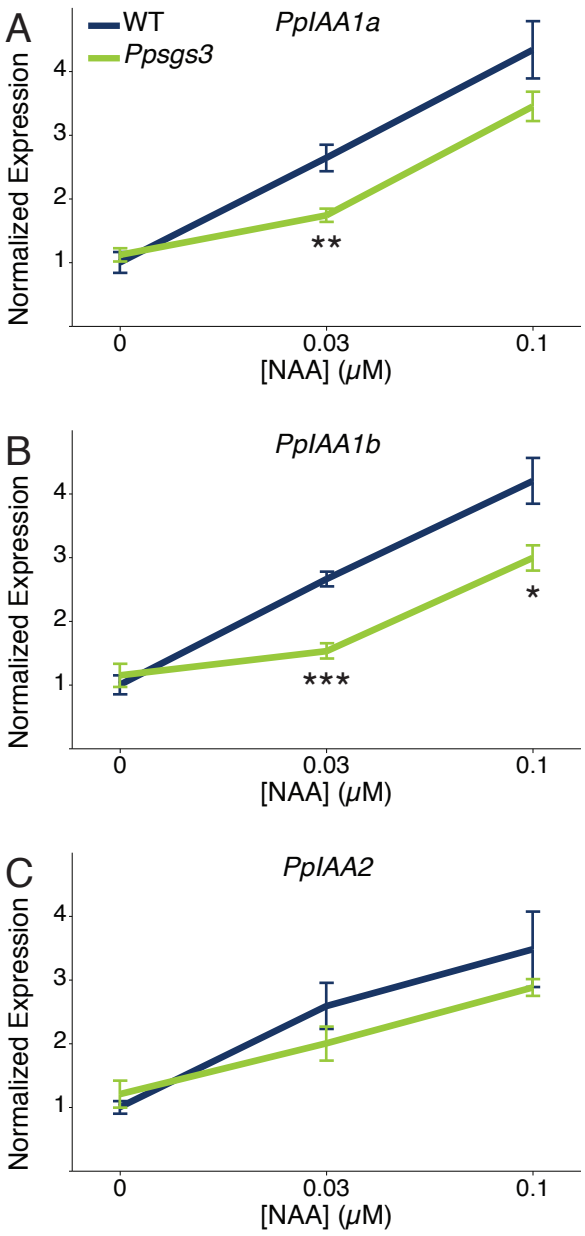

Figure 4.2: The molecular auxin response is decreased in *Ppsgs3* plants
Relative expression levels of the auxin-responsive genes **(A)** *PpIAA1a*, **(B)** *PpIAA1b* and **(C)** *PpIAA2* in 15-day-old plants grown on media supplemented with 0, 0.03, or 0.1μM NAA. Although levels of all three genes are similar in WT and *Ppsgs3* plants grown without auxin, auxin-treated plants show significant differences in auxin-responsive gene expression. WT plants show upregulation of all three genes in response to 0.03μM NAA. *Ppsgs3* plants show a much smaller magnitude of *PpIAA1a* and *PpIAA1b* upregulation in response to auxin (A-B).
All expression values were normalized to GAPDH, and displayed relative to the expression level in WT plants grown on media without added NAA. *p < .05, **p < .01, ***p < .001.

Figure 4.2

scriptional regulatory network motif (Alon, 2007), and play an especially important role in the auxin response. The observation that auxin induces miR390 expression in *Arabidopsis* roots presents the possibility that tasiRNA levels are auxin-regulated (Marin et al., 2010). Such feedback regulation may lend key properties and information-processing functions to the auxin response GRN. We set out to explore feedback regulation in the auxin response network in *Physcomitrella* by investigating the regulation of tasiRNAs and their targets by auxin signaling.

We tested the effect of auxin on miR390, tasiRNA, and miR1219 expression by comparing the levels of these sRNAs in plants grown on media with and without 0.1 μM NAA (Fig 4.3a). We found that while miR390 was upregulated $\sim$1.5–3-fold in plants grown on auxin-containing media, miR1219 levels in the same plants decreased $\sim$5-fold. tasiR-ARFa and tasiR-ARFb/e, which appear to be expressed at similar levels in the absence of exogenous auxin, also have opposite responses to the addition of auxin to growth media: tasiR-ARFa is downregulated $\sim$2-fold, whereas tasiR-ARFb/e are upregulated $\sim$7-fold. These results reveal a complex relationship between auxin signaling and tasiRNA/miR1219 levels, which are difficult to interpret in terms of an effect on target levels.

To directly assay the effect of auxin signaling on tasiRNA target expression, we measured the levels of *PpARFb1*, *PpARFb2*, and *PpARFb4* in plants grown on BCDAT media with and without 0.1 μM NAA. Levels of all three genes were elevated $\sim$2.5-3.5-fold on auxin-containing media (Fig 4.3b), indicating that auxin signaling promotes their expression. We next investigated the effect of this auxin-induced upregulation on the spatial domain of PpARFb4 expression by growing WT and sRNA-resistant *PpARFb4-GUS* plants on increasing concentrations of auxin. We found that auxin treatment results in an expanded domain of PpARFb4 expression, with expression observed in a higher proportion of filaments on 0.1 μM NAA (Fig 4.3d), and in cells further from the protonemal edge on 1 μM NAA (Fig 4.3e). This expression pattern is similar to that observed for sRNA-resistant PpARFb4 in m^*t^* plants (Fig 3.6d), raising the possibility that sRNAs no longer repress their targets in high-auxin conditions. We investigated whether sRNA regulation shows an additive effect to auxin on the spatial domain of ARF expression. We observed that on both 0.1 and 1 μM NAA, sRNA-resistant *PpARFb4*

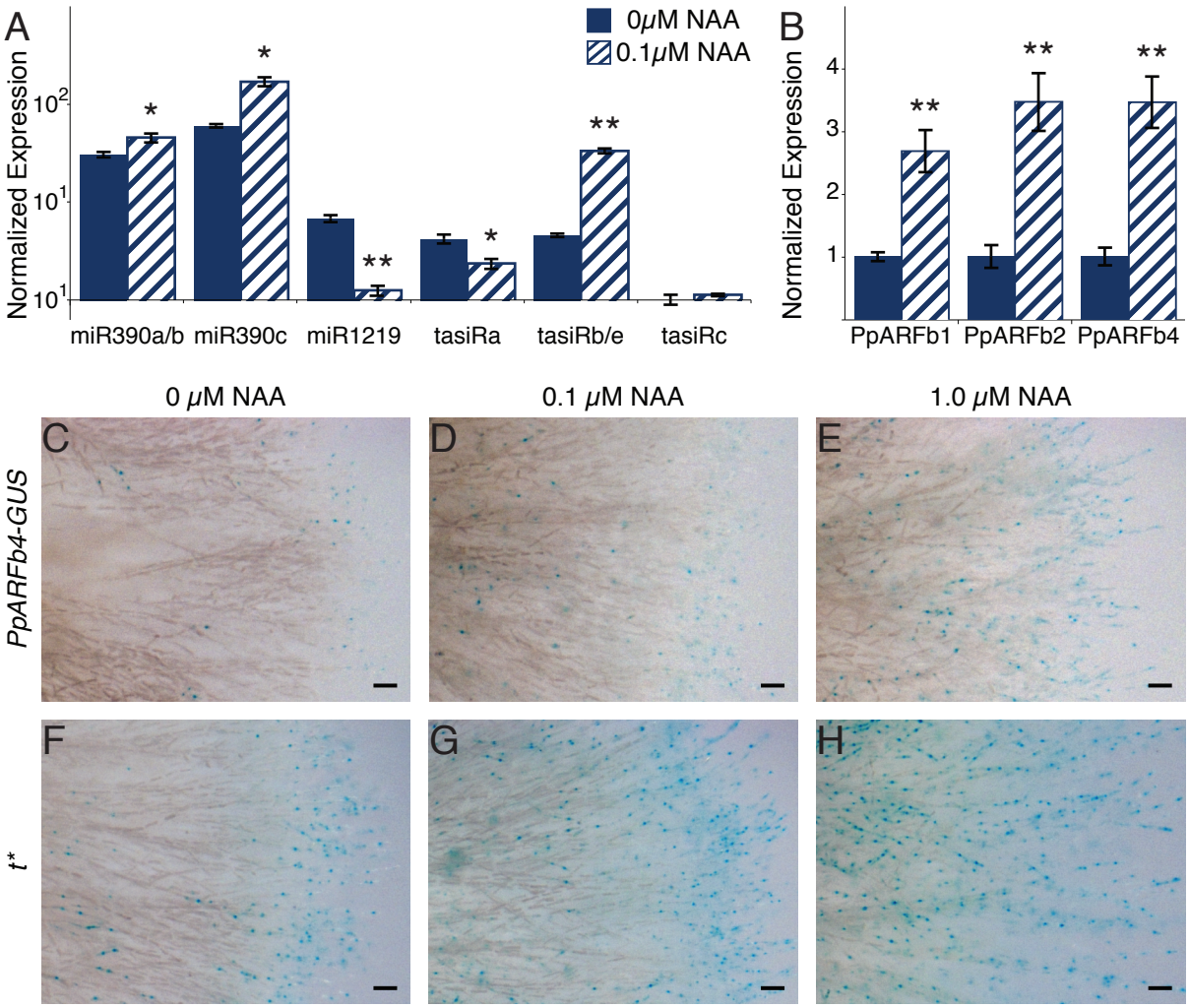

Figure 4.3: tasiRNAs and their targets are auxin-regulated
(A) sRNAs show a complex auxin response. miR390 is slightly upregulated in plants grown on 0.1μM NAA, while miR1219 is downregulated nearly 5-fold. The two dominant tasiR-ARF species, tasiRa and tasiRb/e, also display opposing auxin responses. tasiRa is down-regulated ~2-fold on 0.1μM NAA, whereas tasiRb/e is upregulated ~7-fold. **(B)** *PpARFb1, PpARFb2,* and *PpARFb4* are upregulated 2.5-3.5-fold in plants grown on 0.1μM NAA. **(C-E)** *PpARFb4-GUS* and **(F-H)** *t** plants grown on 0, 0.1, and 1μM NAA, respectively. Auxin induces both an increase in expression strength and an expansion of the expression domain of PpARFb4.
Plants were collected 15 days post-transplation. All expression values were normalized to GAPDH. In (A), values are displayed relative to the levels of tasiRc, to highlight relative expression levels of various sRNAs; in (B), expression values are shown relative to the expression level of each gene in WT plants grown on media without added NAA.
*p < .05, **p < .01. Pictures shown in (C) and (F) are the same as in 3-6.a and 3-6.d, respectively.

Figure 4.3

displayed an expanded domain of expression as compared to WT *PpARFb4* (Fig 4.3f-h). In t^* plants grown on 1 μM NAA, PpARFb4 expression extended nearly to the center of the protonemal mat (Fig 4.3h); in m^*t^* plants grown on the same auxin concentration, PpARFb4 expression was ubiquitous in the protonema (data not shown).

Together, there data indicate that *PpARFb1*, *PpARFb2*, and *PpARFb4* are upregulated in response to auxin; that this upregulation results in the expansion of the PpARFb4 expression domain towards the center of the protonemal mat; and that, despite a complex pattern of auxin regulation of these sRNAs, miR1219 and tasiRNAs continue to exclude their targets from the center of the protonemal mat in plants grown on exogenous auxin.

Ppsgs3 plants are impaired in the auxin-dependent induction of a gene regulating caulonemal differentiation

We sought to explore the effect of perturbing tasiRNA biogenesis on genes known to regulate the developmental processes found to be defective in *Ppsgs3* mutants. Previous studies showed that the transcription factor *PpRSL1* is upregulated in response to auxin and is necessary for auxin-dependent caulonemal formation (Jang and Dolan, 2011; Jang et al., 2011; Menand et al., 2007b). To investigate the possibility that the absence of auxin-dependent caulonemal runners in *Ppsgs3* is the result of *PpRSL1* downregulation, we assayed *PpRSL1* expression levels in WT and *Ppsgs3* plants. We did not detect an effect of the *Ppsgs3* mutation on *PpRSL1* transcript levels in 15-day-old plants (data not shown). However, this may be the result of a low level of caulonemal runner formation at this early developmental stage, and we next compared *PpRSL1* expression in 22-day-old WT and *Ppsgs3* plants.

PpRSL1 levels are indistinguishable between these two genotypes in 22-day-old plants grown on media without NAA. However, WT and *Ppsgs3* respond differently to the addition of exogenous auxin. In WT plants, we observe an increase in *PpRSL1* transcript levels in in plants grown on media with 0.03 μM NAA. This is consistent with published data from cellophane-cultured protonemal tissue treated with high auxin concentrations (Jang and Dolan, 2011; Lavy et al., 2012). By contrast, in *Ppsgs3*, addition of 0.03 μM NAA to growth media results in a $\sim$3-fold decrease in *PpRSL1* transcript levels (Fig 4.4). This result suggests

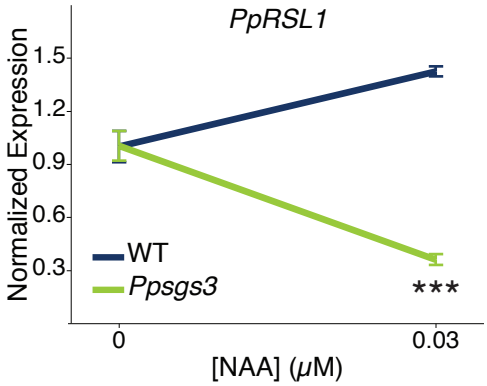

Figure 4.4: Auxin-responsiveness of *PpRSL1* is compromised in *Ppsgs3* plants

Relative expression levels of *PpRSL1* in 22-day-old plants grown on BCDAT media supplemented with 0 or 0.03μM NAA. Although expression levels are indistinguishable between WT and *Ppsgs3* plants grown without auxin, auxin-treated plants show significant differences. WT plants show induction of *PpRSL1* expression in response to 0.03μM NAA, whereas in *Ppsgs3*, expression is downregulated on auxin relative to untreated plants. All expression values were normalized to GAPDH, and displayed relative to the expression level in WT plants grown on media without added NAA. ***p < .001.

that *PpRSL1* may be repressed by B-group ARFs, which are misregulated in *Ppsgs3*. This is consistent with our previous finding that *PpRSL1* and *PpARFb4* have complementary expression patterns in developing protonema (Fig 3.6a,e). The decrease in *PpRSL1* expression levels in *Ppsgs3* plants grown on auxin, rather than an absence of induction, is likely the result of increased levels of repressive ARFs following auxin induction in these tasiRNA biogenesis mutants. The auxin-induced expression of PpARFb4 in the absence of tasiRNA regulation encroaches on the *PpRSL1* expression domain towards the center of the plant, causing a decrease in the expression levels of this gene.

These data confirm that in *Ppsgs3* plants grown on media containing low amounts of exogenous auxin, the loss of caulonemal runners accompanies a drop in the levels of *PpRSL1*, a transcription factor that acts as a key inducer of caulonemal development. A decrease in *PpRSL1* alone, however, is not sufficient to account for the full spectrum of phenotypes observed in *Ppsgs3* mutants. For example, although plants harboring deletions in *PpRSL1* and its paralog *PpRSL2* lack caulonemal runners, they do not display the decrease in gametophore formation observed in *Ppsgs3*. In fact, our data suggests that the phenotypes observed in *Ppsgs3* are the result of the repression of a range of auxin-regulated processes.

Discussion

Complex feedback regulation in the moss auxin response network

Negative feedback plays a key role in the auxin response pathway in flowering plants, and may provide the auxin response GRN with key regulatory properties (Middleton et al., 2010). If conserved, these properties may have favored the repeated cooption of the auxin response GRN over the course of evolution (see Chapter 1). In *Physcomitrella*, Aux/IAAs are upregulated in response to auxin signaling (Prigge et al., 2010), suggesting that this negative feedback loop is an ancestral component of the auxin response network in land plants. We explored feedback in an additional repressive component of the auxin response GRN, the repressive ARFs, and found that these are also induced by auxin signaling. This may represent a

partially conserved aspect of the auxin response network, as some repressive ARFs, including the tasiRNA target *AtARF4*, are also auxin-regulated in *Arabidopsis* (Paponov et al., 2008).

Our investigations revealed that tasiRNAs and miR1219 are a key component of the auxin response GRN in moss. These tasiRNAs feed into the auxin pathway via the regulation of repressive *ARF* gene expression. A complex system of feedback also regulates tasiRNAs via auxin signaling. Some of these sRNAs (tasiR-ARFb/e) are upregulated in response to auxin signaling, presumably resulting in a positive feedback loop through the downregulation of repressive *ARF*s. Other sRNAs (miR1219 and tasiR-ARFa) are repressed in response to auxin, forming a negative feedback loop. We investigated the sum of these feedback loops by observing the effect of auxin treatment on the spatial expression domain of one tasiRNA target, PpARFb4. We found that while auxin induced an expansion of the PpARFb4 expression domain, sRNAs continued to exclude PpARFb4 expression from the center of the protonemal mat. Further work is needed to address this complex feedback system, which provides a potential mechanism for spatial, temporal, growth condition-specific, or even auxin concentration-dependent feedback loops regulating the auxin response.

The readout of the auxin response GRN is the induction of auxin-responsive genes, and their regulation of downstream developmental processes, including chloronemal branch determinacy, caulonemal runner initiation, and gametophore bud formation (summarized in Fig 4.5a). We have demonstrated that a key role of miR390-dependent tasiRNAs is to sensitize the auxin response GRN to auxin signaling by regulating repressive ARF expression. In the absence of tasiRNAs, moss plants are impaired in their ability to induce auxin-regulated genes, such as *PpRSL1* and *Aux/IAA*s, in response to auxin signaling, resulting in developmental defects. The observation that auxin-responsive gene expression, such as *Aux/IAA*s and *PpRSL1*, is not altered between WT and *Ppsgs3* moss grown on media without exogenous auxin may appear inconsistent with this model. This apparent inconsistency may be explained by the fact that auxin response genes act in most or all protonemal cells, as evidenced by the broad activity of the *PpRSL1* promoter throughout the protonema, and the ubiquitous effect of *Ppiaa* mutations in the developing plant. By contrast, caulonemal formation in response to auxin, as well as the major contribution of the tasiRNA pathway to ARF repression, is limited to the

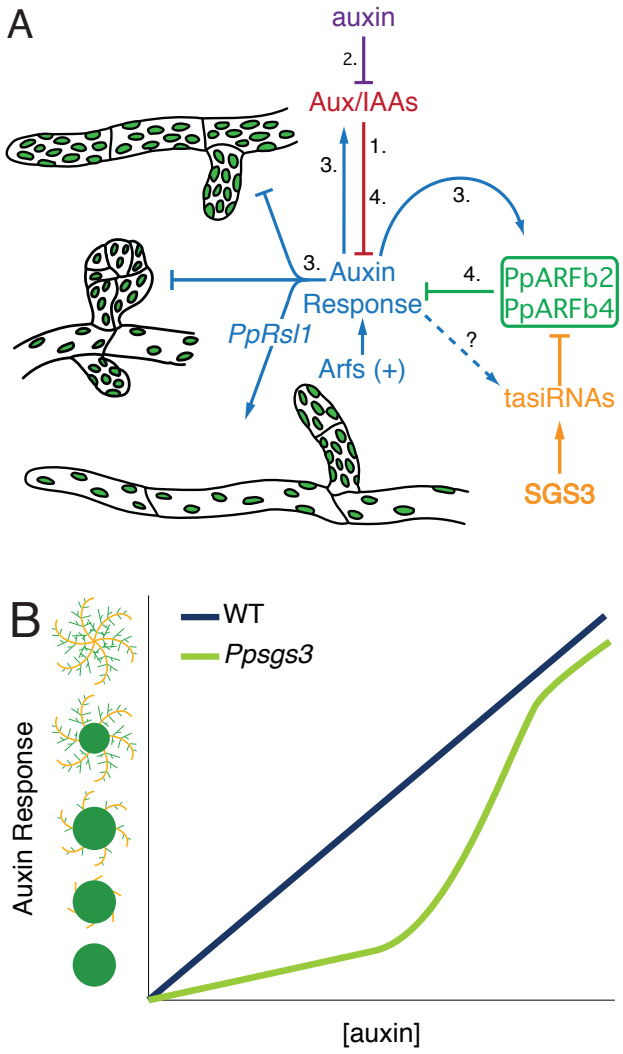

Figure 4.5: tasiRNAs modulate the auxin response in moss
(A) Feedback in the auxin response pathway in moss. 1 - Aux/IAAs repress the auxin response. 2 - In the presence of auxin, Aux/IAAs are degraded, and the auxin response is initiated via the activating ARFs. 3 - The auxin response controls a number of downstream genes and developmental processes. It promotes caulonemal runner growth via PpRSL1, and represses branching and gametophore bud formation. It also upregulates the expression of repressive ARFs and Aux/IAAs. In addition, it may result in an increase in the overall level of tasiRNAs. 4 - The upregulation of repressive ARF and Aux/IAA proteins results in the repression of the auxin response. (B) Model of the role of tasiRNAs in the auxin response. Our data suggest that while both tasiRNA-defective and WT plants can respond to auxin, the activity of tasiRNAs results in a smooth gradient of auxin response level accross a wide range of auxin concentrations.

Figure 4.5

edge of the protonemal mat.

The work presented in this chapter elaborates on our understanding of the auxin response GRN by identifying multiple instances of feedback regulation, and demonstrating that the deregulation of tasiRNA targets results in a decreased sensitivity to auxin. One caveat of these conclusions is that, rather than measuring the direct effect of auxin treatment on the expression of auxin-responsive genes, we are quantifying the steady state of their expression after 2–3 weeks of growth on auxin-containing media. However, the continuous growth of moss on auxin-containing media likely represents a condition that is close to what is found in nature. Mosses secrete a wide range of molecules into their substrate, including polypeptides (Neuenschwander et al., 1994) and hormones; in fact, studies in liquid-cultured *Physcomitrella* found that >60% of cytokinin and >90% of auxin was found in the culture media, rather than inside the moss tissue (Reutter et al., 1998). These data strongly suggest that exogenous hormones represent a key mode of intercellular signaling in bryophytes (Shaw and Goffinet, 2000; Chapter 2). Thus, by assaying gene expression in *P. patens* grown on low concentrations of exogenous auxin, we are closely recapitulating the natural state of moss development. Moreover, alternative approaches to measuring auxin responsiveness in plants must be performed on cellophane-subcultured protonemal tissue (as in Prigge et al. (2010)), which has a drastically different gene expression profile from individually grown plants (Fig 2.6).

The complexity of the auxin response GRN likely provides certain favorable properties to the auxin response. The negative feedback loop acting via Aux/IAAs, for example, may create a robust, switch-like auxin response (Lau et al., 2011). Interestingly, our finding that repressive ARFs are also regulated by auxin in *Physcomitrella* points to an additional negative feedback loop. This feedback loop is expected to yield different properties from the Aux/IAA loop, as unlike the ARFs, Aux/IAAs are degraded in response to increasing auxin concentrations. Computational modeling may reveal the properties lent to the auxin response GRN by this new circuit. We are especially interested in the possibility, proposed based on modeling of the *Arabidopsis* auxin response GRN, that repressive ARFs may buffer cells against fluctuations in auxin signaling. Finally, we identify tasiRNAs as a key component of the auxin response GRN, both feeding into the network and receiving complex feedback from it. Understanding

the properties that these sRNAs impart to the auxin response GRN may be key to elucidating the reasons behind their repeated cooption.

tasiRNAs as a dial to tune developmental response to auxin

In flowering plants, the auxin response governs a number of processes that demonstrate a graded developmental output, in which the response to varying levels of auxin produces a series of intermediate states, rather than an 'on/off' response. Examples of such processes include lateral root formation, lateral root outgrowth (Malamy, 2005), and hypocotyl growth (Lilley et al., 2012). We observe a similar graded response across varying concentrations of auxin in *Physcomitrella* caulonemal formation, with an increasing number of cells switching to caulonemal runner fate with increasing auxin concentration (Fig 4.1a–e). Such a graded output may be beneficial to the plant in responding to a diverse set of external stimuli, where a different level of caulonemal runner or gametophore production may be necessary in distinct conditions.

Strikingly, in the range of auxin concentrations that elicit a graded response in WT plants, we failed to observe such a response in *Ppsgs3*. We envision two possible explanations for this observation. It may result from a shift in the responsive range of *Ppsgs3*, such that the slope of the response to increasing auxin concentrations remains the same, but *Ppsgs3* fails to respond to auxin in the 0–0.1 μM NAA range. Alternatively, the auxin response phenotype of *Ppsgs3* may reflect a change in the shape of the auxin response curve in these plants (Fig 4.1b). Rather than the graded auxin response of WT, *Ppsgs3* may display a sigmoid, switch-like behavior to increasing auxin concentrations. In this model, the auxin response is repressed by a high level of PpARFb expression, until a concentration ($<$0.3 μM NAA) is reached that overrides this repression. In either situation, the defect in tasiRNA biogenesis likely leads to a decreased sensitivity of *P. patens* to subtle changes in the level of auxin signaling.

In *Arabiodopsis*, modeling of a simple system containing one self-regulating activating ARF and one auxin-regulated repressive Aux/IAA demonstrated a switch-like response to increasing auxin concentrations (Lau et al., 2011). Our data demonstrate that, much like the Aux/IAAs, tasiRNA-targeted repressive ARFs are auxin-inducible in *Physcomitrella*, making

the case for a plausible extension of the model proposed in Lau et al. (2011) et al to include repressive ARFs. One key question is how the switch-like auxin response of individual cells can be translated into a graded response on the level of the entire plant. This may be achieved by slight differences in the state of the auxin response GRN between chloronemal cells at the protonemal edge. Although each of these cells responds to an increase in auxin levels in a switch-like manner, the level of auxin signaling at which this switch is triggered differs between individual cells. Thus, gradual increases in the level of auxin will trigger the auxin response and caulonemal runner fate in progressively more cells.

Our phenotypic data thus suggests that tasiRNAs sensitize the auxin response network to allow cells to respond to low levels of auxin. The effect of this on a tissue-wide scale is that the protonema can tune its development by responding to small changes in auxin concentration. Additional phenotypic, gene expression, and computational modeling data are needed to test the validity of this hypothesis. If correct, this model suggests that the tasiRNA biogenesis pathway may have been conserved over the course of 450 million years of plant evolution because it lends the auxin response GRN the ability to tune its output across a range of auxin concentrations.

Chapter 5

Discussion and perspective

Introduction

Despite their conservation over the course of ~450 million years of plant evolution, miR390-dependent tasiRNAs do not appear to share a common developmental output across land plants. Rather, they form a conserved part of the ancient auxin response GRN, which has itself been coopted for multiple developmental functions. A key question at the outset of our research was why the miR390-dependent tasiRNA pathway has been so frequently reused over the course of plant evolution. Our work with *Physcomitrella* suggests that the properties that tasiRNAs lend to the auxin response may have been a key reason for this pathway's recurrent utilization in plant development.

Our data demonstrate that in moss, SGS3 plays a conserved role in the biogenesis of tasiRNAs. We have also shown that tasiRNAs regulate chloronemal determinacy, and promote caulonemal runner and gametophore bud formation by downregulating repressive ARF proteins and limiting their expression to the edge of the protonemal mat. These results demonstrate that tasiRNAs in *Physcomitrella* are key regulators of the development of the protonema, a derived tissue type that evolved within the mosses (Mishler and Churchill, 1984). Thus, the developmental role of tasiRNAs in *Physcomitrella* appears to represent an independent cooption event, rather than an ancestral function.

In addition to determining the developmental role of the tasiRNA pathway in moss, we explored the regulatory properties of tasiRNAs and their targets. miR390-dependent tasiRNAs form a part of the auxin response network, in which they regulate the expression of repressive ARFs, which in turn prevent the activating ARF-mediated upregulation of auxin-responsive genes. Experiments with plants expressing tasiRNA- and miR1219-resistant *PpARFb4* demonstrate that the activity of these sRNAs lends robustness to auxin-regulated developmental processes, allowing plant-to-plant uniformity in the levels of caulonemal runner formation. We also identified extensive feedback between auxin signaling, tasiRNAs, and repressive ARFs, with the latter being auxin-inducible. Previous studies have suggested that repressive ARFs stabilize the auxin response against fluctuations in auxin signaling by decreasing the ability of cells to activate auxin-regulated genes in response to small changes in auxin levels

(Vernoux et al., 2011). Interestingly, repressive PpARFb4 is expressed at the protonemal edge in *Physcomitrella*, the 'differentiating zone' where auxin likely acts to induce caulonemal runner formation. This raises the possibility that its role is to buffer cells against spurious fluctuations in auxin signaling, ensuring that cell fate decisions are made in response to legitimate increases in auxin levels. In the absence of tasiRNAs, the overexpression of repressive ARFs results in the insensitivity of the plant to increases in the auxin concentration.

Our findings indicate that tasiRNAs create a balance in the level of the protonemal auxin response, allowing repressive ARFs to buffer cells against small fluctuations in auxin signaling while simultaneously sensitizing the plant to changes in the auxin concentration, thus allowing it to tune its developmental response by varying the levels of input into auxin signaling. This property of tasiRNAs may have been key to their repeated cooption over the course of evolution.

tasiRNAs modulate the auxin response in moss as part of a complex GRN

Spatial regulation by tasiRNAs allows for a robust and sensitive auxin response in cells at the protonemal edge

tasiRNAs and miR1219 play a crucial role in establishing the pattern of repressive ARF expression within the plant. Our results indicate that the promoter of the repressive *PpARFb4* is active in nearly all filaments, in 5–12 cells from the edge of the protonemal mat (and in additional cells in conditions with high amounts of exogenous auxin), as well as in developing gametophore buds. tasiRNAs and miR1219 act together to limit the expression of this gene to the 1–3 cells at the tip of some filaments, and to completely eliminate its expression in many others. sRNA-mediated silencing of *PpARFb4* appears strongest further from the protonemal edge, suggesting that tasiRNAs and/or miR1219 may be expressed in a gradient originating near the center of the protonemal mat. Such sRNA gradients have been proposed to help establish a sharp spatial boundary in target gene expression (Levine et al., 2007), and a gradient of tasiRNAs participates in patterning the adaxial-abaxial leaf axis in flowering plants (Chitwood et al., 2009). In protonema, which elongate solely by division of the tip cell, tasiRNA

mobility may provide an extra useful property: by moving into the newly formed cells near the tips of filaments, tasiRNAs would continue to restrict PpARFb expression to the edge of the growing protonemal mat.

The restriction of repressive B-group ARFs to the protonemal edge suggests that they may be playing a special role in regulating the auxin response in this domain. Recent work in flowering plants has shown that distinct meristematic regions display differences in their capacity to respond to auxin as a result of the differential expression patterns of ARFs, Aux/IAAs, and TIR-family auxin receptors. These patterns result in a meristem periphery that is able to respond to auxin maxima by initiating lateral organs, and a meristematic central zone that is not responsive to the high levels of auxin it often experiences (Vernoux et al., 2011). Similarly, we hypothesize that differential auxin response in different domains of the plant plays a key role in regulating moss development. The expression of tasiRNA-targeted repressive ARFs at the protonemal edge may allow for the selective repression of the auxin response in this domain. However, additional observations hint at a more complex scenario of repressive ARF function.

We observe both an expansion of PpARFb4 expression and an increase in auxin-regulated processes in plants grown on exogenous auxin. This seemingly paradoxical result hints at the possibility that in WT plants, PpARFb4 may act to stabilize the auxin response in those parts of the plant where auxin signaling induces caulonemal differentiation. Such rheostat-like function has already been proposed to be a key role of the repressive ARFs expressed in the periphery of the flowering plant shoot apical meristem. Here, at the site of organ initiation, the capability to respond to auxin must remain high while responses to spurious and frequent stochastic fluctuations in auxin signaling are prevented. To achieve this, activating ARFs responsible for inducing auxin-responsive genes are coexpressed with repressive ARFs, which dampen this response and prevent auxin-regulated genes from being activated as a result of small fluctuations in auxin signaling levels (Vernoux et al., 2011).

Our hypothesis for the mechanism of tasiRNA- and ARFb-mediated regulation of the auxin response is summarized in Fig 5.1. In the absence of repressive ARFs, chloronemal tip cells are sensitive to auxin, responding at low concentrations by switching to caulonemal

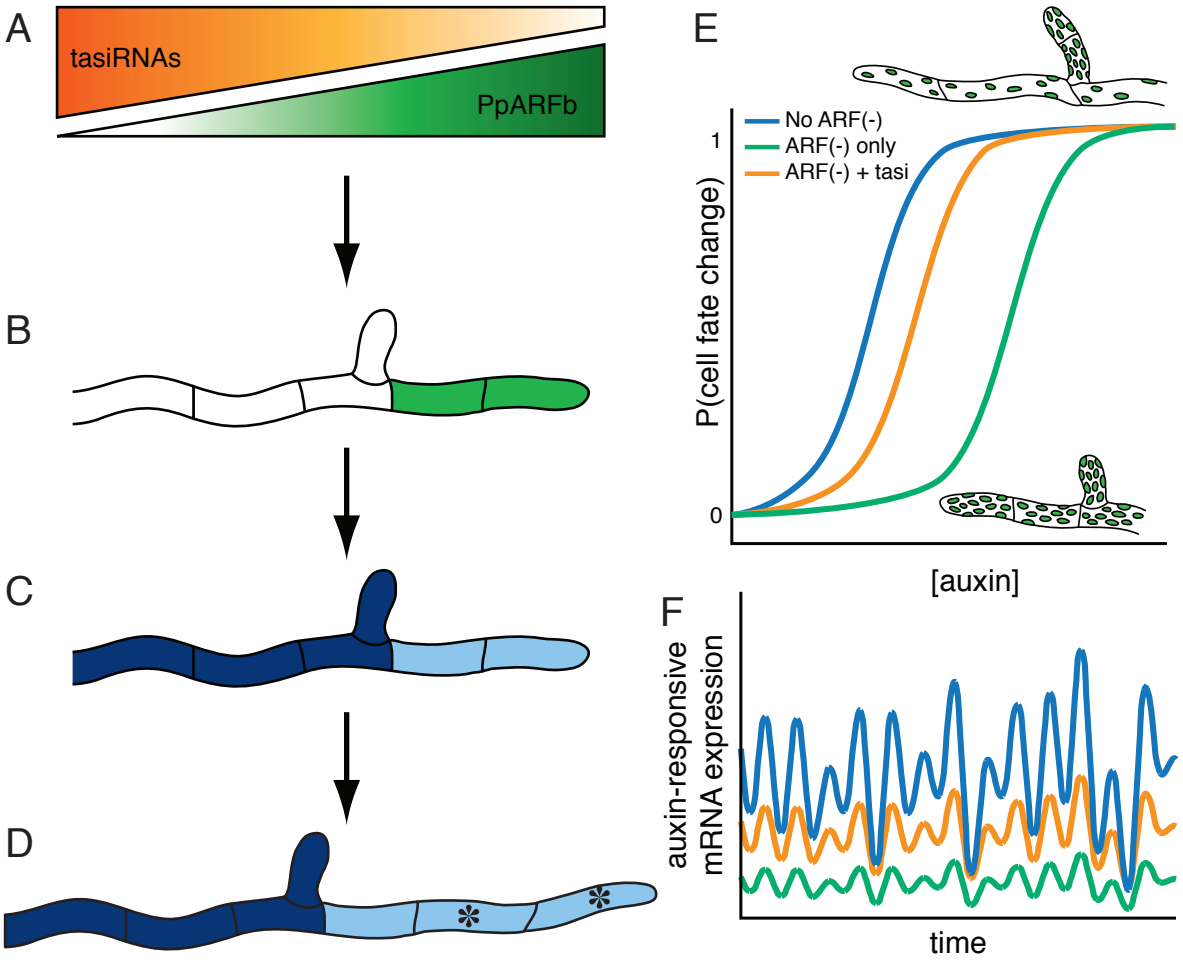

Figure 5.1: A model of spatial regulation of the auxin response in moss
(A) tasiRNAs act more strongly further from the protonemal edge, and we propose that they may form a gradient from the center of the protonemal mat. This gradient opposes the expression pattern of B-group ARFs. **(B)** The opposing gradients of tasiRNAs and *PpARFB* promoter activity result in a boundary of PpARFb expression 1-3 cells from the tip of chloronemal filaments. **(C)** Expression of B-group ARFs represses auxin-regulated genes, such as *PpRSL1*, in cells closest to the protonemal edge. **(D)** In response to auxin signaling, expression of auxin-regulated genes is induced in the sensitive cells at the chloronemal tip, causing their differentiation into caulonema (*). **(E-F)** The proposed model of the effect of ARF expression on the dynamics of the auxin response in chloronemal tip cells. In the absence of repressive ARFs (blue line), cells are sensitive to auxin, but fluctuations in auxin signaling cause strong fluctuations in the auxin response (F, blue line). Strong expression of repressive ARFs (green line) solves the problem of robustness by decreasing the sensitivity of the auxin response to noise, but also requires a very high concentration of auxin to trigger caulonemal runner formation . In the presence of tasiRNAs (orange line), repressive ARF expression is decreased, increasing the sensitivity of the cell to auxin while maintaining a degree of robustness to auxin signaling fluctuations.

runner cell fate. However, they are also sensitive to fluctuations in auxin signaling, which can force the cell to pass auxin response 'threshold' for caulonemal runner differentiation (Fig 5.1e–f, blue line). This high level of noise can be mitigated by the expression of repressive ARFs; however, cells now require a very high amount of auxin to initiate caulonemal runner formation, as is seen in *Ppsgs3* mutants (Fig 5.1e–f, green line). The expression of tasiRNAs decreases repressive ARF levels in the cell, creating a balance between robustness to fluctuations in auxin signaling and sensitivity to auxin (Fig 5.1e–f, orange line). As shown in Fig 5.1a, the tasiRNAs are expressed throughout filaments, potentially in a gradient originating towards the filament base, near the center of the protonemal mat. These sRNAs downregulate B-group repressive *ARF* genes throughout the filament. PpARFb expression is thus cleared in most of the filament, and weak expression remains in the cells closest to the tip. This pattern results in the weaker but stable expression of auxin-regulated genes, such as *PpRSL1*, in the tips of growing filaments at the protonemal edge. However, ARFb-mediated repression in these cells is weak enough that auxin, either applied exogenously or produced by the plant, can induce high levels of auxin-regulated gene expression, and cause the differentiation of chloronemal tip cells into caulonema.

Stochastic local variation in the auxin response

Stochasticity in cell fate decisions is thought to play an important role in many developmental processes across a range of organisms. It is especially important for allowing the even distribution of a certain cell type across a large field of cells (Losick and Desplan, 2008). This is reminiscent of caulonemal runner formation in WT plants. Under nitrogen-rich growth conditions, most protonemal cells remain chloronema, but a number of cells along the circumference of the protonemal mat switch to become caulonemal runners. Some additional observations also point to stochastic variations in local auxin response in moss protonema. For example, although *Ppsgs3* plants rarely form caulonemal runners on BCDAT media, individual plants occasionally have multiple caulonemal runners emerging from one spot or sector along the protonemal edge (for example, Fig 4.1f). These sectors may represent areas

of increased auxin signaling. Expression of PpARFb4 similarly displays a seemingly stochastic pattern. The auxin-inducible nature of this gene suggests that this stochasticity reflects filament-to-filament differences in the level of auxin signaling.

Interestingly, in both caulonemal formation in *Ppsgs3* and PpARFb4 expression in WT plants, stochastic differences in the auxin response appear not just at the level of individual filaments, but in sectors. The rare caulonemal runner formation in *Ppsgs3* always occurs in contiguous sections of the protonemal edge, and certain patches of the protonemal mat display an increased number of PpARFb4-expressing filaments. One possible explanation for these local differences in auxin signaling levels, spanning multiple filaments, is the uneven distribution of auxin within the substratum. Experiments in liquid-cultured moss have found that the majority of auxin and cytokinin produced by protonema are secreted, including 95% of the auxin (Reutter et al., 1998). Thus, exogenous auxin concentration may play a key role in regulating moss development. Spatial variations in exogenous hormone concentration could easily be created by local differences in synthesis and secretion levels (for example, due to protonemal density), substratum composition, and the movement of water through the substratum. Such variation may create the observed spatial differences in auxin signaling, although the rapid diffusion of auxin may prevent the long-term buildup of the hormone in one location. Instead, other sources of spatial differences in the state of the auxin response GRN at the protonemal edge may play a role in local variation in protonemal development.

tasiRNAs allow for a graded auxin response

As a result of tasiRNA-mediated modulation of the auxin response, WT plants respond to increasing auxin concentrations with graded phenotypic changes. In the absence of tasiRNAs, moss plants display insensitivity to low concentrations of exogenous auxin, resulting in a "switch-like" auxin response (Fig 4.4b). The graded response observed in WT may allow plants to modulate their development in response to a wide range of stimuli. However, how tasiRNAs allow for such behavior to occur from a mechanistic point of view is not immediately clear.

Both modeling of cell fate decisions and experimental evidence across multiple species and developmental contexts have demonstrated that cell fate decisions often display switch-like behavior (Ferrell, 2002). Such switch-like responses to signaling allow their outputs to be robust to small perturbations across much of the range of signaling, and many common regulatory motifs result in a switch-like output (Masel and Siegal, 2009). Even in cases where changes in input level result in a graded molecular response, downstream cell fate decisions often display switch-like behavior (Mackeigan et al., 2005). Modeling of simple auxin response circuits suggests that auxin signaling may also result in a switch-like response (Lau et al., 2011). These switch-like mechanisms allow cells to 'commit' to a cell fate decision. The transition from chloronemal cell to caulonemal runner cell may represent a similar, all-or-nothing decision, in which case a switch-like auxin response may be beneficial.

Although the output of the auxin response in individual chloronemal cells is likely switch-like, the moss plant as a whole appears to respond to auxin signaling in a graded manner. A classic example of this difference between the dynamics of individual- and population-level responses is found in *Xenopus* oocytes. Here, the activation of MAPK in response to progesterone is highly switch-like in individual oocytes. However, inter-oocyte differences in the concentration of progesterone required to activate MAPK lead to the appearance of a graded response when groups of oocytes are examined together (Ferrell and Machleder, 1998). Similarly, we believe that cell-to-cell differences in auxin signaling, either as a result of uneven auxin distribution throughout the substratum or stochastic differences between cells in the state of the auxin response network, result in a graded response of the protonemal tissue to increasing auxin concentrations.

In the absence of tasiRNAs, *Physcomitrella* is responsive to exogenous auxin, but only at high levels, and displays a seemingly switch-like response across the entire plant. This suggests that the role of tasiRNAs is to decrease the threshold for auxin responsiveness in chloronemal cells. Although individual cells display variability in their auxin responsiveness, tasiRNAs (together with miR1219) lower repressive ARF expression across the protonemal edge to such a level as to allow a significant number of cells there to respond to auxin in physiological ranges of this hormone. In the absence of tasiRNAs, the threshold for auxin

response is set too high for the levels of auxin signaling in most cells at the protonemal edge, resulting in a failure to make caulonemal runners. This threshold can be overcome with the application of sufficient amounts of exogenous auxin, but such high auxin levels result in the simultaneous triggering of the auxin response across most chloronemal cells.

The modulation of the auxin response in moss presents a fascinating direction for additional research. We hypothesize that the auxin response is switch-like in individual cells, and experiments on moss with a transcriptional auxin reporter will be able to directly test this model. Such a system can also be used to test the effect of other auxin GRN components on this response, and would allow further examination of detailed properties of the auxin response network in *P. patens*, including the spatiotemporal pattern of the auxin response and the effect of changes in the levels of sRNAs feeding into the network. In light of our results, the examination of the role of another conserved sRNA that targets putative repressive *ARF* genes—miR160—should be examined in the context of the auxin response. Finally, computational modeling of the auxin response GRN, integrating sRNAs as well as our findings on feedback loops within the network, may allow further examination and refinement of our hypothesis regarding the role of tasiRNAs in setting a threshold for the auxin response.

Environmental regulation of moss development via modulation of the auxin response

The auxin response as a developmental effector of exogenous signaling

Unlike most animals, plants are sessile, and thus unable to escape unfavorable environmental conditions. This, combined with the continuous development they undergo throughout their lives, necessitates mechanisms of modulating development based on external signals. Mosses are no exception, as demonstrated by the effect of soil type and media nutrient content on *Physcomitrella* development (Fig 5.2a–f). Experiments in cultured mosses have allowed the developmental effect of varying environmental conditions to be tested one-by-one. Many conditions were found to profoundly affect moss development. Caulonemal formation appeared

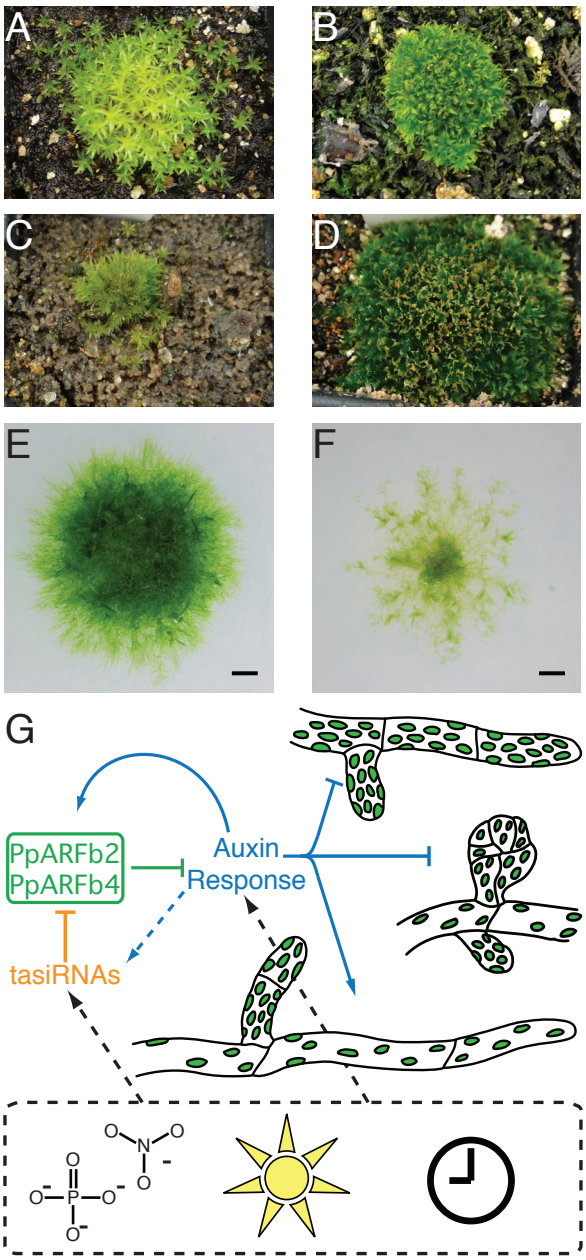

Figure 5.2: Environmental conditions profoundly influence moss development and may feed into the auxin response GRN via tasiRNAs
(A - D) 7-week-old *Physcomitrella* grown on Rediearth, Metromix, maize potting soil, and soil from Uplands Farm at Cold Spring Harbor Laboratory, respectively. Plants exhibit differences in color, plant size, gametophore density, gametophore morphology, and caulonemal runner/satellite gametophore formation, depending on soil type.
(E - F) 22-day-old moss plants grown on BCDAT and BC(D) media, which differs only in Nitrogen content, display differences in branching, caulonemal runner formation, and gametophore number. Scalebar = 1 mm. **(G)** tasiRNAs may provide an input node that allows exogenous signals, such as time, light, and substrate nutrient content, to feed into the auxin response gene regulatory network. This network's many inputs and developmental outputs place it in a unique position to intergrate exogenous signals and modulate the plant's development accordingly.

Figure 5.2

especially susceptible, and can be modulated by the levels of nutrients such as Calcium, Phosphorus, and Nitrogen, as well as light levels; gametophore formation and branching are also regulated by light (reviewed in Reski (1998)), and anecdotal evidence suggests that nutrient levels may also play a role in their formation, although this effect may not be direct. Finally, as discussed in Chapter 2, developmental timing plays a critical role in regulating the initiation of gametophore buds and caulonemal runners.

Multiple regulatory networks likely participate in translating exogenous signals into a developmental output in moss. However, the auxin-mediated regulation of nearly all developmental processes modulated by exogenous signals in moss—including branching, caulonemal runner formation, and gametophore formation—suggest that the auxin response network likely plays a key role in moss environmental response. Indeed, studies of cryptochrome (CRY) function in *Physcomitrella* revealed that blue light regulated the auxin response in a CRY-dependent manner (Imaizumi et al., 2002). Other exogenous signals may also affect moss development by feeding into the auxin response GRN.

A role for tasiRNAs in mediating exogenous signals

The role of tasiRNAs in modulating the auxin response makes them ideal mediators of exogenous signals (Fig 5.2g). Changes in tasiRNA levels via regulation by environmentally responsive transcription factors, such as cryptochromes or phytochromes, would cause changes in the auxin responsiveness of the plant, altering developmental output. Experiments are currently ongoing to test the responsiveness of tasiRNA biognesis mutants to environmental perturbations, especially changes in Nitrogen levels. Interestingly, preliminary observations indicate an especially strong effect of the *PpARFb4-m*t** mutation on development on media containing low concentrations of Nitrogen. Additional research is needed to determine the effect of a range of environmental conditions on the levels of tasiRNAs and auxin signaling in *Physcomitrella*, especially in light of preliminary data demonstrating that the levels of tasiRNAs (and potentially their targets) are changed in response to developmental time (Fig 2.6). Tools are now available to address the role of tasiRNA- and miR1219-mediated ARF regulation in the developmental response of *Physcomitrella* to environmental and timing signals.

Direct modulation of tasiRNA levels by exogenous signals, however, is not necessary for tasiRNAs to play a key role in the response to these signals in *Physcomitrella*. By maintaining protonema in an auxin-sensitive state, tasiRNAs potentiate the response to changes in auxin signaling, allowing an effect of exogenous cues on any of a number of nodes in the auxin signaling GRN to be translated into a developmental output.

Evolutionary perspective on the role of tasiRNAs

Regulation of diverse developmental processes by tasiRNAs

Of the tasiRNA pathways found across plants, only the miR390-dependent biogenesis pathway and its targets are conserved between mosses and flowering plants. In flowering plants, these tasiRNAs have been coopted to regulate the development of a diverse set of evolutionarily novel organs, including leaves, meristems, and lateral roots (see Chap 1). Since tasiRNAs do not appear to control shared developmental processes between mosses and angiosperms, they may have been coopted due to certain properties that they lend to the processes they regulate. Detailed analysis of the role of miR390-dependent tasiRNAs in flowering plant development may help reveal the cause of this repeated cooption.

The role of tasiRNAs in the regulation of lateral root outgrowth may be especially instructive with regards to conserved properties of these sRNAs. Much like the developmental processes regulated by tasiRNAs in *Physcomitrella*, lateral root outgrowth in flowering plants is auxin-regulated, and sensitive to environmental conditions, especially substratum nutrient content (Malamy, 2005). Moreover, lateral root formation and outgrowth increase progressively with increasing auxin concentrations (Malamy, 2005), thus displaying the same graded response to auxin as caulonemal runner formation. The role of tasiRNAs in regulating lateral root outgrowth suggests that the modulation of auxin-responsive developmental processes may have been the ancestral function of this pathway. We are currently exploring the lateral root response to auxin in WT and tasiRNA biogenesis mutants in *Arabidopsis* to determine whether, as in moss, tasiRNAs allow the plant to tune the developmental output of its auxin response.

Interestingly, our results hint at an additional potential link between tasiRNAs and root development. In moss, the levels of the auxin-responsive gene *PpRSL1* can be modulated by tasiRNAs (Fig 4.2a). *PpRSL1* is a conserved transcription factor with a role in regulating the development of tip-growing cells across land plants. In *Physcomitrella*, *PpRSL1* is involved in caulonemal and rhizoid specification, whereas in *Arabidopsis*, its homologs *AtRHD6* and *AtRSL1* function in the specification of root hairs (Jang and Dolan, 2011; Jang et al., 2011; Menand et al., 2007b). However, the parallels between developmental processes controlled by *RSL* genes in mosses and flowering plants do not stop there. Much like caulonemal runner formation in *Physcomitrella*, root hair development in *Arabidopsis* is an auxin-regulated process (Masucci and Schiefelbein, 1994) with high sensitivity to substratum nutrient composition (Ma et al., 2001). The similarities between the environmental, hormonal, and genetic factors regulating root hair and caulonemal runner development present a compelling case for future experiments examining the role of tasiRNAs in root hair formation in flowering plants.

tasiRNAs play an important role in regulating developmental timing in *Arabidopsis* (Hunter et al., 2003; 2006), although the degree to which this is conserved in moss is unclear. Previous studies suggested that tasiRNAs delay the transition of protonema to bud formation, promoting 'juvenile' traits, much as they do in *Arabidopsis* (Cho et al., 2008; 2012; Talmor-Neiman et al., 2006). Our data contradicts this finding, which likely reflects the perturbation of additional sRNA biogenesis pathways in the *Pprdr6* mutants analyzed. Nevertheless, we observe that tasiRNAs play a role in the development of many timing-regulated traits, including caulonemal runner and gametophore formation, and that their levels increase as development progresses. The heteroblasty of phyllid development in gametophores, however, does not appear to be affected. Further work is required to determine whether tasiRNAs directly modulate heteroblasty in *Physcomitrella*. Interestingly, the effect of tasiRNAs on developmental timing in *Arabidopsis* appears to be indirect: rather than being regulated over developmental time, tasiRNAs have been hypothesized to set a constant threshold for a developmental signal by downregulating their *ARF* targets (Hunter et al., 2006). The similarity of this model to our model of tasiRNA-mediated modulation of development in *P. patens* has led us to wonder whether auxin signaling may feed into miR156, which in turn provides the signal for the

'juvenile' characteristics promoted by tasiRNAs in *Arabidopsis* development (Wu and Poethig, 2006).

In all attempts to reconcile the role of the tasiRNA pathway between flowering plants and mosses, it is important to remember that cooption can work in many ways. Regulatory networks need not be coopted for the same reason every time, and a pathway that was coopted once because of its ability to modulate the response to a developmentally important hormone may be coopted another time in a different way because of its favorable expression pattern or developmental output. The cooption of tasiRNAs for the regulation of flowering plant adaxial-abaxial leaf development may represent one such alternative cooption. tasiRNAs act to restrict the expression of their target ARFs to the abaxial side of the developing leaf, where these targets act as determinants of abaxial cell fate. However, unlike the processes described above, leaf polarity does not display a graded developmental output, and is primarily not an environmentally regulated process. On the contrary, there is evidence that tasiRNAs are necessary for robust adaxial-abaxial patterning, buffering against environmental perturbations rather than allowing them to be integrated into development (Timmermans et al., 1998). Other properties of tasiRNAs, such as their ability to form a gradient and to spatially regulate their targets, may have contributed to their cooption for establishing adaxial-abaxial leaf polarity. Thus, the conserved role of the tasiRNA pathway as a modulator of auxin-responsive developmental processes appears especially compelling in some cases, such as its role in lateral root outgrowth, but may present a weaker case in others.

Regulatory properties of the auxin response GRN, and especially the role of tasiRNAs, may have contributed to its frequent cooption

Our data uncovered a number of feedback loops in the auxin response GRN. These include a complex regulatory effect of auxin on tasiRNA and miR1219 levels that warrants further investigation. In addition, our results indicate an auxin-responsive upregulation of repressive ARFs, which is likely to play a key role in the dynamics of the auxin response. This regulatory circuit constitutes one of two major negative feedback loops in the auxin response GRN in *Physcomitrella*. However, the two circuits demonstrate important differences. The

inhibitory effect of Aux/IAA upregulation on the auxin response can be directly counteracted by increased auxin levels, which cause the degradation of Aux/IAA proteins. By contrast, repressive ARF activity is likely unaffected by auxin levels (Vernoux et al., 2011), and thus the increase in repressive ARF levels in response to auxin represents constitutive negative feedback. Interestingly, this subcircuit of the auxin response GRN may also be conserved in flowering plants, as *AtARF4*—a tasiRNA target—is one of the few repressive *ARF*s whose transcript levels are upregulated in response to auxin signaling in *Arabidopsis* (Paponov et al., 2008). Modeling of this constitutive negative feedback loop is necessary to further understand its effect on auxin response dynamics.

Our data demonstrate that tasiRNAs promote sensitivity to auxin, allowing plants to respond to a range of auxin concentrations with graded developmental outputs. Sensitivity to auxin could be increased by simply eliminating repressive ARF expression, but instead, this task is accomplished by a highly conserved tasiRNA/repressive ARF circuit. Additionally, another group of putative repressive *ARF*s is regulated by a conserved miRNA, miR160, across all land plants. The key to explaining this seemingly convoluted mechanism of increasing sensitivity to auxin may lie in the ability of sRNAs to confer robustness to the expression of the genes they regulate (Ebert and Sharp, 2012). Indeed, a breakdown in the robustness of caulonemal runner formation is observed in miR1219- or tasiRNA-resistant mutants of *PpARFb4*. Thus, tasiRNAs may have been conserved due to their ability to provide a robust way to maintain auxin sensitivity while allowing the plant to be buffered against small perturbations in auxin levels through the low-level expression of repressive ARFs.

The ability of tasiRNAs to modulate auxin response levels uniquely positions them to serve as inputs for exogenous signals. By regulating tasiRNA levels, such signals can affect the many developmental processes regulated by auxin signaling. It has been proposed that certain 'input/output genes' that occupy a central position in developmental GRNs are more likely to be coopted over the course of evolution (Stern and Orgogozo, 2008; 2009). In plants, the entire auxin response GRN can be thought of as the input/output node of a larger developmental regulatory network. We suspect that tasiRNAs may function as an 'input' module of this node, integrating exogenous signals into the auxin response GRN, thus altering the expression of

ARF-regulated genes and the developmental processes that they control.

Auxin-regulated processes are iconically ubiquitous in modern land plants. The reason for the cooption of the auxin signaling pathway to regulate the development of such a wide array of tissues and organs, in plants as different as mosses and angiosperms, remain a key question in plant evolution. This question is further complicated by the fact that the auxin response GRN does not appear to regulate a consistent set of morphogenic processes across organisms and developmental contexts. Thus, rather than being coopted because of its role in the regulation of a key set of downstream effector genes, the properties lent to the auxin response by its network organization may have been a key factor in this hormone's repeated repurposing (see Fig5.3). Our results indicate that sRNA regulation imparts a number of key properties to the auxin response, including robustness, sensitivity, and potentially, flexibility of inputs. These data hint that the ancient association of the auxin response network with tasiRNAs, and perhaps with miR160, may have played a key role in its evolutionary success.

Perspective

Our work in *Physcomitrella* identifies multiple regulatory subcircuits in the GRN regulating plants' response to the ancient phytohormone auxin, and suggests that tasiRNAs may play a conserved role in the development of land plants by promoting sensitivity of the auxin response while maintaining its robustness. This model allows us to conceive of a number of testable hypotheses regarding the mechanism of tasiRNA-mediated developmental regulation in flowering plants. It is our hope that further experimental work in model angiosperms will put these hypotheses to the test. While some of these may prove correct, the ones that don't will provide new models to explain why certain genetic networks are coopted for novel functions. Such crosstalk between evolutionary questions and hypotheses and developmental analysis is crucial for understanding both the proximal mechanisms and ultimate causes of the genetic regulation of development, and we hope that the work presented here contributes to this scientific feedback loop.

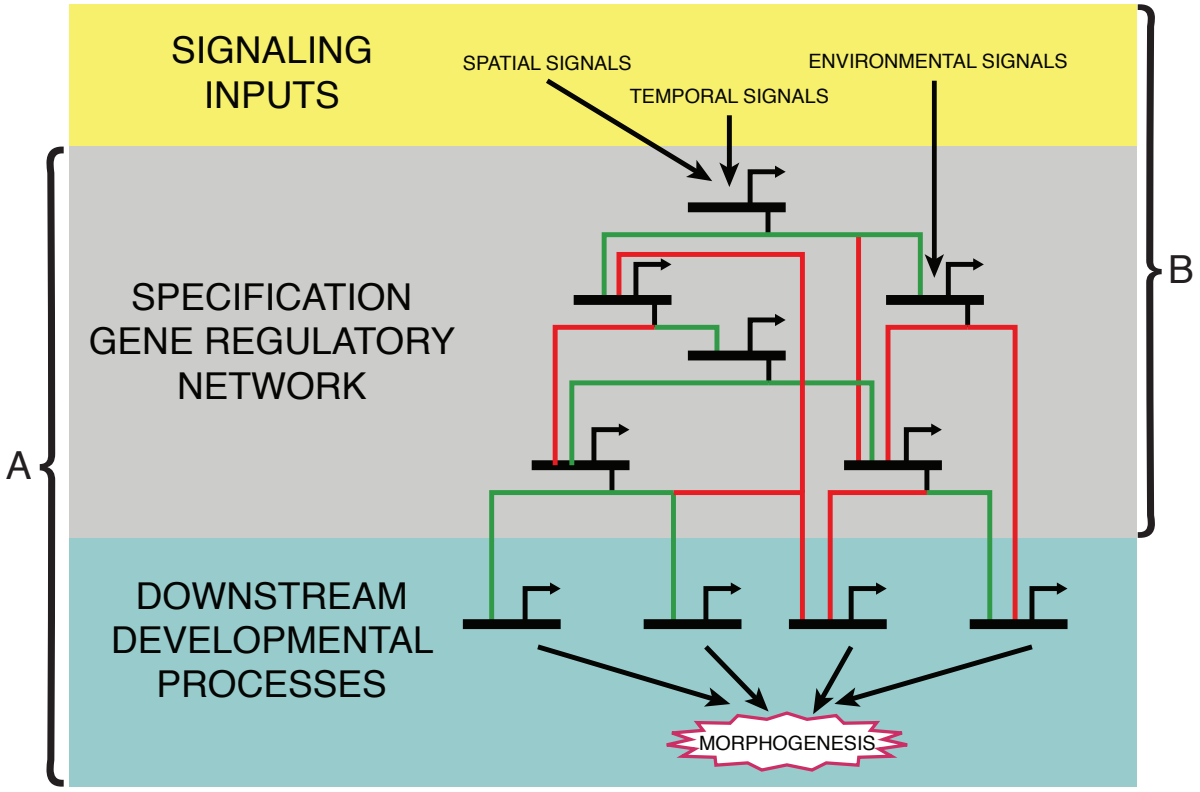

Figure 5.3: Cooption of regulatory networks
A hierarchical gene regulatory network, with signaling inputs feeding into a complex specification GRN, which includes complex feedback regulation, and the outputs of the specification GRN regulating downstream developmental effectors, which in turn control morphogenesis. **(A)** Cooption of a specification GRN component coopt with it downstream effector genes as well, resulting in the transplantation of existing morphogenic processes to a new developmental context. Cooption of the Dll genes in insect limb evolution is likely one example of this evolutionary mechanism. **(B)** Alternatively, a network can be coopted - often with many upstream inputs intact - but the downstream genes it regulates can be changed over the course of evolution. In this case, rather than the specific developmental processes it regulates, the properties of the regulatory network - such as robustness and sensitivity - likely play the key role in the network's cooption. This is likely the case with the auxin response GRN, which regulates a range of developmental processes across land plants, but whose internal organization appears to be conserved over evolutionary time.

Chapter 6

Materials and methods

Identification of a *Physcomitrella* SGS3 homolog

Physcomitrella SGS3 homologs was identified by using AtSGS3 as a query for a blastp search (Altschul et al., 1997) against the *Physcomitrella* genome (Rensing et al., 2008). Alignment of the protein sequences of *Arabidopsis*, maize, and *Physcomitrella* SGS3 was performed using M-COFFEE (Moretti et al., 2007). The XS domain was identified using the Conserved Domain Database (Marchler-Bauer et al., 2002). Sequence similarity and identity was calculated using ClustalW (Larkin et al., 2007).

Moss culture

The Grandsen strain of *P. patens* was kindly donated by the Quatrano Lab. Moss was cultured under continuous light and at 25°C on BCD media enriched with 5mM Ammonium Tartrate (aka 'BCDAT'), as described in Cove et al. (2009a), but without including $FeSO_4$ in media. Sporophyte development was induced on BC media containing 0.5 mM KNO_3 and 90 μM $FeSO_4$ (aka 'BC(D)'). Moss subculture was performed by vortexing protonemal tissue in water with a glass bead for approximately one minute in a 10 mL plastic screwcap centrifuge tube. Homogenized protonema was then plated onto BCDAT media overlaid with cellophane discs (AA Packaging) and grown for 5–7 days.

For experiments on individual plants, moss was subcultured 2–5 times, and plantlets 1–3mm in diameter were transplanted to solid media 5 days after the final subculture. Plant age is reported as the number of days a plant was grown after transplantation. For experiments on moss grown from spores, spores were sterilized as described in Cove et al. (2009a), suspended in water, kept at 4°C in the dark for $\sim$1 week, and plated onto solid media.

Creation of transgenic plants

Cloning of transformation constructs

To clone the construct used to create *Ppsgs3* mutants, 5′ and 3′ homology regions were PCR-amplified using Phusion DNA polymerase (NEB) from genomic *Physcomitrella* DNA with

EP23–EP24B and EP27E–EP28E, respectively. PCR products were cloned using pCRII-TOPO TA cloning kit (Invitrogen). Insertion in the desired direction was verified, and plasmids were digested using *Bgl*II + *Not*I and *Kpn*I + *Xba*I, and cloned between the *Bam*HI + *Not*I and *Kpn*I + *Xba*I sites of the BHSNR vector (Menand et al., 2007b), respectively.

To clone the construct used to create *PpARFb4-GUS* plants, DNA segments were amplified using Phusion DNA polymerase, and overlap extension PCR (Higuchi et al., 1988) was performed on combinations of segments in a stepwise manner until the full linearized construct was assembled. The assembled linear construct was then treated with Polynucleotide Kinase (NEB) and self-ligated using the Rapid DNA Liagation Kit (Roche). The 5′ homology region was amplified from *Physcomitrella* genomic DNA with EP196–EP81, and then again with EP196–EP376, to add the necessary overlap region. The 3′ homology region was amplified using EP197–EP197. The *GUS* transgene and 35S terminator were amplified using EP378–EP379 from the pKGWFS7 vector (Karimi et al., 2002). Fragments of the pCR8 vector backbone (Invitrogen) were amplified using EP273–EP179 and EP180–EP276. The *NptII* resistance cassette was amplified from the BNRF vector (Menand et al., 2007b) using EP377–EP198.

To create the m^* mutation in the *PpARFb4-GUS* construct, two segments were amplified using EP273–EP207 and EP206–EP276, and overlap extension PCR and self-ligation were performed as described above. To create the t^* mutation, segments of *PpARFb4-GUS* were amplified with EP273–EP209 and EP208–EP276, followed by overlap PCR and self-ligation.

Moss transformation

Moss was transformed as described in (Cove et al., 2009b) with the following minor adjustments. For protoplast isolation, protoplasts were digested for 30 minutes in 2% Driselase, followed by one round of filtering using 40 μm Cell Strainers (BD Falcon). Washes were performed using 8% D-mannitol without $CaCl_2$. Post-transformation dilution in D-mannitol was performed over the course of 30 mins.

Transformations were performed using 10-30 μg linearized DNA. Linearization was performed by digesting transformation constructs using *Hind*III for the creation of *Ppsgs3.20*

and *Bgl*II for *PpARF2a-GUS*, m^*, t^*, and m^*t^*. For *Ppsgs3.152* and *Ppsgs3.173*, PCR amplification from the SGS3-KO construct was performed with primers EP430–EP55E using ExTaq DNA polymerase (TaKaRa).

PCR validation of targeted insertion

Initial transformants were screened using PCR screening with GoTaq DNA polymerase (Promega). *Ppsgs3* mutants were screened using EP119–EP120, EP123–EP124, and EP122–EP61I to test for the presence of the WT locus. EP119–EP126 and EP61I–EP121 were used to test for the targeted 5′ and 3′ transgene insertion, respectively. *PpARF2a-GUS*, m^*, t^*, and m^*t^* plants were tested using EP128–EP70 to test for targeted 5′ transgene insertion. EP91F–EP210 were used to amplify a fragment of DNA containing the miR1219 and tasiR-ARF binding sites, and digests were performed with *Nhe*I and *Stu*I to test for the m^* and t^* mutations, respectively.

Transgene copy number quantification

For DNA extraction, 3-9 cellophane-covered plates of protonemal tissue were harvested, blotted on a paper towel, and ground in liquid Nitrogen. Ground tissue was then mixed with Extraction Buffer containing 100 mM Tris-HCl (pH 8.0), 1.42 M NaCl, 2% CTAB, 20 mM EDTA, 1.4 X 10^{-3} 2, beta-mercaptoethanol, 5 X 10^{-4} ascorbic acid and 2% PVP-40, and extracted twice with 24:1 Chloroform-Isoamyl Alcohol. Southern blots were then performed as described in Sambrook et al. (2001). To assay transgene copy number in *Ppsg3.20* plants, blots were hybridized with a probe amplified from the hygromycin resistance cassette using EP61H–EP125. To assay transgene copy number in *PpARF2a-GUS*, m^*, t^*, and m^*t^* plants, blots were hybridized with a probe amplified from the 5′ homology region using EP354–EP64B.R.

To determine transgene copy number by quantitative PCR (qPCR), reactions were performed on 5–20 ng purified DNA. To assay transgene copy number in *Ppsgs3.152* and *Ppsgs3.173*, EP502–EP431 and EP503–EP504 were used to test for the presence of the 5′ and

3' homology regions, respectively, with EP505–EP506 serving as a genomic control. Copy number was calculated using the formula $2^{(C(t)_{homologyregion_{WT}} - C(t)_{genomic_{WT}})}$.

Transformants with more than one insertion of the transformation cassette were discarded, with the exception of *Ppsgs3.20*, in which the transformation cassettes were shown by Southern blot to be inserted in tandem into the target locus.

Quantification of gene and sRNA expression

RNA Isolation

Total RNA was extracted from *Physcomitrella* using Trizol reagent (Invitrogen) according to the manufacturer's suggested protocol. For extractions from cellophane-grown tissue, protonema were subcultured 2–5 times, then cultured for 5 days on cellophane-overlaid BCDAT media, blotted dry on a paper towel and frozen for RNA extraction.

For extractions from solid media-grown plants, moss was subcultured and individual mosslets planted out as described in Phenotyping. Individual plants were cut out of solid media, minimizing the amount of media attached to the plant but taking care not to damage the tissue. Samples were incubated ∼3 mL Buffer QG (Qiagen), to dissolve agar. Plants were then vortexed on the lowest setting for 5 minutes, Buffer QG was replaced, and the process was repeated. This was followed by two 5–10-minute-long washes with double-distilled water. Tissue was then blotted dry on paper towels, and frozen for RNA extraction. Forty 4-day-old, fifteen 8-day-old, six 15-day-old, or one to two 22-day-old plants of a genotype were pooled for each biological replicate. To minimize environmental effects on gene expression, mutant and WT plants were grown simultaneously on the same plates. 3–6 replicates were used in total.

sRNA qRT-PCR

RNA was extracted from moss plantlets as described in RNA Isolation in 3 biolgical replicates; unless otherwise stated, tissue from moss plants 15 days post-transplantation was

used. For sRNA cDNA synthesis and qPCR, we followed a protocol modified from (Varkonyi-Gasic et al., 2007), using the Superscript III kit (Invitrogen). The major change to the protocol was that distinct hairpin primers with variants in the loop sequence were used for every unique sRNA, to allow for a unique reverse qRT-PCR primer for each sRNA amplified. Stem loop primers for miR390, miR1219, and tasiR-ARFs, as well as the reverse primer for the U6 snRNA, were pooled into one synthesis reaction for each RNA sample. A separate set of synthesis reactions was performed using the U6 primer and tasiR-AP2 stem loops. A list of the primers used is provided in Appendix A. qRT-PCR was performed on 2–3 technical replicates using the IQ SYBR Green Supermix (Bio Rad). Reactions were performed at an annealing temperature of 60°C and an extension time of 30 seconds. The formula $2^{(C(t)_{U6} - C(t)_{sRNA})}$ was used to normalize sRNA expression levels to U6 levels.

transcript qRT-PCR

RNA was extracted from moss plantlets as described in RNA Isolation in 3-6 biolgical replicates; unless otherwise stated, tissue from moss plants 15 days post-transplantation was used. cDNA was synthesized with oligo(dT) primers using the Superscript III kit (Invitrogen) following the manufacturer's suggested protocol. A list of primers used for qPCR are provided in Appendix A. qRT-PCR was performed at an annealing temperature of 57°C and an extension time of 30 seconds, except in the case of the data presented in Fig 2.6b, for which an annealing temperature of 59°C was used. Each reaction was performed in 3 technical replicates; any clear outliers among the technical replicates were discarded. The $2^{(C(t)_{GAPDH} - C(t)_{gene})}$ was used to normalize gene expression levels to GAPDH levels.

RLM 5' RACE

RNA was extracted from cellophane-grown tissue as described in RNA Isolation. RLM 5' RACE was performed as described in Axtell et al. (2007), using forward primers from the GeneRacer RACE kit (Invitrogen) and Phusion DNA polymerase (NEB). For *PpARFb1*, a PCR reaction was performed with EP367 at annealing temperature of 64°C and an extension time of 30 seconds. Nested PCR was performed using EP368 and the following 'touchdown' PCR

regime: 98°C for 30″; 98°C for 10″, 80°C (and stepping down by 1°C at every cycle) for 10 cycles; 98°C for 30″, 68°C for 30″, 72°C for 30″, for 30 cycles; 72°C for 5′. For *PpARFb1*, a PCR reaction with EP370, 64°C annealing temperature, 30 seconds extension time was followed by a nested PCR reaction with EP370 at 70°C annealing temperature, 30 seconds extension time.

Phenotyping

Unless otherwise stated, phenotyping experiments and RNA extractions were performed on tissue grown on modified BCDAT media containing 90μM $FeSO_4$. To minimize environmental effects on gene expression, all plants constituting a single experiment were grown simultaneously on the same plates, and all plates were placed on the same incubator shelf. Unless otherwise stated, all experiments were performed under continuous light. In most cases, experiments were repeated two or more times, and representative results are presented here.

Gametophore counts

Gametophores were counted by visually examining plants using a dissecting microscope, without taking them apart. Only buds with at least one phyllid were counted. Each data point represents the average of ten plants, and the same plants were followed over the timecourse presented.

Soil experiments

Cellophane-cultured plantlets were transplanted 5–7 days post-subculture to moist soil and were grown under a plastic dome for two months at ∼22°C under a 16/8 light/dark regime. Soil was kept moist throughout the course of the experiment. Unless otherwise stated, experiments were performed on Rediearth (Sungro).

Branching analysis

Branching analysis was performed on plants ∼3 weeks post-transplantation. Plants were cut out from plates together with surrounding agar and fixed in FAA (3.7% formaldehyde, 5% acetic acid, 50% ethanol, by vol). Sections of agar were then cut out, starting close to the center of the plant. Under a dissecting microscope, individual filaments running from the center of the plant to the edge of the protonemal mat were selected and pulled out of the agar with extreme care. For photography, filaments were immobilized in 0.2% agarose. For branch tracing, filaments were observed at high magnification and every protonemal cell, gametophore bud, and branch position was noted from the growing tip of the filament to the oldest cell originating near the center of the plant (usually 25–40 cells in one filament). At least 8 filaments from 3 or more plants were analyzed in each genotype.

Cell length measurements

Plants were collected and fixed as described in Branching Analysis. Protonema near the protonemal edge, including primary filaments and branches, were removed from agar, flattened on slides covered with a thin pad of 4% agarose, and photographed on a compound microscope. ImageJ (Collins, 2007) was used to measure chloronemal cells 3–5 cells from the tip. 8 or more filaments from 2–3 plants of each genotype were analyzed.

Chemical treatments

Chemical treatments of *Physcomitrella* were performed by adding ethanol-dissolved NAA, PCIB, or beta-estradiol to moss growth media. Ethanol did not make up more than 0.1% of media by volume, and all plates in a given experiment—regardless of hormone concentration—contained the same concentration of ethanol.

Protein experiments

Individual plants were pulled out from agar, frozen, and protein was extracted from individual plants and analyzed with SDS-PAGE as described in Sambrook et al. (2001). Proteins

were transferred to a membrane and detected with a polyclonal anti-HA antibody (Roche) using SuperSignal West Femto Chemiluminescent Substrate (Pierce) according to the manufacturer's suggested protocol.

Histochemical staining

Plants were cut out of plates, together with surrounding agar, taking care not to damage tissue, and added to staining solution containing 50 mM sodium phosphate (pH 7.0), 10 mM EDTA, 0.05% Triton-X, 2 mM ferrocyanide, 2 mM ferricyanide, 0.05% X-Gluc, 75 mg/L Kanomycin, and 150 mg/L Spectinomycin and vacuum-infiltrated for 30–60 mins at $\sim$600 mm Hg. *PpARF2a-GUS*, m^*, t^*, m^*t^* and WT plants were then incubated in staining solution for 14 days at 37°C, with staining solution being exchanged every 3 days. *PpRSL1p::GUS* plants were stained in the same conditions, but for 1 hour, or for 13 hours in the case of 'extended' staining shown in Fig 3.5e inset. After staining, plants were vacuum-infiltrated as before but with FAA, cleared in 70% ethanol, and examined with a dissecting microscope.

Appendix A

Primers

Primer	Sequence	Purpose
EP367	ATCTGCACGTGGGAACCAGCTTTGCT	5' RACE
EP368	GGCTTGACGTTCCACGAGGTATTTCG	5' RACE
EP369	CACTCGACACGTCGTTGCTGAGAGTT	5' RACE
EP370	ATGAGGAGGTCCGGGAGGATTCGATA	5' RACE
EP464	GTTGGCTCTGGTGCCCACGTGCTTCGATTCGCACCAGAGCCAACAAGCTA	cDNA synthesis: miR1219a-c
EP453	GTTGGCTCTGGTGCAGGGTCCGAGGTATTCGCACCAGAGCCAACGGCGCT	cDNA synthesis: miR390a-c
EP521	GTTGGCTCTGGTGCCCACGTGCTTCGATTCGCACCAGAGCCAACTGAAGC	cDNA synthesis: tasiR-AP2a
EP522	GTTGGCTCTGGTGCTGCCGTCCACTGATTCGCACCAGAGCCAACGGAAGC	cDNA synthesis: tasiR-AP2b
EP523	GTTGGCTCTGGTGCCACGCTGGAGCAATTCGCACCAGAGCCAACCTAAGC	cDNA synthesis: tasiR-AP2d
EP524	GTTGGCTCTGGTGCGTGATGGCGAACATTCGCACCAGAGCCAACATAAGC	cDNA synthesis: tasiR-AP2f
EP466	GTTGGCTCTGGTGCTGCCGTCCACTGATTCGCACCAGAGCCAACTGCCCA	cDNA synthesis: tasiR-ARFa
EP468	GTTGGCTCTGGTGCCACGCTGGAGCAATTCGCACCAGAGCCAACCAACCA	cDNA synthesis: tasiR-ARFb/c/e
EP180	ATGGTCATAGCTGTTTCCTGG	cloning
EP196	AACGACGGCCAGTAGATCTCCGTTGTTGTTTGAGGACGTG	cloning
EP197	CAGCTATGACCATAGATCTTCTGGTTTAGGGGACTACGG	cloning
EP198	CTCGTCACAGTTGGGCGGCCGCGAATTCGAGCTCGG	cloning
EP199	CGCGGCCGCCCAACTGTGACGAGGACGATG	cloning
EP206	CCGCTAGCGACCGACACGAGCGGGTATCACCATGGGAG	cloning
EP207	GCTCGTGTCGGTCGCTAGCGGATTCGTCCCACTCCACTTTC	cloning
EP208	AGGCCTCCAACATTCGTAACCGACTCGTCCCCGCAG	cloning
EP209	GGTTACGAATGTTGGAGGCCTGCGCTTTGGCCTAGGC	cloning
EP23	TATGGGCCCGCGGCCAAGCAATGCTGTCGTCCTCTC	cloning
EP24B	CCGGCCAGATCTATAGTCCTGCAAAGTGGACTATAATCAG	cloning
EP273	AGAACATAGCGTTGCCTTGG	cloning
EP27E	AATCCAGATCCCCCGGGACGTTCTCTTGAAGCGAATTCACGGAGAGGTAG	cloning
EP28E	ACCGAGCTCCACCGGTGGTGGCTGTTGCGGTGCTTTTGTTCCAGTTCC	cloning
EP376	GGTTTCTACAGGACGTAACATGTCGACAGCTCCACCTCCACCTCC	cloning
EP377	GATTGTCGTTTCCCGCGTCGACATAACTTCGTATAATG	cloning
EP378	GGAGGTGGAGGTGGAGCTGTCGACATGTTACGTCCTGTAGAAACC	cloning
EP379	CATTATACGAAGTTATGTCGACGCGGGAAACGACAATC	cloning

Primer	Sequence	Purpose
EP430	TTCTCCCGCAATATTCAAGC	cloning
EP55E	GGTGCTTTTGTTCCAGTTCC	cloning
EP81	AGCTCCACCTCCACCTCCGCCACTGCTCTGAACTGC	cloning
EP128	TTCGTAGGATGACAAACTGGAG	*PpARFb4-GUS PCR* test
EP170	TGATAGCGCGTGACAAAAAC	*PpARFb4-GUS PCR* test
EP210	CCGTTGATTTGGGATACGTC	*PpARFb4-GUS PCR* test
EP91F	CCGGCTGTATTCATGACTTTG	*PpARFb4-GUS PCR* test
EP119	TCTTCCAAGTTCCGATCACC	*Ppsgs3* PCR test
EP120	GGCTTTTTCCGTTCTTGTCTC	*Ppsgs3* PCR test
EP121	GCTTCATGCTGTTGCTTTTG	*Ppsgs3* PCR test
EP122	GCGCTTGATACAGTGGATTG	*Ppsgs3* PCR test
EP123	AGGATCGAACAGGAACAACG	*Ppsgs3* PCR test
EP124	GTACGCACCTTTCCTTCGTC	*Ppsgs3* PCR test
EP126	ATGGAATCCGAGGAGGTTTC	*Ppsgs3* PCR test
EP61I	GGTTTCGCTCATGTGTTGAG	*Ppsgs3* PCR test
EP410	CCAACTTACGTGGTGGGAGT	qPCR - *GAPDH*
EP411	GATCCCAAACTTCTCGTCCA	qPCR - *GAPDH*
EP457	TGGATTCTTCCTGCCTCTCAC	qPCR - miR1219a-c
EP465	GTGCCCACGTGCTTCG	qPCR - miR1219a-c/tasiR-AP2a
EP452	TGGATTAAGCTCAGGAGGGAT	qPCR - miR390a-b
EP454	GTGCAGGGTCCGAGGT	qPCR - miR390a-c
EP481	TGGATTGAGCTCAGGAGGGAT	qPCR - miR390c
EP515	GTCTTTAGGGCAGGCGAGTGAGCAATC	qPCR - *PpAP2a*
EP516	GTGTGGCATGCTGCAAACTATTGGGTG	qPCR - *PpAP2a*
EP517	AAAGTACAGGCGTCTATAGCTGGTGC	qPCR - *PpAP2b*
EP518	GGCTTATTTGAAACGGACCGCGAA	qPCR - *PpAP2b*
EP519	GCAAGCAGTCTACTCATCATGCCA	qPCR - *PpAP2c*
EP520	TTGATGCTGGCGGCTTTCAGCTTT	qPCR - *PpAP2c*
EP375	AGCCAATTTGTTCGACTGGT	qPCR - *PpARFb1*
EP373	GTGAAAGGCACGAAAGGGTA	qPCR - *PpARFb1/PpARFb4*
EP479	GTGATAGGCACGAAAGGGTT	qPCR - *PpARFb2*

Primer	Sequence	Purpose
EP480	CCCTGCAGGACCTTAAACAG	qPCR - *PpARFb2*
EP394	CCAACTTGTTGGACTGCTGA	qPCR - *PpARFb4*
EP398	ATCCGGGAGTCCGAGCTTC	qPCR - *PpIAA1a*
EP399	GGTTCTGCGCAGGAGGTG	qPCR - *PpIAA1a*
EP494	AGAACCAGACTGTGGGTTGG	qPCR - *PpIAA1b*
EP495	TACTGCCCGCTGATGTACTG	qPCR - *PpIAA1b*
EP511	AGGTGAATTTGCACCAAAGC	qPCR - *PpIAA2*
EP512	GCCAACCCACTGTCTGATTC	qPCR - *PpIAA2*
EP418	CCATGCTGGAGAAGGCTATC	qPCR - *PpRSL1*
EP419	TCGGTTTCTCTGACGACTCC	qPCR - *PpRSL1*
EP525	TGGATTTAGGGTGTGATGAGT	qPCR - tasiR-AP2a/b/f
EP526	TGGATTTGGGGTGTGATGACT	qPCR - tasiR-AP2d
EP497	GTGCGTGATGGCGAAC	qPCR - tasiR-AP2f
EP455	TGGATGTATCACAAGGGTAGG	qPCR - tasiR-ARFa
EP467	GTGCTGCCGTCCACTG	qPCR - tasiR-ARFa/tasiR-AP2b
EP469	GTGCCACGCTGGAGCA	qPCR - tasiR-ARFb/c/e
EP462	TGGATTTGTCTCAAGGGTACG	qPCR - tasiR-ARFb/e
EP463	TGGATTTGTCTCAAGGGTAGC	qPCR - tasiR-ARFc
EP459	CGATACAGAGAAGATTAGCATGG	qPCR - *U6*
EP460	GGACCATTTCTCGATTTGTG	qPCR - *U6*
EP125	GGAACCCTAATTCCCTTATCTG	Southern Probe
EP354	TGCATAAGCATGCGTGGTAG	Southern Probe
EP61H	GACGGCAATTTCGATGATG	Southern Probe
EP64B.R	TTTTTGTGGACCCTTCATCG	Southern Probe
EP431	CGAATCCGCACCATAATTTC	Transgene quantification qPCR
EP502	GGTTTTGGTTGTTGCAGCTT	Transgene quantification qPCR
EP505	CAAGCTGGTGAAGGAGGAAG	Transgene quantification qPCR
EP506	ACACCAACAAACCCTTCTGC	Transgene quantification qPCR

Appendix B

Signals and prepatterns: new insights into organ polarity in plants.

Published as Husbands AY, Chitwood DH, Plavskin Y, Timmermans MCP. 2009. Signals and prepatterns: new insights into organ polarity in plants. *Genes & Development* **23**: 1986–1997.

Downloaded from genesdev.cshlp.org on October 6, 2009 - Published by Cold Spring Harbor Laboratory Press

REVIEW

Signals and prepatterns: new insights into organ polarity in plants

Aman Y. Husbands,[1] Daniel H. Chitwood,[1,2] Yevgeniy Plavskin,[1,2] and Marja C.P. Timmermans[1,2,3]

[1]Cold Spring Harbor Laboratory, Cold Spring Harbor, New York 11724, USA; [2]Watson School of Biological Sciences, Cold Spring Harbor, New York 11724, USA

The flattening of leaves results from the interaction between upper (adaxial) and lower (abaxial) domains in the developing primordium. These domains are specified by conserved, overlapping genetic pathways involving several distinct transcription factor families and small regulatory RNAs. Polarity determinants employ a series of antagonistic interactions to produce mutually exclusive cell fates whose positioning is likely refined by signaling across the adaxial–abaxial boundary. Signaling candidates include a mobile small RNA—the first positional signal described in adaxial–abaxial polarity. Possible mechanisms to polarize the incipient primordium are discussed, including meristem-derived signaling and a model in which a polarized organogenic zone prepatterns the adaxial–abaxial axis.

The flattening of the leaf has been an important innovation in the evolution of land plants. The extension of the lamina is an outcome of dorsoventral (adaxial–abaxial) patterning of the developing primordium. Establishment of adaxial–abaxial polarity also directs the differentiation of distinct cell types within the leaf's adaxial/top and abaxial/bottom domains (Waites and Hudson 1995). For example, water-conducting xylem tissue in the vasculature forms adaxially to the sugar-bearing phloem cells. In many plant species, the adaxial side of the leaf also develops a thickened waxy cuticle and a tightly packed layer of palisade mesophyll cells that optimizes the capture of light, while the abaxial side contains loosely packed spongy mesophyll and a higher density of stomatal pores to facilitate gas exchange and regulate transpiration (Fig. 1A,B). The differentiation of these distinct cell fates and the extension of the leaf lamina are important adaptations that maximize photosynthesis while minimizing water loss to the environment.

Unlike animals, plants exhibit indeterminate growth and continuously give rise to new organs, such as leaves, from their shoot. The growing tip of the plant shoot, the shoot apical meristem (SAM), contains a population of pluripotent stem cells that divide to replenish themselves and to provide a persistent source of daughter cells for the formation of new organ primordia (see Maughan et al. 2006). Lateral organs arise at the meristem periphery and become patterned along the adaxial–abaxial axis early in development while the primordium is still closely associated with the meristem. As primordia arise on the flank of the SAM, their adaxial side develops in closer proximity to the meristem tip than their abaxial side, leading botanists as early as the 1940s to suggest that this inherent asymmetry may direct the patterning of the leaf (Fig. 1C,D; Wardlaw 1949).

The first insights into the mechanisms that establish adaxial–abaxial polarity came from elegant surgical experiments conducted soon after. Incipient leaves separated from the meristem by a small incision emerge as abaxialized organs, which suggested the idea that a meristem-derived positional signal, now referred to as the Sussex signal, is required to specify adaxial fate (Sussex 1951, 1954). In addition, such surgically isolated primordia display radial symmetry, implying that abaxial cell fate alone is not sufficient to direct laminar outgrowth in the developing leaf. A recent extension of the Sussex experiments specifically implicates the epidermal layer (L1) in adaxial fate specification, as ablation of L1 cells between incipient primordia and the meristem similarly results in the formation of centric, abaxialized organs (Reinhardt et al. 2005). Interestingly, proximal regions of primordia separated at the P1 stage of development remain abaxialized, despite the correct adaxial–abaxial polarization of the leaf's distal end ("P" referring to plastochron stage or the time between subsequent leaf initiations, such that P0/I1 is the incipient primordium; P1, the first primordium visibly protruding from the SAM; P2, the second oldest primordium; etc.). This suggests that the acquisition of organ polarity occurs gradually and does not spread from distal to proximal regions of primordia, but rather depends on sustained positional information provided by the meristem. Such positional information is, however, required over only a short developmental window. Surgical experiments indicate that by the P2 stage of primordium development, mechanisms within the organ are in place to maintain the separation of adaxial and abaxial domains throughout organ development (Reinhardt et al. 2005).

[*Keywords*: Organ polarity; pattern formation; signaling network; small RNAs]
[3]Corresponding author.
E-MAIL timmerma@cshl.edu; FAX (516) 367-8369.
Article is online at http://www.genesdev.org/cgi/doi/10.1101/gad.1819909.

Downloaded from genesdev.cshlp.org on October 6, 2009 - Published by Cold Spring Harbor Laboratory Press

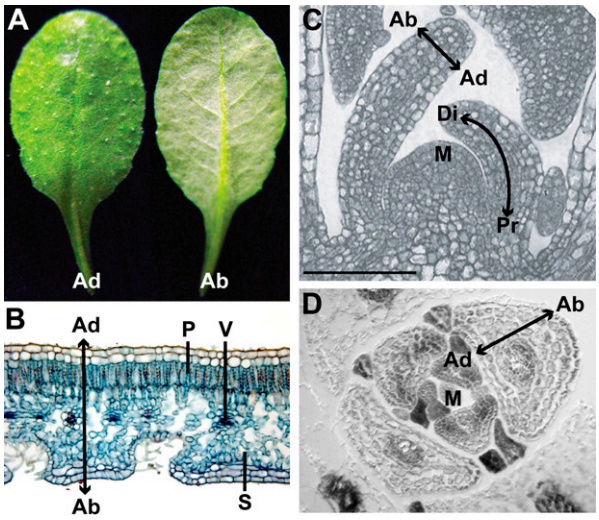

Figure 1. Adaxial–abaxial leaf polarity. (*A*) The adaxial side of an *Arabidopsis* leaf is dark green and trichome-rich, whereas the abaxial leaf surface is gray-green and trichome-poor. (*B*) Transverse section through a *Nerium* leaf illustrating the differentiation of distinct cell types within the adaxial and abaxial domains. Rectangular palisade mesophyll (P) cells form a tightly packed file beneath the adaxial epidermis, whereas spongy mesophyll (S) cells separated by large intercellular air spaces differentiate abaxially. Within the vasculature (V), water-bearing xylem cells differentiate adaxial to sugar-bearing phloem cells. (*C*) Longitudinal section of an *Arabidopsis* apex, showing the proximal–distal and adaxial–abaxial axes of leaf primordia relative to the SAM (marked M). (*D*) Transverse section of an *Arabidopsis* vegetative shoot apex, showing the positions of the adaxial and abaxial sides of leaf primordia relative to the meristem (M). Note the spiral phyllotaxis of leaves around the SAM with increasingly older primordia at a greater distance from the meristem. (The image in *B* is used with permission from the University of Wisconson Plant Teaching Collection at http://botit.botany.wisc.edu/images/130/Leaf.)

While the nature of the positional information from the meristem that polarizes the developing primordium remains unknown, genes involved in adaxial–abaxial patterning have been identified in evolutionarily diverse model organisms, such as *Antirrhinum majus* (snapdragon), *Arabidopsis thaliana*, *Zea mays* (maize), and *Oryza sativa* (rice). Among these polarity determinants are several transcription factor and small RNA families that act in conserved and partially redundant genetic pathways to promote adaxial or abaxial fate. Here, we review the contributions of these genetic pathways to adaxial–abaxial patterning in diverse plant lineages, highlighting in particular the unique role of small regulatory RNAs. We propose that the maintenance of precisely defined adaxial and abaxial domains throughout primordium development is achieved through mutually antagonistic relationships between polarity determinants and signaling across the adaxial–abaxial boundary, perhaps mediated by a mobile small RNA. Finally, we present possible patterning mechanisms that set up the initial polarization of the incipient primordium, including patterning via a meristem-derived adaxializing signal and a model in which the organogenic zone of the SAM is prepatterned along the adaxial–abaxial axis.

Transcriptional regulators of leaf polarity

Adaxial determinants

PHANTASTICA. The first gene recognized to function in the control of leaf polarity—*PHANTASTICA* (*PHAN*), which encodes a MYB domain transcription factor—was cloned from *Antirrhinum* nearly 50 years after surgical experiments suggested the existence of a meristem-derived adaxializing signal (Waites and Hudson 1995; Waites et al. 1998). *phan* mutants display a range of phenotypic severities, governed in part by temperature and leaf position. Basally positioned *phan* leaves exhibit a weak polarity phenotype, developing adventitious blade outgrowths on their upper surface. These outgrowths are associated with sectors of cells that have lost adaxial fate and instead have taken on abaxial identity. The most severe *phan* mutant leaves completely lack flattened lamina and show radial symmetry with abaxial cell types encircling central xylem tissue (see Fig. 2A,B for comparable phenotypes in maize). These phenotypes demonstrate that *PHAN* is necessary to specify adaxial fate in *Antirrhinum*, and support the idea that extension of the leaf blade results from the juxtaposition of adaxial and abaxial tissues (Waites and Hudson 1995). Exactly how an adaxial–abaxial boundary coordinates blade outgrowth, however, is still unclear. In addition to their polarity

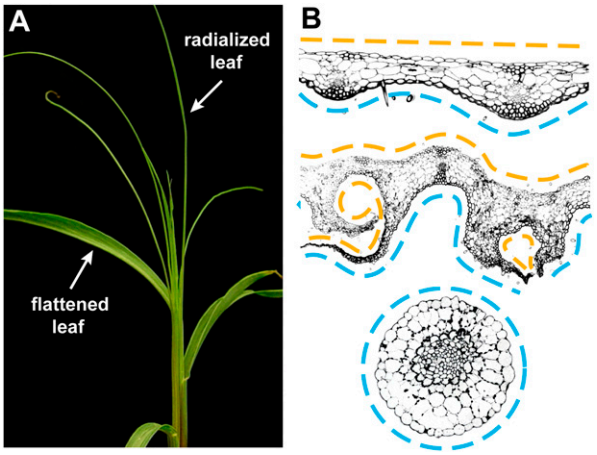

Figure 2. Phenotypes of mutants with perturbed adaxial–abaxial patterning. (*A*) Normal maize leaves develop flattened blades due to interaction between the adaxial and abaxial domains. *lbl1* mutants interfere with ta-siRNA biogenesis and adaxial cell fate specification and consequently their leaves are often radial and abaxialized. (*B*) Transverse sections through a wild-type (*top*), weakly adaxialized *mwp1* (*middle*), and fully abaxialized *lbl1* (*bottom*) leaf. Note the formation of ectopic blade outgrowths at the boundaries of adaxialized tissue sectors on the abaxial leaf surface of the *mwp1* leaf (marked by orange lines), and the radial symmetry of the *lbl1* leaf. (Orange lines) Adaxial; (blue lines) abaxial. (The images in *B* are reproduced with permission from Candela et al. [2008] [© 2008 American Society of Plant Biologists] and Timmermans et al. [1998].)

Downloaded from genesdev.cshlp.org on October 6, 2009 - Published by Cold Spring Harbor Laboratory Press

phenotypes, the most severe *phan* alleles frequently lead to meristem arrest. This observation, in conjunction with data from surgical experiments, points to a mutually promotive relationship between adaxial identity and meristem activity.

The role of *PHAN* in adaxial–abaxial patterning is conserved in tobacco, tomato, and several other compound-leafed species (Kim et al. 2003a; McHale and Koning 2004; Hay and Tsiantis 2006). Surprisingly, mutations in the maize and *Arabidopsis PHAN* orthologs *ROUGH SHEATH2* (*RS2*) and *ASYMMETRIC LEAVES1* (*AS1*), respectively, cause no obvious polarity defects (Timmermans et al. 1999; Tsiantis et al. 1999; Byrne et al. 2000). *PHAN*, *RS2*, and *AS1* are expressed uniformly throughout developing primordia, suggesting that any contributions to adaxial–abaxial patterning are regulated by interacting protein partners. Supporting this, AS1 and RS2 interact with AS2, a LOB domain transcription factor that localizes to the adaxial-most cell layers of young leaf primordia (Xu et al. 2003; Phelps-Durr et al. 2005; Husbands et al. 2007; Iwakawa et al. 2007). Although organ polarity is not obviously perturbed in *as1 as2* double mutants, *Arabidopsis* plants that constitutively express *AS2* develop leaf and vascular defects consistent with an adaxialized phenotype (Lin et al. 2003). These findings indicate that the AS pathway in *Arabidopsis* contributes to organ polarity, but does so redundantly with other genetic pathways. Indeed, screens for mutations that enhance the *as1* or *as2* defects have implicated several regulatory networks, including chromatin-remodeling, RNAi, and protein synthesis pathways in the regulation of adaxial–abaxial cell fate (Fig. 3A; Li et al. 2005; Garcia et al. 2006; Ueno et al. 2007; Pinon et al. 2008). Some of these are discussed elsewhere in this review and illustrate how molecularly conserved polarity determinants can have diverse contributions to adaxial–abaxial patterning in divergent species.

The class III homeodomain-leucine zipper (HD-ZIPIII) genes. The prominent contribution of *PHAN* to adaxial fate in *Antirrhinum* is mirrored by that of members of the HD-ZIPIII family of transcription factors in *Arabidopsis*, rice, and maize (McConnell et al. 2001; Emery et al. 2003; Juarez et al. 2004a,b; Itoh et al. 2008). The HD-ZIPIII genes were recognized as polarity determinants based on the phenotypes resulting from semidominant gain-of-function mutations. *Arabidopsis* plants expressing such dominant alleles of *PHABULOSA* (*PHB*), *PHAVOLUTA* (*PHV*), or *REVOLUTA* (*REV*) possess an enlarged SAM and develop adaxialized lateral organs, due to the altered expression of mutant transcripts (McConnell et al. 2001; Emery et al. 2003). *PHB*, *PHV*, and *REV* are normally expressed on the adaxial side of developing leaf primordia. However, transcripts derived from gain-of-function HD-ZIPIII alleles accumulate ectopically on the abaxial side as well, indicating that *PHB*, *PHV*, and *REV* are sufficient to specify adaxial cell fate (McConnell et al. 2001; Juarez et al. 2004a; Itoh et al. 2008).

HD-ZIPIII genes are expressed not only on the adaxial side of leaf primordia, but also within the tip of the meristem, and *PHB* forms rays of expression that connect the meristem with predicted sites of organ initiation. This pattern of expression presents the possibility that the HD-ZIPIII genes coordinate the bidirectional communication between the SAM and the adaxial side of organ primordia (McConnell et al. 2001). As HD-ZIPIII

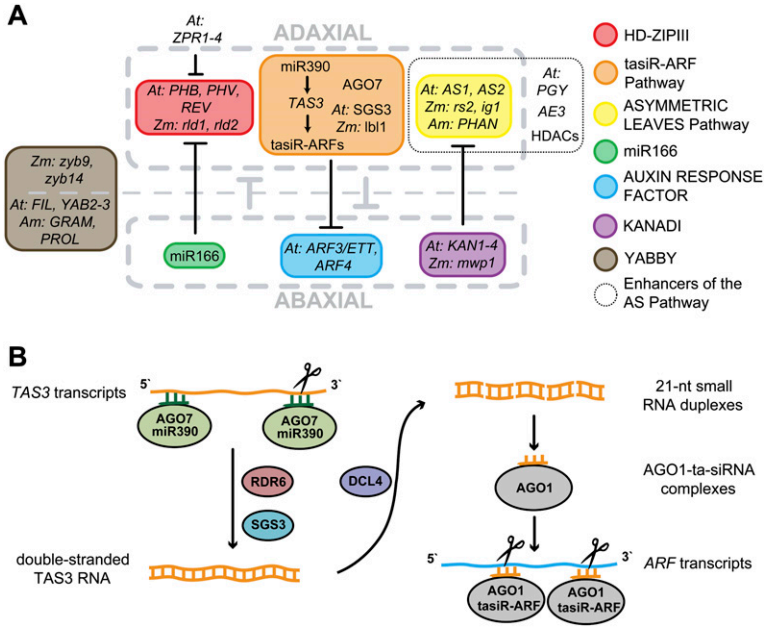

Figure 3. A network of conserved transcription factors and small RNA pathways maintains adaxial–abaxial polarity. (*A*) The HD-ZIPIII, AS, and *TAS3* ta-siRNA pathways contribute to the specification of adaxial cell fate. In *Arabidopsis*, HD-ZIPIII activity is regulated via a negative feedback loop involving the ZPR proteins, while the PIGGYBACK ribosomal proteins (PGY) (Pinon et al. 2008), ASYMMETRIC LEAVES ENHANCER3 (AE3) (Huang et al. 2006), and histone deacetylase proteins (HDAC) (Ueno et al. 2007) enhance the AS pathway (dotted outline). Members of the KANADI and ARF families, together with the miRNA miR166, contribute to the specification of abaxial identity. The site of YABBY activity varies between species but its contribution to organ outgrowth may be conserved. Antagonistic interactions between the polarity determinants create mutually exclusive adaxial and abaxial cell fates that contribute to the stable maintenance of organ polarity throughout development. Direct interactions are marked with a bold line. (*B*) Diagram of the *TAS3* ta-siRNA pathway. miR390-loaded AGO7 targets *TAS3* transcripts, which upon cleavage of the 3′ target site are converted into dsRNAs through the activities of RDR6 and SGS3/LBL1 and subsequently processed by DCL4 into phased 21-nt species. The *TAS3*-derived ta-siRNAs, tasiR-ARFs, act in *trans* to repress the expression of the abaxial determinants *ARF3* and *ARF4*.

Downloaded from genesdev.cshlp.org on October 6, 2009 - Published by Cold Spring Harbor Laboratory Press

proteins contain a putative lipid/sterol-binding START domain (Ponting and Aravind 1999; Schrick et al. 2004), part of this communication could include the control of HD-ZIPIII activity via a mobile lipid signal. Perhaps reflective of their prominent role in adaxial fate specification, HD-ZIPIII activity is subject to additional levels of regulation. The nature of the dominant HD-ZIPIII mutations revealed microRNA (miRNA)-mediated regulation at the post-transcriptional level (see below), and more recent studies have shown that HD-ZIPIII function in *Arabidopsis* is further modulated by interaction with LITTLE ZIPPER (ZPR) proteins. These small leucine zipper-containing proteins prevent HD-ZIPIII dimerization, an obligate requirement for the binding of these polarity determinants to DNA (Wenkel et al. 2007; Kim et al. 2008). ZPR expression is induced by HD-ZIPIII activity, suggesting that a negative feedback loop modulates HD-ZIPIII function. Although the enlarged SAMs of *zpr* loss-of-function mutants illustrate the significance of this feedback loop in meristem regulation, its contribution to organ polarity is less clear.

The replacement of adaxial cell types with their abaxial counterparts in *phan* loss-of-function mutants and the converse effects seen in HD-ZIPIII gain-of-function mutants suggest that adaxial and abaxial cell fates are mutually exclusive. Negative feedback regulation, as observed between the HD-ZIPIII and ZPR genes, could conceivably separate adaxial and abaxial identities defining distinct domains of activity. However, *ZPR1* and *ZPR3* transcripts accumulate late in primordium development and only adaxially (Wenkel et al. 2007; Kim et al. 2008), instead suggesting a role for these proteins in fine-tuning HD-ZIPIII function. Insights into the molecular basis underlying the mutual exclusivity of adaxial and abaxial cell fates came from analyses of determinants involved in the specification of abaxial identity.

Abaxial determinants

The KANADI (KAN) genes. The KAN genes are contributors to abaxial identity in both monocot and dicot plant species (Kerstetter et al. 2001; Eshed et al. 2001, 2004; Candela et al. 2008; Zhang et al. 2009). These genes encode transcription factors containing a MYB-like GARP DNA-binding domain and are expressed in the abaxial domain of lateral organs. Mutations in the KAN family members *milkweed pod1* from maize and *SHALLOT-LIKE1* from rice lead to the formation of partially adaxialized leaves (Fig. 2B; Candela et al. 2008; Zhang et al. 2009). A role for the four *Arabidopsis* KAN genes in adaxial–abaxial patterning is clear from phenotypes of higher-order mutants. Double and triple mutants develop ectopic outgrowths on their abaxial leaf surface or produce radially symmetric adaxialized organs. The latter phenotype closely resembles those of HD-ZIPIII gain-of-function mutants; indeed, HD-ZIPIII transcripts accumulate ectopically throughout radialized *kan1 kan2* organs (Eshed et al. 2001, 2004). Conversely, ectopic expression of *KAN1* or *KAN2* throughout the developing leaf leads to fully abaxialized organs, with a concomitant loss of HD-ZIPIII expression, implicating the KAN genes as possible negative regulators of the HD-ZIPIII genes (Kerstetter et al. 2001; Eshed et al. 2004). Likewise, loss-of-function *phb phv rev* triple-mutant embryos develop a single abaxialized cotyledon in lieu of a meristem—a phenotype that can be suppressed by additional mutations in *kan1*, *kan2*, and *kan4* (Emery et al. 2003; Izhaki and Bowman 2007). These genetic interactions point to a reciprocal role for the HD-ZIPIII genes in excluding KAN gene expression from the SAM to maintain meristem activity. An antagonistic relationship between these polarity determinants in the developing leaf could provide a possible basis for the mutually exclusive and opposing nature of adaxial and abaxial cell fates.

A further antagonistic interaction has been reported recently between KAN proteins and the AS pathway. KAN1 binds a *cis*-element in the promoter of *AS2* to repress its expression at the transcriptional level, thereby restricting AS2 activity to the adaxial side of leaves (Wu et al. 2008). This transcriptional repression of *AS2* by KAN1 is likely to represent only a single facet of its role in leaf polarity, as *as2* mutants fail to suppress the *kan1 kan2* phenotype. KAN1 may negatively regulate adaxial determinants beside *AS2* or, alternatively, polarity determinants like the KAN genes may have dual activities and be required for the induction of abaxial-promoting pathways as well. These findings, in conjunction with the likely repressive nature of the AS pathway (Guo et al. 2008), illustrate the complexity of interactions between polarity determinants that lead to mutual exclusivity of adaxial and abaxial cell fates (Fig. 3A). These opposing cell fates, in turn, are likely an integral part of the mechanism that maintains the separation between adaxial and abaxial domains throughout organ development.

The AUXIN RESPONSE FACTORs (ARFs). A strikingly similar phenotype to that of the *kan1 kan2* mutants can be seen in *Arabidopsis* plants mutant for the *ARF* family members *ARF3*/*ETTIN* (*ARF3*) and *ARF4* (Pekker et al. 2005). ARF genes encode transcription factors that control downstream responses to the plant hormone auxin, which regulates numerous developmental processes (for review, see Guilfoyle and Hagen 2007). *arf3* single mutants suppress the *KAN1* overexpression phenotype, positioning ARF3 as a potential downstream target of KAN activity (Pekker et al. 2005). However, neither *ARF3* nor *ARF4* expression is altered in a *kan1 kan2* background. Further, expression of *ARF3* from a ubiquitously expressed promoter does not induce the formation of abaxialized lateral organs, as is the case with ectopic *KAN1* or *KAN2* expression (Pekker et al. 2005). This discrepancy is not simply explained by the fact that *ARF3* and *ARF4* are targets of small RNA-mediated gene regulation (see below), as the ubiquitous expression of a small RNA-insensitive *ARF3* allele also negligibly affects adaxial–abaxial patterning (Fahlgren et al. 2006; Hunter et al. 2006). Together, these data suggest that ARF3, ARF4, and the KAN proteins have overlapping roles as abaxial determinants, but differ in their interactions with other components of the adaxial–abaxial patterning network.

Downloaded from genesdev.cshlp.org on October 6, 2009 - Published by Cold Spring Harbor Laboratory Press

YABBY genes: downstream components in adaxial–abaxial polarity. While the relative contributions to organ polarity of the factors described above may vary between species, their functions as adaxial or abaxial determinants are evolutionarily conserved. This is not the case for the YABBY genes. In *Arabidopsis*, members of this transcription factor family—including *FILAMENTOUS FLOWER* (*FIL*), *YAB2*, and *YAB3*—promote abaxial identity (Sawa et al. 1999; Siegfried et al. 1999). Higher-order *yabby* loss-of-function mutants show weak adaxialized phenotypes, while constitutive expression of YABBY proteins abaxializes lateral organs and terminates the meristem. Consistent with this activity, YABBY genes are expressed on the abaxial side of lateral organs in *Arabidopsis*. Abaxial-specific YABBY expression is conserved in a number of dicot species, including *Antirrhinum*, tomato, and tobacco (Kim et al. 2003b; Eshed et al. 2004; Golz et al. 2004; Navarro et al. 2004). In rice, however, YABBY genes show a nonpolarized expression pattern and their ectopic expression has no effect on adaxial–abaxial patterning (Yamaguchi et al. 2004; Dai et al. 2007). Most strikingly, the maize YABBY homologs *zyb9* and *zyb14* are expressed on the adaxial side of developing lateral organs (Juarez et al. 2004b), indicating that, although YABBY genes in *Arabidopsis* promote abaxial fate, this function is not conserved throughout the angiosperms.

Several observations suggest that the YABBY genes act downstream from other polarity determinants to direct blade outgrowth at the adaxial–abaxial boundary. Expression of YABBY genes begins later in primordium development than that of the HD-ZIPIII and KAN genes (Heisler et al. 2005; Toriba et al. 2007), and the ectopic blade outgrowths seen in weak polarity mutants show strong YABBY gene expression irrespective of whether such outgrowths arise on the upper or lower leaf surface (Eshed et al. 2004; Juarez et al. 2004b). In fact, YABBY genes are required for their production, as *kan1 kan2 fil yab3* quadruple mutants lack the ectopic blade outgrowths seen in *kan1 kan2* mutants (Eshed et al. 2004). The ancestral function of YABBY genes may therefore be to drive blade outgrowth along planes dictated by an adaxial–abaxial boundary, and in this regard it is interesting to note that YABBY expression in potato and maize becomes localized to the presumptive site of this boundary during primordium development (Eshed et al. 2004; Juarez et al. 2004b).

Thus, while the function of polarity determinants in specifying either adaxial or abaxial fate is conserved, their input into the regulation of YABBY genes must have diverged during plant evolution. In addition to regulating YABBY gene expression, adaxial and abaxial determinants employ a series of negative interactions to define mutually opposing cell fates (Fig. 3A). Although the molecular basis for the majority of these interactions remains unknown, they likely form part of a larger regulatory network that preserves the separation of adaxial and abaxial domains during primordium growth. This network must also include positive interactions that reinforce the identity within each domain, as well as signaling between the domains to provide positional inputs that refine the boundary. As none of the transcription factors described above are known to be mobile, their activities are likely patterned in response to positional signals. At least one of these signals is now known to be a mobile small RNA whose contribution to organ polarity is discussed below.

Novel small RNA-based patterning mechanisms in adaxial–abaxial polarity

Small RNAs as adaxial and abaxial determinants

Because HD-ZIPIII genes are sufficient to specify adaxial fate, their polarized expression is vital to the proper patterning of leaves. Dominant alleles that lead to ectopic abaxial expression of HD-ZIPIII transcripts result from mutations in a target site recognized by the miRNA miR166 (McConnell et al. 2001; Juarez et al. 2004a; Mallory et al. 2004; Itoh et al. 2008). In maize and *Arabidopsis*, mature miR166 accumulates on the abaxial side of leaf primordia in a pattern complementary to that of its HD-ZIPIII targets (Juarez et al. 2004a; Kidner and Martienssen 2004). miR166 directs the cleavage of HD-ZIPIII transcripts (Tang et al. 2003), and the functional significance of this relationship is demonstrated not only by the adaxializing phenotypes caused by dominant HD-ZIPIII alleles, but also by the development of severely abaxialized organs upon ectopic expression of miR166 (Alvarez et al. 2006). The negative regulation of HD-ZIPIII genes by miR166 therefore reveals an additional component of the regulatory network maintaining distinct adaxial and abaxial fates.

Given the significant role for miR166 in organ polarity, mechanisms must exist to precisely define its spatiotemporal pattern of accumulation. Insight into one such regulatory mechanism came from analyses of the maize mutant *leafbladeless1* (*lbl1*). Severe recessive alleles of *lbl1* lead to the formation of centric abaxialized leaves in which HD-ZIPIII expression is dramatically reduced (Fig. 2A,B; Timmermans et al. 1998; Juarez et al. 2004b). *lbl1* encodes the functional ortholog of SUPPRESSOR OF GENE SILENCING3 (SGS3), an essential component in the *Arabidopsis trans*-acting siRNA (ta-siRNA) biogenesis pathway (Nogueira et al. 2007). This specialized RNAi pathway has been reviewed elsewhere (Chapman and Carrington 2007); however, in brief, miRNA-guided cleavage triggers conversion of ta-siRNA precursor (*TAS*) transcripts into long dsRNAs via an *RNA-DEPENDENT RNA POLYMERASE6* (*RDR6*)- and *lbl1*/*SGS3*-dependent pathway and sets the register for phased, 21-nucleotide (nt) ta-siRNA production by DICER-LIKE4 (DCL4) (Peragine et al. 2004; Vazquez et al. 2004; Allen et al. 2005). ta-siRNAs are then loaded into an ARGONAUTE (AGO)-containing RNA-induced silencing complex (RISC) and, like miRNAs, act in *trans* to post-transcriptionally repress the expression of target genes (Fig. 3B).

The molecular identity and loss-of-function phenotype of *lbl1* demonstrate that ta-siRNAs act as adaxial determinants in maize. Their effect is mediated via miR166, as

Downloaded from genesdev.cshlp.org on October 6, 2009 - Published by Cold Spring Harbor Laboratory Press

mir166c and *mir166i* precursors are specifically up-regulated in *lbl1* mutant apices and mature miR166 accumulates ectopically on the adaxial side of incipient and developing *lbl1* leaf primordia (Nogueira et al. 2007). Adaxial–abaxial polarity in the maize leaf thus employs a novel patterning mechanism, relying on the opposing activities of two distinct small RNAs: (1) ta-siRNAs that define the adaxial side of leaf primordia by spatially restricting the domain of miR166 accumulation; and (2) miR166, which in turn delineates the abaxial side by restricting expression of the adaxializing HD-ZIPIII genes.

Unlike maize, the contribution of ta-siRNAs to adaxial–abaxial patterning in *Arabidopsis* is not immediately apparent. Mutations in ta-siRNA biogenesis components, such as *SGS3*, confer subtle leaf development phenotypes consistent with an accelerated transition from the juvenile to the adult phase, but adaxial–abaxial patterning is not conspicuously altered (Peragine et al. 2004; Vazquez et al. 2004). The functional contributions of ta-siRNAs to leaf development are mediated through the subspecialized *TAS3* ta-siRNA pathway, which requires the unique association of miR390 with its effector AGO7 to trigger ta-siRNA biogenesis (Figs. 3B, 4A; Allen et al. 2005; Adenot et al. 2006; Montgomery et al. 2008). A subset of *TAS3* ta-siRNAs, termed tasiR-ARFs, targets the abaxial determinants *ARF3* and *ARF4* (Allen et al. 2005). Expression of *ARF3* transgenes insensitive to tasiR-ARF regulation results in vegetative phase change defects similar to ta-siRNA biogenesis mutants but does not disrupt adaxial–abaxial polarity (Fahlgren et al. 2006; Hunter et al. 2006). Exactly why the loss of tasiR-ARF activity in *Arabidopsis* confers no obvious leaf polarity phenotypes has yet to be resolved. Functional overlap exists between the *TAS3* ta-siRNA and AS pathways, as tasiR-ARF biogenesis mutants enhance the *as1* and *as2* phenotypes and the expression levels of *FIL* are elevated specifically in mutants compromised for both pathways (Li et al. 2005; Garcia et al. 2006; Xu et al. 2006). Further, additively with the AS pathway, tasiR-ARFs in *Arabidopsis* repress levels of miR166, a function reminiscent of the contribution of *lbl1* to adaxial–abaxial patterning in maize (Xu et al. 2006). However, as the leaves of such double mutants largely retain correct adaxial–abaxial polarity, additional redundancies or differences in the patterning of the *TAS3* ta-siRNA pathway and downstream targets must exist between *Arabidopsis* and maize.

Small RNAs as generators of pattern

In maize, adaxial–abaxial polarity in the incipient leaf is specified through a novel patterning mechanism in which miR390 is positioned at the top of a cascade of small RNA activities. miR390 localizes to the adaxial side of the incipient primordium, where it triggers the biogenesis of *TAS3* ta-siRNAs that then restrict miR166 abaxially (Fig. 4C; Nogueira et al. 2007, 2009). As other components of the *TAS3* ta-siRNA biogenesis pathway are expressed more broadly throughout the SAM, miR390 is the restrictive factor that precisely positions ta-siRNA accumulation. Surprisingly, miR390 remains polarized to the upper "adaxial" side of abaxialized *lbl1* primordia, suggesting that the polar accumulation of miR390 is regulated independently of the ta-siRNA pathway and downstream polarity determinants, such as miR166 and the HD-ZIPIII genes (Nogueira et al. 2009). miR390

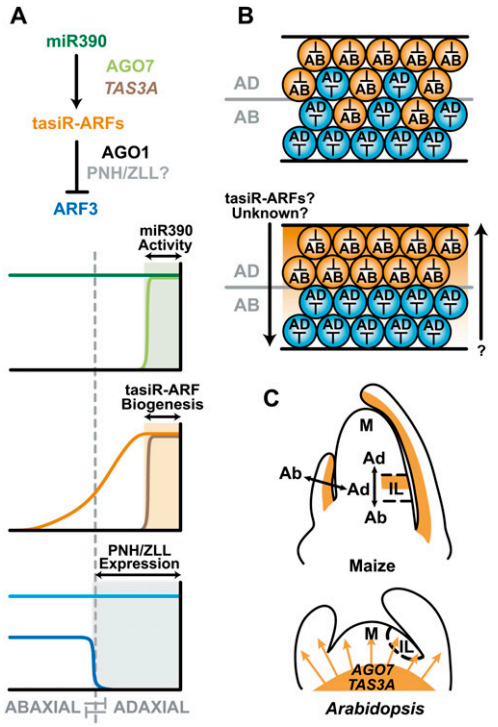

Figure 4. Diverse contributions of *TAS3* ta-siRNAs to adaxial–abaxial patterning. (*A*, *top* graph) In *Arabidopsis*, mature miR390 (dark green) accumulates throughout the leaf, but its activity (gray-green box) is restricted to the adaxial side by localized expression of AGO7 (light green). (*Middle* graph) tasiR-ARF biogenesis (pale orange box) is further confined to the two most adaxial cell layers by the restricted expression of the *TAS3A* precursor (brown). Mobility of tasiR-ARFs (orange) creates a gradient of accumulation across the developing leaf that is strongest near its adaxial site of biogenesis. (*Bottom* graph) This gradient yields regions of high and low tasiR-ARF activity, perhaps patterned in part via adaxial expression of PHN/ZLL (gray box), that restrict ARF3 protein accumulation (dark blue) to the abaxial side even though *ARF3* transcripts (light blue) are present throughout leaf primordia. (*B*) The mutually opposing nature of adaxial and abaxial cell fates, resulting in part from antagonistic interactions between cell-autonomous polarity determinants, contributes to the maintenance of organ polarity, but is unlikely sufficient to define a precise boundary between adaxial and abaxial organ domains. Superimposed intercellular signals that act between the domains can provide positional inputs to refine the adaxial–abaxial boundary. The adaxially derived mobile tasiR-ARFs are candidates for such a signal and may act in conjunction with positional signals from the abaxial domain. (*C*) In maize, miR390 and tasiR-ARFs (orange) accumulate adaxially in initiating and developing leaf primordia. In *Arabidopsis*, tasiR-ARFs move from their site of biogenesis below the SAM into the meristem proper and therefore accumulate uniformly throughout incipient primordia (IL).

Downloaded from genesdev.cshlp.org on October 6, 2009 - Published by Cold Spring Harbor Laboratory Press

accumulation may instead be regulated by positional information inherent to the SAM. This positional information may act to pattern small RNA-related factors. Expression of the miR390 precursors in the SAM is not limited to the incipient primordium, indicating that the discrete accumulation of mature miR390 in just the incipient leaf is regulated at the level of small RNA processing and/or stability (Nogueira et al. 2009). Irrespective of the underlying mechanism, as ta-siRNAs delineate the adaxial and abaxial sides through repression of miR166, the precise spatiotemporal regulation of miR390 accumulation in the incipient primordium is critical to adaxial–abaxial patterning in maize.

While tasiR-ARFs in *Arabidopsis* do not overtly contribute to organ polarity, localization of *TAS3* ta-siRNA pathway components reveals additional RNAi-based mechanisms underlying adaxial–abaxial patterning (Chitwood et al. 2009). Unlike maize, miR390 accumulates throughout the SAM and developing leaf primordia in *Arabidopsis* (Fig. 4C). The extent of miR390 activity is, however, curtailed by the highly restricted localization of AGO7 to the adaxial side of leaves and in the vasculature and pith region beneath the SAM. Likewise, *TAS3A*, the functional contributor of tasiR-ARFs during leaf development (Adenot et al. 2006; Addo-Quaye et al. 2008), localizes to the few adaxial-most cell layers of leaf primordia in a pattern similar to *AGO7* (Chitwood et al. 2009). Thus, in contrast to maize, where the post-transcriptional regulation of miR390 accumulation polarizes the *TAS3* ta-siRNA pathway, in *Arabidopsis* the localized expression of the miR390 substrate (*TAS3A*) and effector complex (AGO7) adaxially positions tasiR-ARF biogenesis.

An ARF3-based sensor for tasiR-ARF activity shows that these small RNAs act across the entire adaxial–abaxial axis, but more so on the adaxial side of the leaf (Chitwood et al. 2009). As tasiR-ARF biogenesis is limited to the two adaxial-most cell layers of leaves, tasiR-ARF activity outside this defined region results from intercellular mobility of this small RNA. Indeed, tasiR-ARFs accumulate in a graded pattern across the leaf blade, strongest near their adaxial source of biogenesis and dissipating toward the abaxial side of the leaf. Additionally, tasiR-ARFs were found to act in the SAM, despite the absence of *AGO7* and *TAS3A* expression in the meristem, suggesting that tasiR-ARFs move from below the SAM into the meristem proper (Chitwood et al. 2009). Such movement might provide an additional explanation for the differing contributions of tasiR-ARFs to leaf polarity in *Arabidopsis* versus maize. Whereas tasiR-ARF activity in maize is polarized in incipient primordia, tasiR-ARFs in *Arabidopsis* are found uniformly throughout the SAM, and their contribution to adaxial–abaxial patterning may not be realized until later in organ development (Fig. 4C). The intercellular trafficking of tasiR-ARFs defines these small RNAs as the first mobile signal in adaxial–abaxial polarity. In addition to the mutual exclusivity of adaxial and abaxial cell fates, signaling between the adaxial and abaxial domains is likely required to maintain leaf polarity. tasiR-ARFs, possibly in conjunction with an abaxial-derived signal, may mediate such interdomain communication and sharpen the adaxial–abaxial boundary that drives laminar outgrowth (Fig. 4B).

Interpreting the tasiR-ARF gradient

Consistent with the idea that tasiR-ARF mobility refines the adaxial–abaxial boundary, the gradient of tasiR-ARF accumulation does not simply translate into an inverse expression gradient of its targets. Instead, it is interpreted into discrete regions of high and low tasiR-ARF activity that creates a sharply defined domain of ARF3 and ARF4 expression on the abaxial side of leaf primordia (Pekker et al. 2005; Chitwood et al. 2009). How tasiR-ARF activity becomes patterned in *Arabidopsis* leaves is not currently understood. This may involve regulation by small RNA effector complexes, just as miR390 activity is limited to the adaxial sides of leaves by the localized expression of AGO7 (Chitwood et al. 2009). tasiR-ARFs act through the ubiquitously expressed AGO1 but perhaps may also act via PINHEAD/ZWILLE/AGO10 (PNH/ZLL), which localizes specifically to the adaxial side of leaf primordia (Fig. 4A; Lynn et al. 1999; Montgomery et al. 2008). PNH/ZLL is required to repress miR166 accumulation in the meristem, a function reminiscent of that of *lbl1* in maize (Nogueira et al. 2007; Liu et al. 2009). An additional link between PNH/ZLL and the tasiR-ARF pathway is suggested by the observation that ARF3 proteins, rather than *ARF3* transcripts, are polarized by tasiR-ARFs (Pekker et al. 2005). In addition to AGO1, PNH/ZLL can mediate small RNA-guided translational repression (Brodersen et al. 2008). This finding, and the superposition of the tasiR-ARF gradient onto the localization of PNH/ZLL and AGO1, could easily account for the discrete patterning of tasiR-ARF activity in leaves (Fig. 4A).

A more tantalizing concept to explain the conversion of the tasiR-ARF gradient into discrete regions of activity would be a morphogen-like patterning mechanism, more commonly found in animal systems. Mathematical modeling of the interaction between tasiR-ARFs and *ARF3* supports the theoretical feasibility of such a scenario (Levine et al. 2007). With this in mind, it is interesting to note that *ARF3* and *ARF4* each possess two tasiR-ARF target sites (Allen et al. 2005). If tasiR-ARFs were to act in a combinatorial fashion on *ARF3* and *ARF4*, this would further facilitate their concentration-dependent, morphogen-like patterning. Critical to such a concept is a dose-dependent response in target expression to tasiR-ARF levels. Although the effect of tasiR-ARF dosage on leaf development is not known, target levels may be important, as increasing the levels of nontargeted *ARF3* transcripts results in increasingly severe leaf defects (Fahlgren et al. 2006; Hunter et al. 2006). Should tasiR-ARFs prove to regulate their target levels in a concentration-dependent morphogen-like manner, this would also provide an efficient, flexible mechanism to position the boundary between the adaxial and abaxial domains of developing leaves (Fig. 4B).

Small RNAs play a prominent role in adaxial–abaxial patterning and, like their protein counterparts, are regulated at the level of biogenesis, stability, activity, and, in

Downloaded from genesdev.cshlp.org on October 6, 2009 - Published by Cold Spring Harbor Laboratory Press

the case of tasiR-ARFs, mobility. tasiR-ARFs in *Arabidopsis* represent the first identified signaling component in the network of interactions that maintains the separation of the adaxial and abaxial domains throughout leaf development. Similar signals from the abaxial side may also be required to further refine the adaxial–abaxial boundary (Fig. 4B). In maize, ta-siRNAs are part of a small RNA cascade that polarizes miR166 in the incipient primordium to delineate the adaxial and abaxial sides. This cascade rests on the adaxial-specific accumulation of miR390, which remains polarized even in molecularly abaxialized *lbl1* primordia. The mechanisms that position this small RNA thus act independently of any known polarity determinant and instead may be patterned by positional information inherent to the SAM.

Establishment of organ polarity

When is the adaxial–abaxial boundary established?

Lateral organs initiate from the peripheral zone (PZ) at the flank of the SAM, a process governed in part by the distribution of the hormone auxin, as discrete auxin maxima presage the sites of incipient primordia (Reinhardt et al. 2003; Heisler et al. 2005). The PZ is uniquely competent to respond to these maxima, as application of exogenous auxin to the stem cell-containing central zone (CZ) at the meristem tip does not result in organ initiation (Reinhardt et al. 2000, 2003). Expression analyses confirm that many polarity determinants are present in the incipient primordium (e.g., Kerstetter et al. 2001; McConnell et al. 2001; Chitwood et al. 2009). Despite this, the temporal relationship between establishment of the adaxial–abaxial axis and the initiation of lateral organs has not been determined and remains a pressing question in the field.

Initial models of the establishment of organ polarity envisioned a uniform distribution of adaxial and abaxial polarity factors in the incipient leaf (Eshed et al. 2001; Emery et al. 2003; Engstrom et al. 2004). A meristem-derived signal, perhaps the hypothetical Sussex signal, would promote adaxial cell fate resulting in polarization along the adaxial–abaxial axis. In the absence of such a signal, the primordium would acquire a default abaxial state. This model is consistent with data from surgical experiments, and the invocation of a meristem-derived signal neatly explains why the adaxial side of leaves always develops closest to the meristem (Fig. 1A,B; Sussex 1951; Reinhardt et al. 2005). However, recent advances in our ability to visualize the dynamics of proteins within the meristem have called this model into question.

Live imaging of *Arabidopsis* inflorescence meristems reveals that REV is restricted to the adaxial side of the incipient floral meristem, even when it is morphologically indistinguishable from the surrounding inflorescence (Heisler et al. 2005). Similarly, many of the polarity determinants in maize exhibit a polarized expression pattern in the initiating leaf, arguing that adaxial and abaxial factors are not uniformly localized throughout incipient primordia (Juarez et al. 2004a,b; Nogueira et al. 2007). Moreover, molecularly abaxialized *lbl1* primordia still exhibit an adaxial-specific accumulation of miR390 (Nogueira et al. 2009). These observations suggest that the incipient organ may be prepatterned into adaxial and abaxial domains. Polarization of the PZ into apical/centric and basal/outer regions, possibly as a consequence of positional information inherent to the SAM, could form the basis for such a prepattern (Fig. 5). This presents the intriguing possibility that organogenesis occurs at sites where an auxin maximum overlaps a prepatterned adaxial–abaxial boundary, criteria that are met only within the PZ. This model can explain the inability of the CZ to produce organs, even in the presence of an auxin maximum, and is not without precedent, as organ formation in other taxa occurs at cell fate boundaries as well (see Wolpert 1998). A similar mechanism may also direct leaflet formation in compound leaves. Leaflets form along the margins of leaves, a site with juxtaposed adaxial and abaxial identities, and mutants with perturbed adaxial–abaxial polarity produce fewer leaflets (Kim et al. 2003a,b). Sites of leaflet initiation are also predicted by auxin maxima, implying their formation is similarly driven by the coincidence of these maxima with adaxial–abaxial boundaries (Fig. 5; Barkoulas et al. 2008).

A prepatterned adaxial–abaxial boundary in the PZ may seem incongruent with surgical experiments, suggesting that a mobile meristem-derived signal is required to specify adaxial fate (Sussex 1951; Reinhardt et al. 2005). However, mobile signaling and prepatterning mechanisms are not necessarily mutually exclusive.

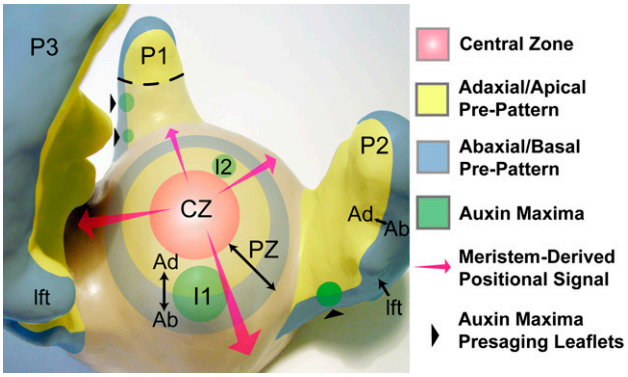

Figure 5. Model for adaxial–abaxial axis specification in the incipient primordium. The SAM comprises a stem cell-containing CZ and organogenic PZ. The PZ is envisioned to be patterned into apical/centric (gray yellow) and basal/outer (gray blue) regions based on positional information inherent to the SAM, possibly signals derived from the CZ and cells basal to the PZ. A lateral organ initiates at the site where an auxin maximum (green circles) overlaps the boundary between these PZ regions (I1). The same boundary also prepatterns the incipient organ into adaxial and abaxial domains. A meristem-derived adaxializing signal (pink arrows) is proposed to maintain this initial polarity until the P2 stage of organ development when maintenance mechanisms within the organ are in place. Compound-leafed species may similarly initiate leaflets (lft) at sites where auxin maxima overlap an adaxial–abaxial boundary at the margins of developing primordia (black arrowheads).

Downloaded from genesdev.cshlp.org on October 6, 2009 - Published by Cold Spring Harbor Laboratory Press

The acquisition of adaxial–abaxial organ polarity may be divided into two temporal phases: (1) establishment of the adaxial–abaxial axis in incipient primordia in response to a prepatterned PZ, and (2) stable maintenance of this axis in developing organs through antagonistic interactions between polarity determinants and interdomain signaling (Figs. 5, 3A, 4B, respectively). If these maintenance mechanisms need time to resolve, as suggested by surgical experiments (Reinhardt et al. 2005), meristem-derived signals could be required to promote adaxial fate in those primordia that have left the prepatterned PZ, but not yet reached the meristem-independent P2 stage of development.

Candidates for the proposed upstream positional information

Assuming prepatterning of the PZ, what positional information could underlie this inherent polarization? One model for adaxial–abaxial polarity suggests that specification of this axis is an extension of embryonic patterning events. The early globular embryo is patterned into a central HD-ZIPIII-expressing region and a peripheral region expressing the KAN genes (McConnell and Barton 1998; Lynn et al. 1999; Kerstetter et al. 2001). The juxtaposition of these two domains drives cotyledon outgrowth; however, it is unclear whether a similar mechanism functions to produce lateral organs in the vegetative SAM. Nonpolar distribution of KAN or HD-ZIPIII transcripts reduces proximal–distal growth but does not prevent organ outgrowth, and neither does the complete loss of HD-ZIPIII expression in incipient leaf primordia of *lbl1* mutants (McConnell et al. 2001; Eshed et al. 2004; Juarez et al. 2004b). In addition, *kan1 kan2 kan4* triple mutants develop ectopic leaf-like outgrowths below the cotyledons that correlate with ectopic expression of PINFORMED1 (PIN1), an auxin efflux carrier required to generate auxin maxima (Izhaki and Bowman 2007; Kuhlemeier 2007). This suggests that KAN proteins may define the lower limit of the organogenic zone through inhibition of PIN1 and further implies that KAN should be excluded from the PZ—a supposition supported by the pattern of *ZmKAN2* expression in the maize apex (Henderson et al. 2006). Likewise, live imaging shows that while REV expression expands into the adaxial domain of the initiating primordium, it is otherwise restricted to regions more apical to auxin maxima within the PZ (Heisler et al. 2005). The HD-ZIPIII and KAN expression domains thus appear to flank the PZ, rather than mark a prepatterned adaxial–abaxial boundary within it, such that expression of these polarity determinants in incipient primordia is likely a downstream consequence of this prepatterning. This, however, does not exclude the possibility that the HD-ZIPIII-expressing and KAN-expressing domains flanking the PZ contribute positional cues to prepattern this region; this idea would be consistent with the promotive relationship that meristems have with adaxial fate (see above).

In maize, the adaxial accumulation of miR390 is independent of known polarity determinants and, given that its precursor transcripts are expressed more broadly than the mature miRNA, suggests regulators of miRNA biogenesis or stability as candidates to prepattern the PZ (Nogueira et al. 2007, 2009). However, as mutants that perturb tasiR-ARF biogenesis in *Arabidopsis* do not show polarity defects (Fahlgren et al. 2006; Hunter et al. 2006), regulators of small RNA activity may not contribute to prepatterning the PZ in all plant species.

A signaling molecule often used to create developmental patterns is auxin, although the relationship between auxin and adaxial–abaxial patterning is still unclear. It is intriguing that auxin is transported primarily through the L1 (Reinhardt et al. 2003), particularly in light of surgical experiments demonstrating a role for the L1 in adaxial fate specification (Reinhardt et al. 2005). However, PIN1 polarization toward a centric convergence point within auxin maxima argues against auxin as a candidate for establishing adaxial or abaxial identity in incipient primordia. Instead, auxin may function during the maintenance phase of adaxial–abaxial polarity. After primordia emerge from the SAM, redistribution of PIN1 proteins results in a depletion of auxin primarily from their adaxial side (Heisler et al. 2005; Bayer et al. 2009). This depletion, coupled with the predominantly abaxial localization of its influx carrier AUXIN-RESISTANT1 (Reinhardt et al. 2003), indicates auxin may preferentially accumulate on the abaxial side of developing primordia. This accumulation correlates with the domains of activity of ARF3 and ARF4, two putative targets of auxin (Pekker et al. 2005). Considering that auxin is a mobile signal, it is tempting to speculate that it may act like tasiR-ARFs and contribute positional information that sharpens the adaxial–abaxial boundary from the abaxial side (Fig. 4B). However, to formally demonstrate a role for auxin in either the prepatterning of the PZ or the maintenance of adaxial–abaxial polarity, more precise knowledge of sites of auxin accumulation will be required (see Vanneste and Friml 2009).

Perspectives

While the meristem-derived signal first proposed nearly 60 years ago is still unknown, significant advances in our understanding of adaxial and abaxial patterning have been made. Numerous antagonistic interactions between polarity determinants, including members of several transcription factor and small RNA families, create mutually opposing cell fates that form the basis for the separation of adaxial and abaxial domains within the developing organ (Fig. 3A). This rudimentary sorting of cell fates is likely refined and maintained through intercellular communication, perhaps via mobile adaxially derived tasiR-ARFs or an equivalent abaxially derived signal, to achieve the complete and stable separation of these domains throughout organogenesis (Fig. 4B). Identification of such positional signals will be an important advance in the field. Determining how the adaxial–abaxial axis is first established also remains a key outstanding question. Recent experiments suggest positional information inherent to the SAM may polarize the PZ to

Downloaded from genesdev.cshlp.org on October 6, 2009 - Published by Cold Spring Harbor Laboratory Press

prepattern the adaxial–abaxial axis of the incipient primordium. This model predicts that organ formation depends on the coincidence of an auxin maximum with this prepatterned adaxial–abaxial boundary (Fig. 5). Polarity determinants differ in their contribution to adaxial–abaxial patterning between species, and the interpretation of a polarized PZ into an adaxial–abaxial axis may similarly vary between plant lineages. Meristem-derived signaling could be required as primordia grow away from this prepatterned PZ until the polarity maintenance network is in place to permanently fix the separation of adaxial and abaxial domains in the developing organ. Identification and characterization of this proposed meristem-derived positional information in diverse plant lineages thus represent an important challenge for the field of leaf polarity.

Acknowledgments

We thank current and former members of the laboratory for helpful discussions, and Cris Kuhlemeier for valuable comments on the manuscript. We apologize to colleagues whose work was not cited due to space limitations. Research on leaf polarity in the laboratory of M.C.P.T. is supported by grants from the USDA (06-03420) and the NSF (0615752). D.H.C. is an NSF graduate research fellow and a George A. and Marjorie H. Matheson fellow, and Y.P. is the recipient of a fellowship from the Watson School of Biological Sciences supported by Grant GM 065094 from the National Institute of General Medical Sciences, National Institutes of Health.

References

Addo-Quaye C, Eshoo T, Bartel D, Axtell M. 2008. Endogenous siRNA and miRNA targets identified by sequencing of the *Arabidopsis* degradome. *Curr Biol* **18:** 758–762.

Adenot X, Elmayan T, Lauressergues D, Boutet S, Bouche N, Gasciolli V, Vaucheret H. 2006. DRB4-dependent *TAS3 trans*-acting siRNAs control leaf morphology through AGO7. *Curr Biol* **16:** 927–932.

Allen E, Xie Z, Gustafson A, Carrington J. 2005. microRNA-directed phasing during *trans*-acting siRNA biogenesis in plants. *Cell* **121:** 207–221.

Alvarez J, Pekker I, Goldshmidt A, Blum E, Amsellem Z, Eshed Y. 2006. Endogenous and synthetic microRNAs stimulate simultaneous, efficient, and localized regulation of multiple targets in diverse species. *Plant Cell* **18:** 1134–1151.

Barkoulas M, Hay A, Kougioumoutzi E, Tsiantis M. 2008. A developmental framework for dissected leaf formation in the *Arabidopsis* relative *Cardamine hirsuta*. *Nat Genet* **40:** 1136–1141.

Bayer E, Smith R, Mandel T, Nakayama N, Sauer M, Prusinkiewicz P, Kuhlemeier C. 2009. Integration of transport-based models for phyllotaxis and midvein formation. *Genes & Dev* **23:** 373–384.

Brodersen P, Sakvarelidze-Achard L, Bruun-Rasmussen M, Dunoyer P, Yamamoto Y, Sieburth L, Voinnet O. 2008. Widespread translational inhibition by plant miRNAs and siRNAs. *Science* **320:** 1185–1190.

Byrne M, Barley R, Curtis M, Arroyo J, Dunham M, Hudson A, Martienssen R. 2000. *Asymmetric leaves1* mediates leaf patterning and stem cell function in *Arabidopsis*. *Nature* **408:** 967–971.

Candela H, Johnston R, Gerhold A, Foster T, Hake S. 2008. The *milkweed pod1* gene encodes a KANADI protein that is required for abaxial/adaxial patterning in maize leaves. *Plant Cell* **20:** 2073–2087.

Chapman E, Carrington J. 2007. Specialization and evolution of endogenous small RNA pathways. *Nat Rev Genet* **8:** 884–896.

Chitwood D, Nogueira F, Howell M, Montgomery T, Carrington J, Timmermans M. 2009. Pattern formation via small RNA mobility. *Genes & Dev* **23:** 549–554.

Dai M, Hu Y, Zhao Y, Liu H, Zhou D-X. 2007. A WUSCHEL-LIKE HOMEOBOX gene represses a YABBY gene expression required for rice leaf development. *Plant Physiol* **144:** 380–390.

Emery J, Floyd S, Alvarez J, Eshed Y, Hawker N, Izhaki A, Baum S, Bowman J. 2003. Radial patterning of *Arabidopsis* shoots by class III *HD-ZIP* and *KANADI* genes. *Curr Biol* **13:** 1768–1774.

Engstrom E, Izhaki A, Bowman J. 2004. Promoter bashing, microRNAs, and KNOX genes. New insights, regulators, and targets-of-regulation in the establishment of lateral organ polarity in *Arabidopsis*. *Plant Physiol* **135:** 685–694.

Eshed Y, Baum S, Perea J, Bowman J. 2001. Establishment of polarity in lateral organs of plants. *Curr Biol* **11:** 1251–1260.

Eshed Y, Izhaki A, Baum S, Floyd S, Bowman J. 2004. Asymmetric leaf development and blade expansion in *Arabidopsis* are mediated by *KANADI* and *YABBY* activities. *Development* **131:** 2997–3006.

Fahlgren N, Montgomery T, Howell M, Allen E, Dvorak S, Alexander A, Carrington J. 2006. Regulation of *AUXIN RESPONSE FACTOR3* by *TAS3* ta-siRNA affects developmental timing and patterning in *Arabidopsis*. *Curr Biol* **16:** 939–944.

Garcia D, Collier S, Byrne M, Martienssen R. 2006. Specification of leaf polarity in *Arabidopsis* via the *trans*-acting siRNA pathway. *Curr Biol* **16:** 933–938.

Golz J, Roccaro M, Kuzoff R, Hudson A. 2004. GRAMINIFOLIA promotes growth and polarity of *Antirrhinum* leaves. *Development* **131:** 3661–3670.

Guilfoyle T, Hagen G. 2007. Auxin response factors. *Curr Opin Plant Biol* **10:** 453–460.

Guo M, Thomas J, Collins G, Timmermans M. 2008. Direct repression of KNOX loci by the ASYMMETRIC LEAVES1 complex of *Arabidopsis*. *Plant Cell* **1:** 48–58.

Hay A, Tsiantis M. 2006. The genetic basis for differences in leaf form between *Arabidopsis thaliana* and its wild relative *Cardamine hirsuta*. *Nat Genet* **38:** 942–947.

Heisler M, Ohno C, Das P, Sieber P, Reddy G, Long J, Meyerowitz E. 2005. Patterns of auxin transport and gene expression during primordium development revealed by live imaging of the *Arabidopsis* inflorescence meristem. *Curr Biol* **15:** 1899–1911.

Henderson D, Zhang X, Brooks L III, Scanlon M. 2006. RAGGED SEEDLING2 is required for expression of KANADI2 and REVOLUTA homologues in the maize shoot apex. *Genesis* **44:** 372–382.

Huang W, Pi L, Liang W, Xu B, Wang H, Cai R, Huang H. 2006. The proteolytic function of the *Arabidopsis* 26S proteasome is required for specifying leaf adaxial identity. *Plant Cell* **18:** 2479–2492.

Hunter C, Willmann M, Wu G, Yoshikawa M, dela Luz Guierrez-Nava M, Poethig S. 2006. *Trans*-acting siRNA-mediated repression of *ETTIN* and *ARF4* regulates heteroblasty in *Arabidopsis*. *Development* **133:** 2973–2981.

Husbands A, Bell E, Shuai B, Smith H, Springer P. 2007. LATERAL ORGAN BOUNDARIES defines a new family of DNA-binding transcription factors and can interact with specific bHLH proteins. *Nucleic Acids Res* **35:** 6663–6671.

References

Abdel-Ghany SE, Pilon M. 2008. MicroRNA-mediated systemic down-regulation of copper protein expression in response to low copper availability in Arabidopsis. *J Biol Chem* **283**: 15932–15945.

Abel S, Theologis A. 1996. Early genes and auxin action. *Plant Physiol* **111**: 9–17.

Addo-Quaye C, Eshoo TW, Bartel DP, Axtell MJ. 2008. Endogenous siRNA and miRNA targets identified by sequencing of the Arabidopsis degradome. *Curr Biol* **18**: 758–762.

Allen E, Xie Z, Gustafson AM, Carrington JC. 2005. microRNA-directed phasing during trans-acting siRNA biogenesis in plants. *Cell* **121**: 207–221.

Allen E, Xie Z, Gustafson AM, Sung GH, Spatafora JW, Carrington JC. 2004. Evolution of microRNA genes by inverted duplication of target gene sequences in Arabidopsis thaliana. *Nat Genet* **36**: 1282–1290.

Alon U. 2006. *An Introduction to Systems Biology: Design Principles of Biological Circuits (Chapman & Hall/CRC Mathematical & Computational Biology)*. Chapman and Hall/CRC, 1 edition.

Alon U. 2007. Network motifs: theory and experimental approaches. *Nat Rev Genet* **8**: 450–461.

Altschul SF, Madden TL, Schäffer AA, Zhang J, Zhang Z, Miller W, Lipman DJ. 1997. Gapped BLAST and PSI-BLAST: a new generation of protein database search programs. *Nucleic Acids Res* **25**: 3389–3402.

Aoyama T, Hiwatashi Y, Shigyo M, Kofuji R, Kubo M, Ito M, Hasebe M. 2012. AP2-type transcription factors determine stem cell identity in the moss Physcomitrella patens. *Development* **139**: 3120–3129.

Arazi T, Talmor-Neiman M, Stav R, Riese M, Huijser P, Baulcombe DC. 2005. Cloning and characterization of micro-RNAs from moss. *Plant J* **43**: 837–848.

Arif MA, Fattash I, Ma Z, Cho SH, Beike AK, Reski R, Axtell MJ, Frank W. 2012. DICER-LIKE3 Activity in Physcomitrella patens DICER-LIKE4 Mutants Causes Severe Developmental Dysfunction and Sterility. *Mol Plant* .

Ashton NW, Grimsley NH, Cove DJ. 1979. Analysis of gametophytic development in the moss, Physcomitrella patens, using auxin and cytokinin resistant mutants. *Planta* **144**: 427–435.

Axtell MJ, Bartel DP. 2005. Antiquity of microRNAs and their targets in land plants. *Plant Cell* **17**: 1658–1673.

Axtell MJ, Bowman JL. 2008. Evolution of plant microRNAs and their targets. *Trends Plant Sci* **13**: 343–349.

Axtell MJ, Jan C, Rajagopalan R, Bartel DP. 2006. A two-hit trigger for siRNA biogenesis in plants. *Cell* **127**: 565–577.

Axtell MJ, Snyder JA, Bartel DP. 2007. Common functions for diverse small RNAs of land plants. *Plant Cell* **19**: 1750–1769.

Axtell MJ, Westholm JO, Lai EC. 2011. Vive la différence: biogenesis and evolution of microRNAs in plants and animals. *Genome Biol* **12**: 221.

Banks JA, Nishiyama T, Hasebe M, Bowman JL, Gribskov M, Depamphilis C, Albert VA, Aono N, Aoyama T, Ambrose BA, et al. 2011. The Selaginella genome identifies genetic changes associated with the evolution of vascular plants. *Science* **332**: 960–963.

Bartel DP. 2004. MicroRNAs: genomics, biogenesis, mechanism, and function. *Cell* **116**: 281–297.

Basu S, Sun H, Brian L, Quatrano RL, Muday GK. 2002. Early embryo development in Fucus distichus is auxin sensitive. *Plant Physiol* **130**: 292–302.

Bergmann DC, Lukowitz W, Somerville CR. 2004. Stomatal development and pattern controlled by a MAPKK kinase. *Science* **304**: 1494–1497.

Bharathan G, Goliber TE, Moore C, Kessler S, Pham T, Sinha NR. 2002. Homologies in leaf form inferred from KNOXI gene expression during development. *Science* **296**: 1858–1860.

Bopp M. 1980. The hormonal regulation of morphogenesis in mosses 351–361.

Carlsbecker A, Lee JY, Roberts CJ, Dettmer J, Lehesranta S, Zhou J, Lindgren O, Moreno-Risueno MA, Vatén A, Thitamadee S, et al. 2010. Cell signalling by microRNA165/6 directs gene dose-dependent root cell fate. *Nature* **465**: 316–321.

Carroll SB, Grenier J, Weatherbee S. 2004. *From DNA to Diversity: Molecular Genetics and the Evolution of Animal Design*. Wiley-Blackwell, 2 edition.

Causier B, Lloyd J, Stevens L, Davies B. 2012. TOPLESS co-repressor interactions and their evolutionary conservation in plants. *Plant Signal Behav* **7**: 325–328.

Chapman EJ, Carrington JC. 2007. Specialization and evolution of endogenous small RNA pathways. *Nat Rev Genet* **8**: 884–896.

Chen X. 2009. Small RNAs and their roles in plant development. *Annu Rev Cell Dev Biol* **25**: 21–44.

Chen JG, Ullah H, Young JC, Sussman MR, Jones AM. 2001. ABP1 is required for organized cell elongation and division in Arabidopsis embryogenesis. *Genes & Development* **15**: 902–911.

Chitwood DH, Nogueira FTS, Howell MD, Montgomery TA, Carrington JC, Timmermans MCP. 2009. Pattern formation via small RNA mobility. *Genes & Development* **23**: 549–554.

Cho SH, Addo-Quaye C, Coruh C, Arif MA, Ma Z, Frank W, Axtell MJ. 2008. Physcomitrella patens DCL3 is required for 22-24 nt siRNA accumulation, suppression of retrotransposon-derived transcripts, and normal development. *PLoS Genet* **4**: e1000314.

Cho SH, Coruh C, Axtell MJ. 2012. miR156 and miR390 Regulate tasiRNA Accumulation and Developmental Timing in Physcomitrella patens. *Plant Cell* .

Chuck G, Cigan AM, Saeteurn K, Hake S. 2007. The heterochronic maize mutant Corngrass1 results from overexpression of a tandem microRNA. *Nat Genet* **39**: 544–549.

Clop A, Marcq F, Takeda H, Pirottin D, Tordoir X, Bibé B, Bouix J, Caiment F, Elsen JM, Eychenne F, et al. 2006. A mutation creating a potential illegitimate microRNA target site in the myostatin gene affects muscularity in sheep. *Nat Genet* **38**: 813–818.

Collins TJ. 2007. ImageJ for microscopy. *Biotechniques* .

Cove DJ, Perroud PF, Charron AJ. 2009a. Culturing the moss Physcomitrella patens. *Cold Spring Harb Protoc* .

Cove DJ, Perroud PF, Charron AJ, McDaniel SF, Khandelwal A, Quatrano RS. 2009b. Transformation of the moss Physcomitrella patens using direct DNA uptake by protoplasts. *Cold Spring Harb Protoc* **2009**: pdb.prot5143.

Crane PR, Friis EM, Pedersen KR. 1995. The origin and early diversification of angiosperms. *Nature* **374**: 27–33.

Cuperus JT, Fahlgren N, Carrington JC. 2011. Evolution and functional diversification of MIRNA genes. *Plant Cell* **23**: 431–442.

De Smet I, Voss U, Lau S, Wilson M, Shao N, Timme RE, Swarup R, Kerr I, Hodgman C, Bock R, et al. 2011. Unraveling the evolution of auxin signaling. *Plant Physiol* **155**: 209–221.

Doebley J, Stec A, Gustus C. 1995. teosinte branched1 and the origin of maize: evidence for epistasis and the evolution of dominance. *Genetics* **141**: 333–346.

Douglas RN, Wiley D, Sarkar A, Springer N, Timmermans MCP, Scanlon MJ. 2010. ragged seedling2 Encodes an ARGONAUTE7-like protein required for mediolateral expansion, but not dorsiventrality, of maize leaves. *Plant Cell* **22**: 1441–1451.

Ebert MS, Sharp PA. 2012. Roles for MicroRNAs in Conferring Robustness to Biological Processes. *Cell* **149**: 515–524.

Eklund DM, Thelander M, Landberg K, Ståldal V, Nilsson A, Johansson M, Valsecchi I, Pederson ERA, Kowalczyk M, Ljung K, et al. 2010. Homologues of the Arabidopsis thaliana SHI/STY/LRP1 genes control auxin biosynthesis and affect growth and development in the moss Physcomitrella patens. *Development* **137**: 1275–1284.

Emery JF, Floyd SK, Alvarez J, Eshed Y, Hawker NP, Izhaki A, Baum SF, Bowman JL. 2003. Radial patterning of Arabidopsis shoots by class III HD-ZIP and KANADI genes. *Curr Biol* **13**: 1768–1774.

Erwin DH, Davidson EH. 2009. The evolution of hierarchical gene regulatory networks. *Nat Rev Genet* **10**: 141–148.

Fahlgren N, Jogdeo S, Kasschau KD, Sullivan CM, Chapman EJ, Laubinger S, Smith LM, Dasenko M, Givan SA, Weigel D, et al. 2010. MicroRNA gene evolution in Arabidopsis lyrata and Arabidopsis thaliana. *Plant Cell* **22**: 1074–1089.

Fahlgren N, Montgomery TA, Howell MD, Allen E, Dvorak SK, Alexander AL, Carrington JC. 2006. Regulation of AUXIN RESPONSE FACTOR3 by TAS3 ta-siRNA affects developmental timing and patterning in Arabidopsis. *Curr Biol* **16**: 939–944.

Ferrell JE. 2002. Self-perpetuating states in signal transduction: positive feedback, double-negative feedback and bistability. *Current Opinion in Cell Biology* **14**: 140–148.

Ferrell JE, Machleder EM. 1998. The biochemical basis of an all-or-none cell fate switch in Xenopus oocytes. *Science* **280**: 895–898.

Finet C, Berne-Dedieu A, Scutt CP, Marlétaz F. 2012. Evolution of the ARF Gene Family in Land Plants: Old Domains, New Tricks. *Mol Biol Evol* .

Finet C, Jaillais Y. 2012. AUXOLOGY: When auxin meets plant evo-devo. *Dev Biol* **369**: 19–31.

Flagel LE, Wendel JF. 2009. Gene duplication and evolutionary novelty in plants. *New Phytol* **183**: 557–564.

Floyd SK, Bowman JL. 2006. Distinct developmental mechanisms reflect the independent origins of leaves in vascular plants. *Curr Biol* **16**: 1911–1917.

Fraser GJ, Hulsey CD, Bloomquist RF, Uyesugi K, Manley NR, Streelman JT. 2009. An ancient gene network is co-opted for teeth on old and new jaws. *PLoS Biol* **7**: e31.

Fujita T, Sakaguchi H, Hiwatashi Y, Wagstaff SJ, Ito M, Deguchi H, Sato T, Hasebe M. 2008. Convergent evolution of shoots in land plants: lack of auxin polar transport in moss shoots. *Evol Dev* **10**: 176–186.

Garcia D, Collier SA, Byrne ME, Martienssen RA. 2006. Specification of leaf polarity in Arabidopsis via the trans-acting siRNA pathway. *Curr Biol* **16**: 933–938.

Gifford EM, Foster AS. 1989. *Morphology and evolution of vascular plants*. W. H. Freeman.

Guilfoyle TJ, Hagen G. 2007. Auxin response factors. *Curr Opin Plant Biol* **10**: 453–460.

Guo M, Thomas J, Collins G, Timmermans MC. 2008. Direct Repression of KNOX Loci by the ASYMMETRIC LEAVES1 Complex of Arabidopsis. *Plant Cell* **20**: 48–58.

Hardtke CS. 1998. The Arabidopsis gene MONOPTEROS encodes a transcription factor mediating embryo axis formation and vascular development. *EMBO J* **17**: 1405–1411.

Harrison CJ, Roeder AHK, Meyerowitz EM, Langdale JA. 2009. Local cues and asymmetric cell divisions underpin body plan transitions in the moss Physcomitrella patens. *Curr Biol* **19**: 461–471.

Havens KA, Guseman JM, Jang SS, Pierre-Jerome E, Bolten N, Klavins E, Nemhauser JL. 2012. A synthetic approach reveals extensive tunability of auxin signaling. *Plant Physiol* **160**: 135–142.

Hay A, Tsiantis M. 2006. The genetic basis for differences in leaf form between Arabidopsis thaliana and its wild relative Cardamine hirsuta. *Nat Genet* **38**: 942–947.

Higuchi R, Krummel B, Saiki RK. 1988. A general method of in vitro preparation and specific mutagenesis of DNA fragments: study of protein and DNA interactions. *Nucleic Acids Res* **16**: 7351–7367.

Hornstein E, Shomron N. 2006. Canalization of development by microRNAs. *Nat Genet* **38**: S20–S24.

Howell MD, Fahlgren N, Chapman EJ, Cumbie JS, Sullivan CM, Givan SA, Kasschau KD, Carrington JC. 2007. Genome-wide analysis of the RNA-DEPENDENT RNA POLYMERASE6/DICER-LIKE4 pathway in Arabidopsis reveals dependency on miRNA- and tasiRNA-directed targeting. *Plant Cell* **19**: 926–942.

Hunter C, Sun H, Poethig RS. 2003. The Arabidopsis heterochronic gene ZIPPY is an ARGONAUTE family member. *Curr Biol* **13**: 1734–1739.

Hunter C, Willmann MR, Wu G, Yoshikawa M, de la Luz Gutiérrez-Nava M, Poethig SR. 2006. Trans-acting siRNA-mediated repression of ETTIN and ARF4 regulates heteroblasty in Arabidopsis. *Development* **133**: 2973–2981.

Husbands AY, Chitwood DH, Plavskin Y, Timmermans MCP. 2009. Signals and prepatterns: new insights into organ polarity in plants. *Genes & Development* **23**: 1986–1997.

Imaizumi T, Kadota A, Hasebe M, Wada M. 2002. Cryptochrome light signals control development to suppress auxin sensitivity in the moss Physcomitrella patens. *Plant Cell* **14**: 373–386.

Ishikawa M, Murata T, Sato Y, Nishiyama T, Hiwatashi Y, Imai A, Kimura M, Sugimoto N, Akita A, Oguri Y, et al. 2011. Physcomitrella Cyclin-Dependent Kinase A Links Cell Cycle Reactivation to Other Cellular Changes during Reprogramming of Leaf Cells. *Plant Cell* .

Itoh JI, Sato Y, Nagato Y. 2008. The SHOOT ORGANIZATION2 Gene Coordinates Leaf Domain Development Along the Central-Marginal Axis in Rice. *Plant Cell Physiol* **49**: 1226–1236.

Jang G, Dolan L. 2011. Auxin promotes the transition from chloronema to caulonema in moss protonema by positively regulating PpRSL1and PpRSL2 in Physcomitrella patens. *New Phytol* **192**: 319–327.

Jang G, Yi K, Pires ND, Menand B, Dolan L. 2011. RSL genes are sufficient for rhizoid system development in early diverging land plants. *Development* **138**: 2273–2281.

Javelle M, Timmermans MCP. 2012. In situ localization of small RNAs in plants by using LNA probes. *Nat Protoc* **7**: 533–541.

Johri MM, Desai S. 1973. Auxin regulation of caulonema formation in moss protonema. *Nature New Biol* **245**: 223–224.

Jones-Rhoades MW, Bartel DP, Bartel B. 2006. MicroRNAS and their regulatory roles in plants. *Annual review of plant biology* **57**: 19–53.

Juarez MT, Kui JS, Thomas J, Heller BA, Timmermans MCP. 2004a. microRNA-mediated repression of rolled leaf1 specifies maize leaf polarity. *Nature* **428**: 84–88.

Juarez MT, Twigg RW, Timmermans MCP. 2004b. Specification of adaxial cell fate during maize leaf development. *Development* **131**: 4533–4544.

Karimi M, Inzé D, Depicker A. 2002. GATEWAY vectors for Agrobacterium-mediated plant transformation. *Trends Plant Sci* **7**: 193–195.

Kasschau KD, Fahlgren N, Chapman EJ, Sullivan CM, Cumbie JS, Givan SA, Carrington JC. 2007. Genome-wide profiling and analysis of Arabidopsis siRNAs. *PLoS Biol* **5**: e57.

Kenrick P, Crane PR. 1997. The origin and early evolution of plants on land. *Nature* **389**: 33–39.

Keys DN, Lewis DL, Selegue JE, Pearson BJ, Goodrich LV, Johnson RL, Gates J, Scott MP, Carroll SB. 1999. Recruitment of a hedgehog regulatory circuit in butterfly eyespot evolution. *Science* **283**: 532–534.

Kidner CA, Timmermans MCP, Byrne ME, Martienssen RA. 2002. Developmental genetics of the angiosperm leaf. *Advances in botanical research* **38**: 191–234.

Kimura S, Koenig D, Kang J, Yoong FY, Sinha N. 2008. Natural variation in leaf morphology results from mutation of a novel KNOX gene. *Curr Biol* **18**: 672–677.

Kramer EM, Irish VF. 1999. Evolution of genetic mechanisms controlling petal development. *Nature* **399**: 144–148.

Larkin MA, Blackshields G, Brown NP, Chenna R, McGettigan PA, McWilliam H, Valentin F, Wallace IM, Wilm A, Lopez R, et al. 2007. Clustal W and Clustal X version 2.0. *Bioinformatics* **23**: 2947–2948.

Lau S, De Smet I, Kolb M, Meinhardt H, Jürgens G. 2011. Auxin triggers a genetic switch. *Nat Cell Biol* **13**: 611–615.

Lauter N, Kampani A, Carlson S, Goebel M, Moose SP. 2005. microRNA172 down-regulates glossy15 to promote vegetative phase change in maize. *Proc Natl Acad Sci USA* **102**: 9412–9417.

Lavy M, Prigge MJ, Tigyi K, Estelle M. 2012. The cyclophilin DIAGEOTROPICA has a conserved role in auxin signaling. *Development* **139**: 1115–1124.

Lee RC, Feinbaum RL, Ambros V. 1993. The C. elegans heterochronic gene lin-4 encodes small RNAs with antisense complementarity to lin-14. *Cell* **75**: 843–854.

Levine E, McHale P, Levine H. 2007. Small regulatory RNAs may sharpen spatial expression patterns. *PLoS Comput Biol* **3**: e233.

Leyser O. 2011. Auxin, self-organisation, and the colonial nature of plants. *Curr Biol* **21**: R331–7.

Liang G, Yang F, Yu D. 2010. MicroRNA395 mediates regulation of sulfate accumulation and allocation in Arabidopsis thaliana. *Plant J* **62**: 1046–1057.

Lilley JLS, Gee CW, Sairanen I, Ljung K, Nemhauser JL. 2012. An endogenous carbon-sensing pathway triggers increased auxin flux and hypocotyl elongation. *Plant Physiol* **160**: 2261–2270.

Liu X, Gorovsky MA. 1993. Mapping the 5′ and 3′ ends of Tetrahymena thermophila mRNAs using RNA ligase mediated amplification of cDNA ends (RLM-RACE). *Nucleic Acids Res* **21**: 4954–4960.

Lodha M, Marco CF, Timmermans MCP. 2008. Genetic and epigenetic regulation of stem cell homeostasis in plants. *Cold Spring Harb Symp Quant Biol* **73**: 243–251.

Losick R, Desplan C. 2008. Stochasticity and Cell Fate. *Science* **320**: 65–68.

Lukowitz W, Roeder A, Parmenter D, Somerville C. 2004. A MAPKK kinase gene regulates extra-embryonic cell fate in Arabidopsis. *Cell* **116**: 109–119.

Ma Z, Bielenberg DG, Brown KM, Lynch JP. 2001. Regulation of root hair density by phosphorus availability in Arabidopsis thaliana. *Plant Cell Environ* **24**: 459–467.

Ma Z, Coruh C, Axtell MJ. 2010. Arabidopsis lyrata small RNAs: transient MIRNA and small interfering RNA loci within the Arabidopsis genus. *Plant Cell* **22**: 1090–1103.

Mackeigan JP, Murphy LO, Dimitri CA, Blenis J. 2005. Graded mitogen-activated protein kinase activity precedes switch-like c-Fos induction in mammalian cells. *Mol Cell Biol* **25**: 4676–4682.

Maizel A, Busch MA, Tanahashi T, Perkovic J, Kato M, Hasebe M, Weigel D. 2005. The floral regulator LEAFY evolves by substitutions in the DNA binding domain. *Science* **308**: 260–263.

Malamy JE. 2005. Intrinsic and environmental response pathways that regulate root system architecture. *Plant Cell Environ* **28**: 67–77.

Mallory AC, Bartel DP, Bartel B. 2005. MicroRNA-directed regulation of Arabidopsis AUXIN RESPONSE FACTOR17 is essential for proper development and modulates expression of early auxin response genes. *Plant Cell* **17**: 1360–1375.

Marchler-Bauer A, Panchenko AR, Shoemaker BA, Thiessen PA, Geer LY, Bryant SH. 2002. CDD: a database of conserved domain alignments with links to domain three-dimensional structure. *Nucleic Acids Res* **30**: 281–283.

Marin E, Jouannet V, Herz A, Lokerse AS, Weijers D, Vaucheret H, Nussaume L, Crespi MD, Maizel A. 2010. miR390, Arabidopsis TAS3 tasiRNAs, and their AUXIN RESPONSE FACTOR targets define an autoregulatory network quantitatively regulating lateral root growth. *Plant Cell* **22**: 1104–1117.

Masel J, Siegal ML. 2009. Robustness: mechanisms and consequences. *Trends Genet* **25**: 395–403.

Masucci JD, Schiefelbein JW. 1994. The rhd6 Mutation of Arabidopsis thaliana Alters Root-Hair Initiation through an Auxin- and Ethylene-Associated Process. *Plant Physiol* **106**: 1335–1346.

Menand B, Calder G, Dolan L. 2007a. Both chloronemal and caulonemal cells expand by tip growth in the moss Physcomitrella patens. *J Exp Bot* **58**: 1843–1849.

Menand B, Yi K, Jouannic S, Hoffmann L, Ryan E, Linstead P, Schaefer DG, Dolan L. 2007b. An ancient mechanism controls the development of cells with a rooting function in land plants. *Science* **316**: 1477–1480.

Meyers BC, Axtell MJ, Bartel B, Bartel DP, Baulcombe D, Bowman JL, Cao X, Carrington JC, Chen X, Green PJ, et al. 2008. Criteria for annotation of plant MicroRNAs. *Plant Cell* **20**: 3186–3190.

Mi S, Cai T, Hu Y, Chen Y, Hodges E, Ni F, Wu L, Li S, Zhou H, Long C, et al. 2008. Sorting of small RNAs into Arabidopsis argonaute complexes is directed by the 5′ terminal nucleotide. *Cell* **133**: 116–127.

Middleton AM, Farcot E, Owen MR, Vernoux T. 2012. Modeling Regulatory Networks to Understand Plant Development: Small Is Beautiful. *Plant Cell* .

Middleton AM, King JR, Bennett MJ, Owen MR. 2010. Mathematical modelling of the Aux/IAA negative feedback loop. *Bull Math Biol* **72**: 1383–1407.

Mishler BD, Churchill SP. 1984. A Cladistic Approach to the Phylogeny of the "Bryophytes". *Brittonia* **36**: 406.

Miyashima S, Koi S, Hashimoto T, Nakajima K. 2011. Non-cell-autonomous microRNA165 acts in a dose-dependent manner to regulate multiple differentiation status in the Arabidopsis root. *Development* **138**: 2303–2313.

Montgomery TA, Howell MD, Cuperus JT, Li D, Hansen JE, Alexander AL, Chapman EJ, Fahlgren N, Allen E, Carrington JC. 2008. Specificity of ARGONAUTE7-miR390 interaction and dual functionality in TAS3 trans-acting siRNA formation. *Cell* **133**: 128–141.

Moretti S, Armougom F, Wallace IM, Higgins DG, Jongeneel CV, Notredame C. 2007. The M-Coffee web server: a meta-method for computing multiple sequence alignments by combining alternative alignment methods. *Nucleic Acids Res* **35**: W645–W648.

Mukherji S, Ebert MS, Zheng GXY, Tsang JS, Sharp PA, van Oudenaarden A. 2011. MicroRNAs can generate thresholds in target gene expression. *Nat Genet* **43**: 854–859.

Nagasaki H, Itoh Ji, Hayashi K, Hibara Ki, Satoh-Nagasawa N, Nosaka M, Mukouhata M, Ashikari M, Kitano H, Matsuoka M, et al. 2007. The small interfering RNA production pathway is required for shoot meristem initiation in rice. *Proc Natl Acad Sci USA* **104**: 14867–14871.

Neuenschwander U, Fleming AJ, Kuhlemeier C. 1994. Cytokinin induces the developmentally restricted synthesis of an extracellular protein in Physcomitrella patens. *Plant J* **5**: 21–31.

Nogueira FTS, Chitwood DH, Madi S, Ohtsu K, Schnable PS, Scanlon MJ, Timmermans MCP. 2009. Regulation of small RNA accumulation in the maize shoot apex. *PLoS Genet* **5**: e1000320.

Nogueira FTS, Madi S, Chitwood DH, Juarez MT, Timmermans MCP. 2007. Two small regulatory RNAs establish opposing fates of a developmental axis. *Genes & Development* **21**: 750–755.

Okano Y, Aono N, Hiwatashi Y, Murata T, Nishiyama T, Ishikawa T, Kubo M, Hasebe M. 2009. A polycomb repressive complex 2 gene regulates apogamy and gives evolutionary insights into early land plant evolution. *Proc Natl Acad Sci USA* **106**: 16321–16326.

Paponov IA, Paponov M, Teale W, Menges M, Chakrabortee S, Murray JAH, Palme K. 2008. Comprehensive transcriptome analysis of auxin responses in Arabidopsis. *Mol Plant* **1**: 321–337.

Parry G, Calderon-Villalobos LI, Prigge M, Peret B, Dharmasiri S, Itoh H, Lechner E, Gray WM, Bennett M, Estelle M. 2009. Complex regulation of the TIR1/AFB family of auxin receptors. *Proc Natl Acad Sci USA* **106**: 22540–22545.

Pekker I, Alvarez JP, Eshed Y. 2005. Auxin response factors mediate Arabidopsis organ asymmetry via modulation of KANADI activity. *Plant Cell* **17**: 2899–2910.

Peragine A, Yoshikawa M, Wu G, Albrecht HL, Poethig RS. 2004. SGS3 and SGS2/SDE1/RDR6 are required for juvenile development and the production of trans-acting siRNAs in Arabidopsis. *Genes & Development* **18**: 2368–2379.

Peterson KJ, Dietrich MR, McPeek MA. 2009. MicroRNAs and metazoan macroevolution: insights into canalization, complexity, and the Cambrian explosion. *Bioessays* **31**: 736–747.

Pires ND, Dolan L. 2012. Morphological evolution in land plants: new designs with old genes. *Philos Trans R Soc Lond, B, Biol Sci* **367**: 508–518.

Prigge MJ, Lavy M, Ashton NW, Estelle M. 2010. Physcomitrella patens Auxin-Resistant Mutants Affect Conserved Elements of an Auxin-Signaling Pathway. *Current Biology* **20**: 1907–1912.

Quatrano R, McDaniel S, Khandelwal A, Perroud P. 2007. Physcomitrella patens: mosses enter the genomic age. *Curr Opin Plant Biol* .

Rademacher EH, Lokerse AS, Schlereth A, Llavata-Peris CI, Bayer M, Kientz M, Freire Rios A, Borst JW, Lukowitz W, Jürgens G, et al. 2012. Different auxin response machineries control distinct cell fates in the early plant embryo. *Dev Cell* **22**: 211–222.

Rademacher EH, Möller B, Lokerse AS, Llavata-Peris CI, van den Berg W, Weijers D. 2011. A cellular expression map of the Arabidopsis AUXIN RESPONSE FACTOR gene family. *Plant J* **68**: 597–606.

Rajagopalan R, Vaucheret H, Trejo J, Bartel DP. 2006. A diverse and evolutionarily fluid set of microRNAs in Arabidopsis thaliana. *Genes & Development* **20**: 3407–3425.

Raser JM, O'Shea EK. 2005. Noise in gene expression: origins, consequences, and control. *Science* **309**: 2010–2013.

Rensing SA, Lang D, Zimmer AD, Terry A, Salamov A, Shapiro H, Nishiyama T, Perroud PF, Lindquist EA, Kamisugi Y, et al. 2008. The Physcomitrella genome reveals evolutionary insights into the conquest of land by plants. *Science* **319**: 64–69.

Reski R. 1998. Development, genetics and molecular biology of mosses. *Botanica acta* .

Reutter K, Atzorn R, Hadeler B, Schmülling T, Reski R. 1998. Expression of the bacterial ipt gene in Physcomitrella rescues mutations in budding and in plastid division - Springer. *Planta* .

Rhoades MW, Reinhart BJ, Lim LP, Burge CB, Bartel B, Bartel DP. 2002. Prediction of plant microRNA targets. *Cell* **110**: 513–520.

Rosin FM, Kramer EM. 2009. Old dogs, new tricks: regulatory evolution in conserved genetic modules leads to novel morphologies in plants. *Dev Biol* **332**: 25–35.

Sakakibara K, Nishiyama T, Sumikawa N, Kofuji R, Murata T, Hasebe M. 2003. Involvement of auxin and a homeodomain-leucine zipper I gene in rhizoid development of the moss Physcomitrella patens. *Development* **130**: 4835–4846.

Sambrook J, Russell DW, Laboratory CSH. 2001. *Molecular cloning : a laboratory manual / Joseph Sambrook, David W. Russell*. Cold Spring Harbor Laboratory Cold Spring Harbor, N.Y, 3rd. ed. edition.

Schaefer DG. 2001. Gene targeting in Physcomitrella patens. *Curr Opin Plant Biol* **4**: 143–150.

Schnable PS, Ware D, Fulton RS, Stein JC, Wei F, Pasternak S, Liang C, Zhang J, Fulton L, Graves TA, et al. 2009. The B73 maize genome: complexity, diversity, and dynamics. *Science* **326**: 1112–1115.

Shaw AJ, Goffinet B. 2000. *Bryophyte Biology*. Cambridge University Press.

Shivaprasad PV, Chen HM, Patel K, Bond DM, Santos BACM, Baulcombe DC. 2012. A microRNA superfamily regulates nucleotide binding site-leucine-rich repeats and other mRNAs. *Plant Cell* **24**: 859–874.

Shomron N, Golan D, Hornstein E. 2009. An evolutionary perspective of animal microRNAs and their targets. *J Biomed Biotechnol* **2009**: 594738.

Shpak ED, McAbee JM, Pillitteri LJ, Torii KU. 2005. Stomatal patterning and differentiation by synergistic interactions of receptor kinases. *Science* **309**: 290–293.

Sieber P, Wellmer F, Gheyselinck J, Riechmann JL, Meyerowitz EM. 2007. Redundancy and specialization among plant microRNAs: role of the MIR164 family in developmental robustness. *Development* **134**: 1051–1060.

Skopelitis DS, Husbands AY, Timmermans MCP. 2012. Plant small RNAs as morphogens. *Current Opinion in Cell Biology* **24**: 217–224.

Stern DL, Orgogozo V. 2008. The loci of evolution: how predictable is genetic evolution? *Evolution* **62**: 2155–2177.

Stern DL, Orgogozo V. 2009. Is genetic evolution predictable? *Science* **323**: 746–751.

Studer A, Zhao Q, Ross-Ibarra J, Doebley J. 2011. Identification of a functional transposon insertion in the maize domestication gene tb1. *Nat Genet* **43**: 1160–1163.

Sunkar R, Girke T, Jain PK, Zhu JK. 2005. Cloning and characterization of microRNAs from rice. *Plant Cell* **17**: 1397–1411.

Talmor-Neiman M, Stav R, Klipcan L, Buxdorf K, Baulcombe DC, Arazi T. 2006. Identification of trans-acting siRNAs in moss and an RNA-dependent RNA polymerase required for their biogenesis. *Plant J* **48**: 511–521.

Tan X, Calderon-Villalobos LIA, Sharon M, Zheng C, Robinson CV, Estelle M, Zheng N. 2007. Mechanism of auxin perception by the TIR1 ubiquitin ligase. *Nature* **446**: 640–645.

Timmermans MC, Schultes NP, Jankovsky JP, Nelson T. 1998. Leafbladeless1 is required for dorsoventrality of lateral organs in maize. *Development* **125**: 2813–2823.

Tiwari SB, Hagen G, Guilfoyle T. 2003. The roles of auxin response factor domains in auxin-responsive transcription. *Plant Cell* **15**: 533–543.

Torii KU, Mitsukawa N, Oosumi T, Matsuura Y, Yokoyama R, Whittier RF, Komeda Y. 1996. The Arabidopsis ERECTA gene encodes a putative receptor protein kinase with extracellular leucine-rich repeats. *Plant Cell* **8**: 735–746.

Townsley BT, Sinha NR. 2012. A new development: evolving concepts in leaf ontogeny. *Annual review of plant biology* **63**: 535–562.

Ulmasov T, Hagen G, Guilfoyle TJ. 1997. ARF1, a transcription factor that binds to auxin response elements. *Science* **276**: 1865–1868.

Ulmasov T, Hagen G, Guilfoyle TJ. 1999a. Activation and repression of transcription by auxin-response factors. *Proc Natl Acad Sci USA* **96**: 5844–5849.

Ulmasov T, Hagen G, Guilfoyle TJ. 1999b. Dimerization and DNA binding of auxin response factors. *Plant J* **19**: 309–319.

Varkonyi-Gasic E, Wu R, Wood M, Walton EF, Hellens RP. 2007. Protocol: a highly sensitive RT-PCR method for detection and quantification of microRNAs. *Plant Methods* **3**: 12.

Vernoux T, Brunoud G, Farcot E, Morin V, Van den Daele H, Legrand J, Oliva M, Das P, Larrieu A, Wells D, et al. 2011. The auxin signalling network translates dynamic input into robust patterning at the shoot apex. *Mol Syst Biol* **7**: 508.

Voinnet O. 2009. Origin, biogenesis, and activity of plant microRNAs. *Cell* **136**: 669–687.

von Goethe JW. 1790. Versuch die Metamorphose der Pflanzen zu erklären.

Wang H, Nussbaum-Wagler T, Li B, Zhao Q, Vigouroux Y, Faller M, Bomblies K, Lukens L, Doebley JF. 2005. The origin of the naked grains of maize. *Nature* **436**: 714–719.

Wartlick O, Kicheva A, González-Gaitán M. 2009. Morphogen gradient formation. *Cold Spring Harb Perspect Biol* **1**: a001255.

Werner T, Koshikawa S, Williams TM, Carroll SB. 2010. Generation of a novel wing colour pattern by the Wingless morphogen. *Nature* **464**: 1143–1148.

Wienholds E, Kloosterman WP, Miska E, Alvarez-Saavedra E, Berezikov E, de Bruijn E, Horvitz HR, Kauppinen S, Plasterk RHA. 2005. MicroRNA expression in zebrafish embryonic development. *Science* **309**: 310–311.

Wightman B, Ha I, Ruvkun G. 1993. Posttranscriptional regulation of the heterochronic gene lin-14 by lin-4 mediates temporal pattern formation in C. elegans. *Cell* **75**: 855–862.

Williams L, Carles CC, Osmont KS, Fletcher JC. 2005. A database analysis method identifies an endogenous trans-acting short-interfering RNA that targets the Arabidopsis ARF2, ARF3, and ARF4 genes. *Proc Natl Acad Sci USA* **102**: 9703–9708.

Wittkopp PJ, True JR, Carroll SB. 2002. Reciprocal functions of the Drosophila yellow and ebony proteins in the development and evolution of pigment patterns. *Development* **129**: 1849–1858.

Wu G, Park MY, Conway SR, Wang JW, Weigel D, Poethig RS. 2009. The sequential action of miR156 and miR172 regulates developmental timing in Arabidopsis. *Cell* **138**: 750–759.

Wu G, Poethig RS. 2006. Temporal regulation of shoot development in Arabidopsis thaliana by miR156 and its target SPL3. *Development* **133**: 3539–3547.

Wu MF, Tian Q, Reed JW. 2006. Arabidopsis microRNA167 controls patterns of ARF6 and ARF8 expression, and regulates both female and male reproduction. *Development* **133**: 4211–4218.

Yifhar T, Pekker I, Peled D, Friedlander G, Pistunov A, Sabban M, Wachsman G, Alvarez JP, Amsellem Z, Eshed Y. 2012. Failure of the Tomato Trans-Acting Short Interfering RNA Program to Regulate AUXIN RESPONSE FACTOR3 and ARF4 Underlies the Wiry Leaf Syndrome. *Plant Cell* **24**: 3575–3589.

Yoshikawa M. 2005. A pathway for the biogenesis of trans-acting siRNAs in Arabidopsis. *Genes & Development* **19**: 2164–2175.

Zhai J, Jeong DH, De Paoli E, Park S, Rosen BD, Li Y, Gonzalez AJ, Yan Z, Kitto SL, Grusak MA, et al. 2011. MicroRNAs as master regulators of the plant NB-LRR defense gene family via the production of phased, trans-acting siRNAs. *Genes & Development* **25**: 2540–2553.

Zhao T, Li G, Mi S, Li S, Hannon GJ, Wang XJ, Qi Y. 2007. A complex system of small RNAs in the unicellular green alga Chlamydomonas reinhardtii. *Genes & Development* **21**: 1190–1203.

Zuo J, Niu QW, Chua NH. 2000. Technical advance: An estrogen receptor-based transactivator XVE mediates highly inducible gene expression in transgenic plants. *Plant J* **24**: 265–273.